A Seismological Comparison of Bezymianny Volcano, Russia, and Mount St. Helens Volcano, Washington

Weston Albert Thelen

A dissertation
submitted in partial fulfillment of the
requirements for the degree of

Doctor of Philosophy

University of Washington

2009

Program Authorized to Offer Degree:
Department of Earth and Space Sciences

University of Washington
Graduate School

This is to certify that I have examined this copy of a doctoral dissertation by

Weston Albert Thelen

and have found that it is complete and satisfactory in all respects,
and that any and all revisions required by the final
examining committee have been made.

Chair of the Supervisory Committee:

Stephen D. Malone

Reading Committee:

Stephen D. Malone

John Vidale

Michael West

Date: _____

In presenting this dissertation in partial fulfillment of the requirements for the doctoral degree at the University of Washington, I agree that the Library shall make its copies freely available for inspection. I further agree that extensive copying of the dissertation is allowable only for scholarly purposes, consistent with “fair use” as prescribed in the U.S. Copyright Law. Requests for copying or reproduction of this dissertation may be referred to ProQuest Information and Learning, 300 North Zeeb Road, Ann Arbor, MI 48106-1346, 1-800-521-0600, to whom the author has granted “the right to reproduce and sell (a) copies of the microform and/or (b) printed copies of the manuscript made from microform.”

Signature_____
_

Date_____

University of Washington

Abstract

A Seismologic Comparison of Bezymianny Volcano, Russia and Mount St. Helens, Washington

Weston A. Thelen

Chair of the Supervisory Committee:

Professor Stephen D. Malone

Department of Earth and Space Sciences

Bezymianny Volcano, Russia and Mount St. Helens, Washington are examples of eruptions involving the sector collapse of a volcano. The study and comparison of Mount St. Helens and Bezymianny has led to a better understanding of the precursory seismicity prior to eruptions. The shallow moment release prior to an eruption is dependent on the time since the last eruption at both volcanoes. This relationship is independent of the type of eruption that ensues, suggesting that overcoming the strength of the plug in shallow conduit must occur prior to the initiation of an eruption. This finding has obvious implications for forecasting eruptions, and more importantly, for forecasting failed eruptions.

The comparison of multiplets at Bezymianny and Mount St. Helens suggests that the physical properties of magma in the shallow conduit controlled the occurrence and behavior of multiplets. When there is shallow crystallization and

active degassing of the plug within the conduit, multiplets are abundant. Alternatively, when there is no shallow crystallization in a semi-open system, as at Bezymianny, multiplets were less abundant. At both volcanoes prior to an explosion, the multiplet percentage of total seismicity drops, and the average amplitude of each multiplet increases. Multiplet characteristics such as the multiplet percentage of total seismicity, multiplet durations, and the number of contemporaneous multiplets can be tracked prior to an eruption to forecast the type of eruption that will ensue.

The future volcanic activity at Mount St. Helens will likely diverge from the current explosive activity at Bezymianny. Without any additional input of mafic material or additional gas content, intermittent viscous dome building at Mount St. Helens will likely continue. In general, the high gas content of the magmas at Bezymianny compared to Mount St. Helens has driven more explosivity during eruptions despite the lower silica content and resultant lower viscosity magma at Bezymianny compared to Mount St. Helens. In future eruptions at Bezymianny and Mount St. Helens, the seismic energy release prior to eruptions will be dictated by the time since the last eruption. Stronger seismicity can be expected in cases where the conduit bends around existing domes.

TABLE OF CONTENTS

Page

LIST OF FIGURES

Figure Number Page

Figure Number Page

Figure Number Page

LIST OF TABLES

Table Number Page

Acknowledgements

I wish to acknowledge several individuals who have made this dissertation possible. My advisor, Steve Malone has always included me in meetings and in conversations that I had no business attending due to my lack of experience. His subtle encouragement and sound advice has kept me hungering for results throughout my graduate career. The financial support and advice that has come from the Pacific Northwest Seismograph Network was instrumental in giving me the practical knowledge and experience to approach and solve a variety of problems. In particular, Bill Steele, Tony Qamar, Karl Hagel and Paul Bodin have been instrumental in my continued learning and experience. Support from the PIRE project has also been key in gaining experience and obtaining data for the Bezymianny portion of this project. I would also like to thank several fellow graduate students including Sanjoy Som, Theresa Kayzar, Aaron Wech and Joe Macgregor for their stimulating conversations and much-needed distractions.

This dissertation would not be possible without the support of my family. Though I did not know at the time, the my interests in geology and volcanoes began on long road trips to places such as Crater Lake, Mount St. Helens, Mount Lassen and Mount Shasta. Only through the positive and supportive environment that I grew up in, could I have accomplished the goals that I have. Lastly, I could not have completed this dissertation without the support of my wife Jenni. She has tolerated my ridiculous work hours and months of absence in Russia or elsewhere. In return for this abuse she has given me love and sanity.

Dedication

To my wife, Jenni and new son, Coen Scott.

I. Introduction

1.1 Objectives

Since the 1980 edifice failure and subsequent eruption at Mount St. Helens, similar collapse deposits have been found at other volcanoes worldwide. In the last 400 years, 17 avalanche calderas have formed and been accompanied by explosions [Siebert, 1984]. In this scenario, the upper several hundred meters of the volcano is removed, resulting in depressurization, and explosion. Shortly after the initial explosions are over, viscous dome building begins. Presumably, dome building stops when the edifice on top of the conduit is restored to pre-collapse conditions. While this zeroth-order model produces a nice story, it lacks the details necessary to apply it to current volcano monitoring and hazard mitigation.

Two volcanoes, Bezymianny and Mount St. Helens, are part-way through the process described above. Bezymianny has had dome building and explosive eruptions intermittently since its 1955-56 sector collapse and lateral blast. Mount St. Helens has also experienced intermittent dome growth since 1980. This dissertation seeks to make a meaningful seismic comparison between morphologically similar volcanoes with a similar initial condition of edifice failure in order to gain information and insight into the activity at both volcanic systems. Comparing and contrasting the pathways for magma transport and pre-eruptive seismicity patterns between the two volcanoes provides insight that is immediately useful in the ongoing hazard mitigation of the future eruptions of Mount St. Helens and Bezymianny. Further, by utilizing the similarities and differences of both volcanoes, one can reduce the number of volcanic parameters that are responsible for the observed seismic activity.

Seismology is a tool often used on volcanoes to gain insight into processes at work under the surface of the earth and to investigate the volcano's geologic structure. At volcanoes worldwide, conduit geometry, dynamic stress states and magma ascent processes have all been studied using earthquakes. Additionally, nearly every major eruption is preceded by earthquake activity. A seismological comparison between Bezymianny Volcano and Mount St. Helens thus has the potential to compare phenomenon at work under the volcano and understand better the underlying processes that lead to the activity that is observed at the surface. A better understanding of the processes causing the seismicity will improve eruption forecasting at both volcanoes.

1.2 Mount St. Helens

Mount St. Helens is located in the Cascade Mountain Range of Washington, USA. The Cascade mountain chain extends from Northern California in the south, to British Columbia in the north, over 1200 km in length. The volcanic arc is the product of the subduction of the Juan de Fuca Plate under the North American Plate. Mount St. Helens is among the youngest and most active volcanoes in the Cascade chain [Hildreth, 2007]. The volcano lies approximately 50 km west of the axis of the arc in a zone of strike-slip faulting that is consistent with compression. The orientation of maximum principal compression is approximately N20E [Giampiccolo et al., 1999]. Regionally, Mount St. Helens is proposed to lie in a small pull-apart basin formed by a step-over in the dextral St. Helens fault zone. This interpretation is based on focal mechanisms, dike orientations and lineations in the regional seismicity (Figure 1.1; Weaver et al., 1983, Musumeci et al., 2002). Presumably, buoyant magma has

exploited this tensional area over the past 50,000 years to build the edifice in its current form.

1.2.1 Eruptive History

The current Mount St. Helens edifice began forming approximately 40,000 years ago [Mullineaux and Crandell, 1981; Clynne et al., 2008]. Dacitic volcanism until 2,500 years BP was discontinuous, including dormant periods of thousands of years. Beginning 2,500 years ago, andesite and basaltic eruptions were found interspersed with more voluminous dacitic eruptions. In the last 2,500 years, dormant periods have lasted between 200 and 700 years. Previous Mount St. Helens eruptions have occurred in the 17, 18 and 19 centuries. The last eruption before the activity beginning in 1980 was between 1800 A.D. and 1857 A. D [Pallister et al., 1992]. This eruption included an explosive summit eruption with a dense rock equivalent of 0.5 km^3, a 5 km-long andesite lava flow (Floating Island Lava Flow), and the extrusion of a dacitic lava dome (Goat Rocks) on the north flank of the volcano.

On March 20, 1980, Mount St. Helens began the volcanic earthquake crisis that led to the lateral blast and sector collapse of May 18, 1980. The buildup in seismic activity was rapid initially, however the number of earthquakes quickly declined in number after a peak on March 24, while keeping a nearly constant moment release (Figure 1.2). The activity remained at a constant level for weeks despite the appearance of phreatic activity and the continued emplacement of a cryptodome within the edifice. The intruded cryptodome eventually reached a volume of 0.11 cubic kilometers [Pallister et al., 1992]. Immediately prior to the eruption on May 18, there were no obvious short-term precursors, suggesting the eruption and

M5.1 earthquake accompanying the eruption was due to spontaneous failure of the destabilized edifice [Qamar et al., 1983]. A plinian eruption with a cloud in excess of 20 km high followed the lateral blast.

After several large explosions in the summer and fall of 1980, Mount St. Helens began a period of discrete dome building events that continued until 1986. Each event was preceded by an increase in seismicity and deformation (Figure 1.3, Swanson et al., 1985). Dome building occurred without any significant explosive activity after October, 1980, with the exception of one event in March, 1982. Dome-building episodes generally were less than 10 days long, however one period of dome building in 1983 lasted for over 1 year [Swanson and Holcomb, 1990]. The total volume of the dome at the end of the dome building eruption in 1986 was 74.1 million cubic meters [Swanson and Holcomb, 1990]. During the dome-building phase between 1980 and 1986, an increase in the strength of precursory seismicity suggested an increased amount of resistance due to the state of the extruding magma, and the size of the growing dome [Neri and Malone, 1989]. Multiplets, or repeating earthquakes, were common, particularly during the later dome-forming eruptions [Fremont and Malone, 1987]. The eruptive products between 1980 and 1986 have all been dacitic in composition, with a SiO_2 content ranging from 60% to 64% [Pallister et al., 1992]. Since 1981, the SiO_2 content has increased slightly from 62% to 64%.

Between 1987 and 2004, the seismicity at Mount St. Helens continued below 2 km deep as low-level background activity at about 2.0-2.5 km deep and as discrete deeper swarms, though the only activity seen at the surface was some minor phreatic

explosions from 1989 to 1991 (Figure 1.4; Mastin, 1994). Earthquake focal mechanisms below 4 km revealed rotated stress fields after the end of dome building in 1986 until 1992 [Barker and Malone, 1991; Moran, 1994]. The rotated stress field was consistent with magma recharge at depths between 4 and 10 km. Recharge continued into the late 1990s below 5.5 km depth [Musumeci et al., 2002].

The latest eruption of Mount St. Helens began in late September 2004 after 18 years of quiescence. Seismicity started approximately 8 days prior to the first explosion on October 1, 2004 and was confined to depths of less than 1 km [Moran et al., 2008]. After several small explosions, dome extrusion was continuous until January 2008 [Scott et al., 2008]. The eruption had low SO_2 (240 t/d max) and CO_2 (2400 t/d max) output compared to dome building between 1980 and 1986, yet the volcano maintained extrusion for 3.5 years at rates initially as high as 6 cubic meters per second [Iverson et al., 2006; Gerlach et al., 2008]. The eruption was notable for the smooth extrusive features (called “Whalebacks”) that formed in late 2004 and 2005, and the abundance of repeating earthquake families (called “Drumbeats”). In January 2008, extrusion stopped, and high frequency earthquake activity resumed below 2 km depth.

1.2.2 Magma Plumbing System

Much is known about the plumbing system under the edifice of Mount St. Helens from a combination of abundant earthquakes during eruptions and a dense seismic network. Seismicity is generally concentrated around the volcanic edifice (Figure 1.5). Scandone and Malone (1985) interpreted earthquake locations immediately following the May 18, 1980 eruption to define a magma reservoir at 7-14

km that is connected to the surface via a relatively thin conduit with a smaller, shallow magma chamber at 2 to 3 km depth (Figure 1.6). There have been occasional deep-long period (DLP) earthquakes in excess of 20 km depth [Malone and Moran, 1997], which are thought to be associated with magma movement into the bottom of the magma chamber [Power et al., 2004]. Thus far, 14 possible DLPs have been identified between 1988 and 2009 under Mount St. Helens [M. Nichols, pers. comm., 2009]. Recent seismic tomography results support the presence of a magma chamber below 7 km depth [Lees, 1992; Waite and Moran, 2009]. The magma chamber is believed to have a volume of 5-7 cubic kilometers based on seismic evidence and volumes of prehistoric eruptions [Pallister et al., 1992]. Petrologic evidence supports the presence of multiple small magma chambers within the conduit system between 1980 and 1986 [Cashman and McConnell, 2005].

Between the last dome forming eruption in 1986 and the 2004 eruption, there was a conspicuous concentration of small earthquakes between 2.1 km and 2.4 km depth (Figure 1.4). The concentration of earthquakes appear to form a cap on the recharge seismicity that occurred during that time period. This cap coincides with the source region of deformation and proposed source of magma during the 1980-1986 dome forming eruptions [Chadwick et al., 1988a]. Seismicity during the dome-forming eruptions bottomed out at depths approximately coincident with the concentration of seismicity. The interface between the bedrock and the overlying edifice is thought to exist at depths of approximately 2 km, coincident with the cap in seismicity [Waite and Moran, 2009; Williams et al., 1987]. Seismic velocities below the cap (3 and 6 km depth) are low with respect to the surrounding crust, and this zone has been interpreted as an additional shallow magma chamber [Waite and

Moran, 2009]. Interestingly, seismicity above the seismic concentration (<2 km depth) was less than below it during periods of surface quiescence. When there was dome extrusion at the surface, such as from 1980 to 1986 and from 2004 to 2008, the seismicity below the cap was low, while seismicity above the cap was high. While much is known about the magma plumbing system under Mount St. Helens, much is yet to be learned including the structure of the lower and mid-crustal supply system under Mount St. Helens, the depth extent of the active magma chamber and the role of the shallow chamber in the eruptive activity of the volcano.

1.3 Bezymianny

Bezymianny Volcano is located on the Kamchatka Peninsula, Russia within the Klyuchevskoy Group of volcanoes (Figure 1.7). The Klyuchevskoy Group includes several large active volcanic centers including Tolbachik, Klyuchevskoy, Zimina, Bezymianny, and Ushkovsky. The group is often referred to as most productive group of arc volcanoes in the world [e.g. Lees et al., 2007]. The volcanoes are a product of subduction of the northern edge of the Pacific Plate under the Okhotsk Plate. The volume and composition of material erupted within the Klyuchevskoy Group is largely influenced by a slab tear of the Pacific Plate, and the subsequent mantle flow around the edge of the tear [Lees et al., 2007]. Bezymianny is overshadowed by nearby Kamen and Klyuchevskoy volcanoes, which tower over a kilometer higher than Bezymianny's summit dome. The edifice of Bezymianny is built on the shoulder of the extinct Kamen volcano. Kamen was active into the Holocene (<12,000 years), however, the exact date of the last eruption is currently unknown [Braitseva et al., 1991].

1.3.1 Eruptive History

The current edifice of Bezymianny volcano began forming only ~10,000 years BP [Braitseva et al., 1991]. The volcano was then active for 3,000 to 4,000 years [Ozerov et al., 1997]. After 3,000 years of dormancy, activity again commenced until approximately 1,000 years BP [Bogoyavlenskaya et al., 1985]. Eruptive products were dominantly domes and pyroclastic materials interspersed with lava flows up to 2 km long. The volcano is largely made up of andesitic volcanic products [Belousov et al., 2007].

In 1955, Bezymianny began an eruption that led to catastrophic sector collapse and a lateral blast on March 30, 1956. The buildup of seismicity prior to the 1956 eruption was very similar to that of Mount St. Helens, although much longer (Figure 1.8). Initially, seismicity built up rapidly then maintained a constant energy release, number, and maximum magnitude until the eruption. The surface activity from Bezymianny was more energetic than at Mount St. Helens, with a considerable amount of ash produced prior to the paroxysmal eruption [Gorshkov, 1959]. At the end of November, 1955, ash explosions were rare and a small dome began to form within the crater formed by the ash explosions. Even with dome extrusion, the flanks of the volcano continued to deform [Gorshkov, 1959]. From the first detected sign of unrest until the catastrophic eruption was approximately 6 months.

After the 1956 eruption, Bezymianny started a series of discrete dome building eruptions and explosions that lasted for over 5 years (Figure 1.9; [Tokarev, 1981]). Dome extrusion was relatively rapid compared to early rates at Mount St. Helens between 1980 and 1986 (Figure 1.10). Between 1965 and 1976 smooth, rigid domes

were predominantly extruded during a period of continuous dome building [Bogoyavlenskaya et al., 1985].

Since 1976, 22 years after the paroxysmal eruption in 1956, long, thick lava flows have accompanied strong explosions that often destroyed large parts of the dome ([Bogoyavlenskaya and Kirsanov, 1981]). During this latest phase of activity, eruptions usually occur 1-2 times each year. Generally, eruptions since 1976 start by extruding a low-temperature, fully crystalline spine from the vent [Malyshev A., 1995; Belousov et al., 2002]. As the spine collapses, rock avalanches are formed off the sides of the dome. Over the course of days to weeks the number of rockfall events increases. Within days to weeks, an explosion normally occurs, which is accompanied by pyroclastic flows. These explosions are often large enough to destroy parts of the dome. The last phase of this general eruptive sequence is the effusion of a long andesitic lava flow, which fills the crater and newly destroyed parts of the dome [Belousov et al., 2002].

Since 2000, there have been at least 11 separate eruptions at Bezymianny with a Volcanic Explosivity Index (VEI) between 2 and 3 [Venzke E et al., 2008]. Eruptions since 2000 have had seismicity up to 7 km deep (4 km below sea level) (Figure 1.11). These eruptions had no obvious correlation to seismicity that occurs at depths greater than 25 km. Recent eruptions were often are preceded by increased shallow seismicity and a large thermal anomaly on the new dome, which has led the Kamchatkan Branch of Geophysical Services (KBGS) to issue eruption predictions up to 2 weeks prior to an eruption, despite the sparse existing network. A graphical comparison of the volcanic activity between Mount St. Helens and Bezymianny is shown in Figure 1.12. The similarity in eruptive phenomenon begs the question if the

explosive eruptive phase described above at Bezymianny lies in the future at Mount St. Helens.

1.3.2 Magma Plumbing System

The KBGS catalog earthquake locations show two large clusters of high-density seismicity in map view (Figure 1.13). The northern cluster is focused under Klyuchevskoy Volcano and is a combination of a high-density earthquake cluster located at the base of the crust (~30 km) and shallow high-density seismic cluster (< 10 km) under Klyuchevskoy Volcano (Figure 1.14). The southern high-density cluster is elongated to the north of Bezymianny. This cluster consists of seismicity above 7 km depth associated with eruptive activity at Bezymianny (Figure 1.11). Small, shallow seismicity (<500 m) is also present at Bezymianny, however the closest seismic stations to Bezymianny in the KBGS network are too far away to precisely constrain the depths of shallow earthquakes.

The shallow magmatic system is far less well studied at Bezymianny than Mount St. Helens, particularly in English publications. This is due to the relatively sparse seismic network that currently exists (nearest seismic station is 13 km away) and the preference of Russian scientists to publish in national journals, which are not widely distributed outside Russia. The sparse seismic network has hindered the discrimination of seismic sources between Bezymianny and nearby Klyuchevskoy volcano [E. Gordeev, pers. comm., 2009].

Large scale tomography studies suggest a large area of partial melt at the base of the curst beneath nearby Klyuchevskoy Volcano [Lees et al., 2007]. Magnetotelluric and gravity surveys also suggest the presence of a magma chamber

beneath Bezymianny at approximately 10 km depth [Balesta et al., 1976-77]. Petrologic evidence shows a connection of the magma chambers between Klyuchevskoy and Bezymianny below 20 km depth [Ozerov et al., 1997].

1.4 Structure of the Thesis

The purpose of this paper is a seismological comparison between Bezymianny Volcano, Russia and Mount St. Helens, Washington. At both volcanoes I first review the volcanologic background and then concentrate on the event occurrence and energy release of pre-eruption seismic sequences. I then synthesize these observations and analyses into a comparison that points out some similarities and differences between the two volcanoes. Finally, I conclude with a general model and speculate on the future activity at Mount St. Helens.

The paper is broken up into 5 chapters and an appendix. The first chapter provides an introduction and background from which to better understand the remainder of the thesis. The second chapter describes the seismic characteristics found at Bezymianny Volcano. The third chapter describes the characteristics of seismicity at Mount St. Helens, Washington. Much of the data and results on Mount St. Helens are encompassed in Appendix A. Any additional analysis to supplement Appendix A is included in the body of Chapter 3. The fourth chapter synthesizes the information from Chapter 1, and the results from Chapters 2, 3 and Appendix A to make a seismological comparison between Bezymianny Volcano and Mount St. Helens. Finally, the fifth chapter concludes by summarizing the important findings of the thesis.

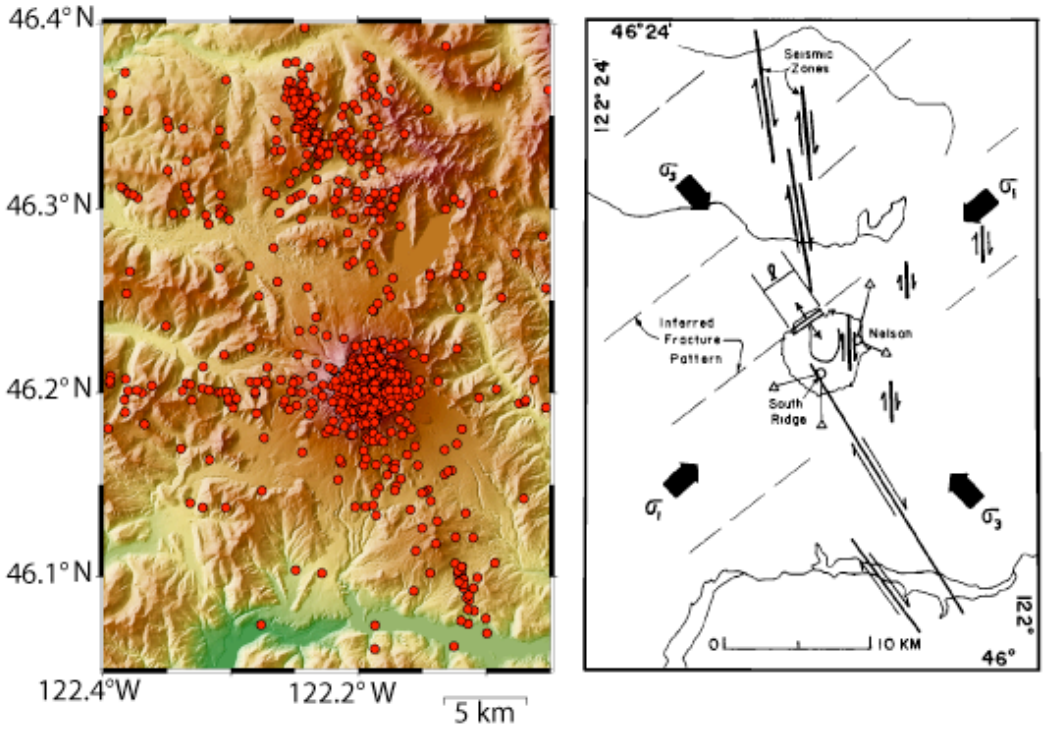

Figure 1.1: Regional seismic activity and tectonics at Mount St. Helens. Left: Map of earthquakes (red dots) between 1970 and 2004 above magnitude 2. Right: Interpretation of Weaver et al., 1987. Thick, dark arrows are stress directions, thin continuous lines are strike slip faults inferred by seismicity. Left pane from Weaver et al.(1987).

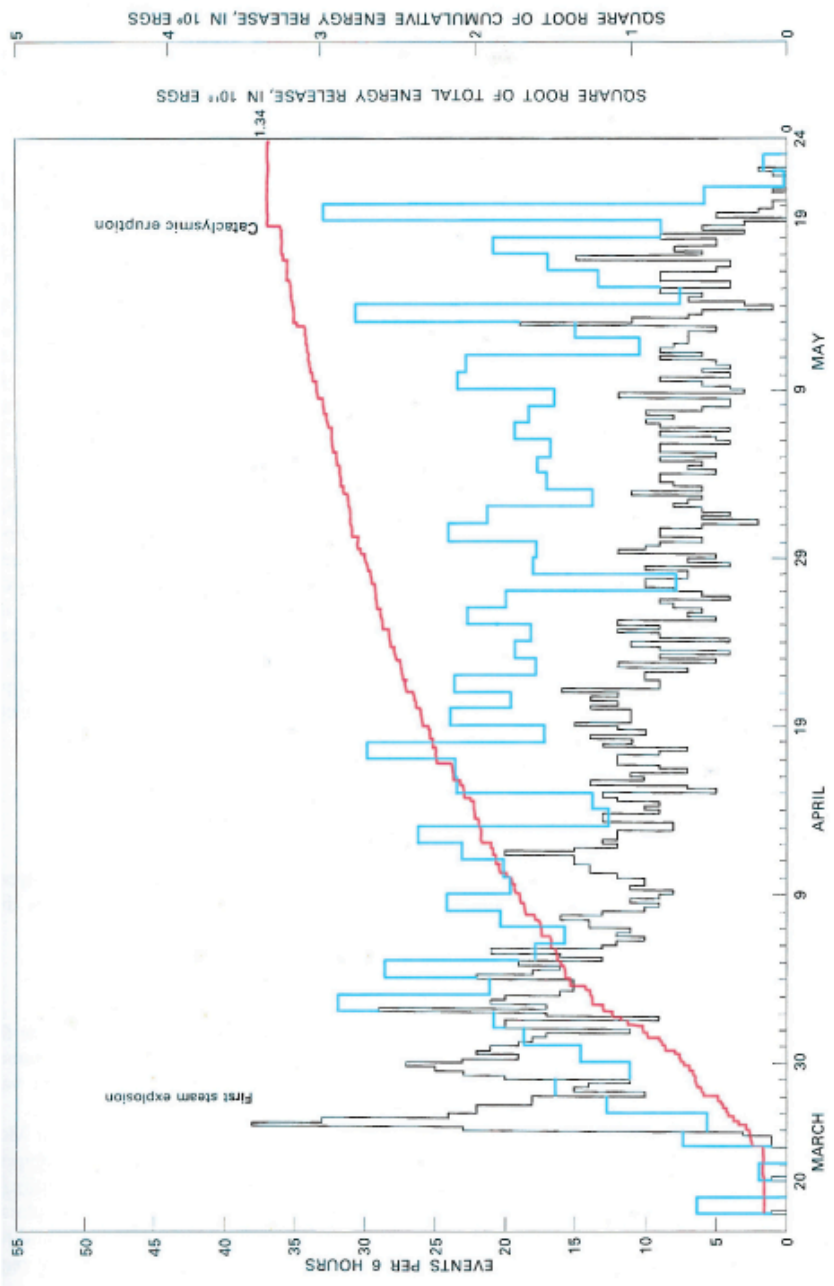

Figure 1.2: Seismic parameters leading to the 1980 eruption at Mount St. Helens. The black line is a count of the events larger than M2.5 per 6 hours (left axis), the blue line is the daily earthquake energy release (far right axis), and the red line is the cumulative moment release through May 24, 1980. Figure from Endo et al. (1981).

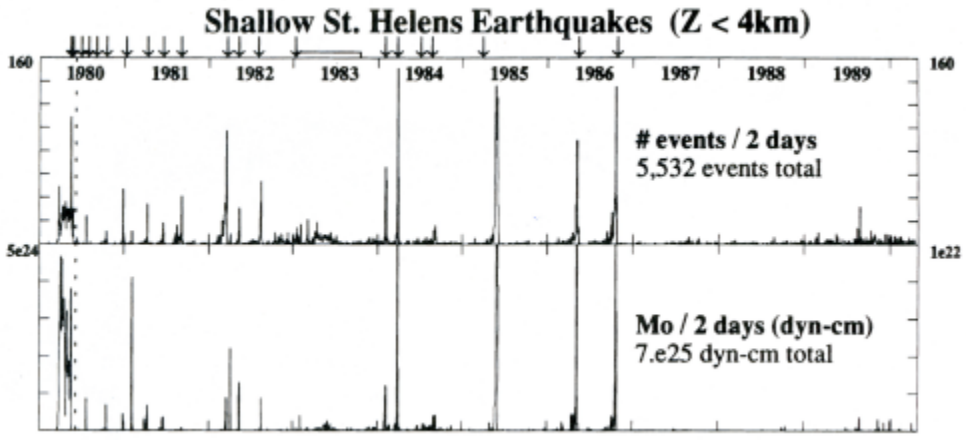

Figure 1.3: Shallow seismic characteristics at Mount St. Helens from Jan. 1, 1980 to May 1, 1990. Arrows at the top of the figure represent eruptions (explosive in 1980, effusive afterward). Figure from Malone et al., 1983.

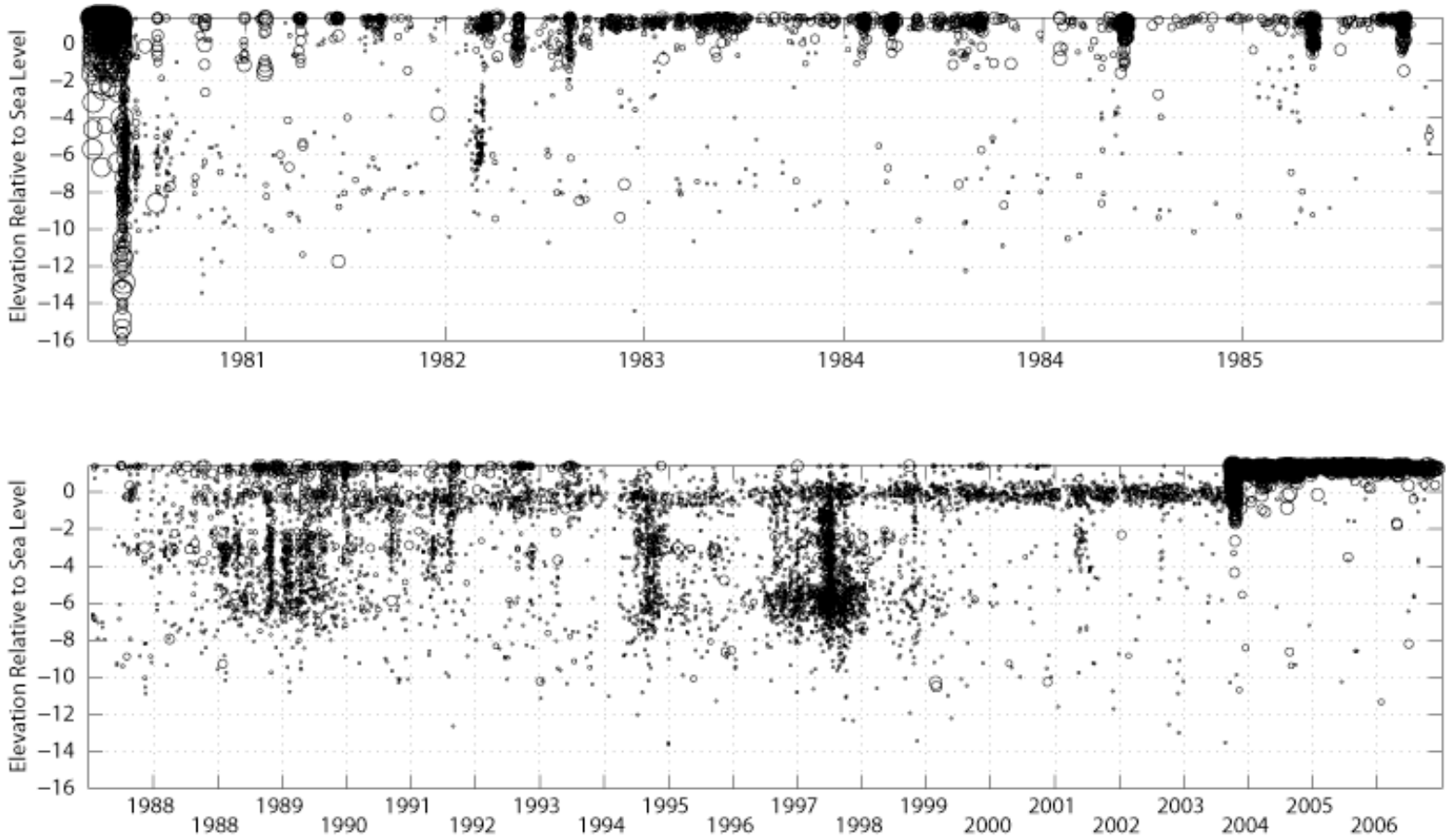

Figure 1.4: Time-depth plot of seismicity at Mount St. Helens between Jan 1, 1980 and Jan 1, 2007. Earthquakes are scaled based on their magnitude. All earthquakes less the M0.5 are the same size. The top of the velocity model in these locations is 1400 m elevation. Earthquakes must have 7 phase picks, a gap less than 135 degrees and a distance to the closest station of less than 10 km. More precise earthquake locations from September to November 2004 are presented in Appendix A.

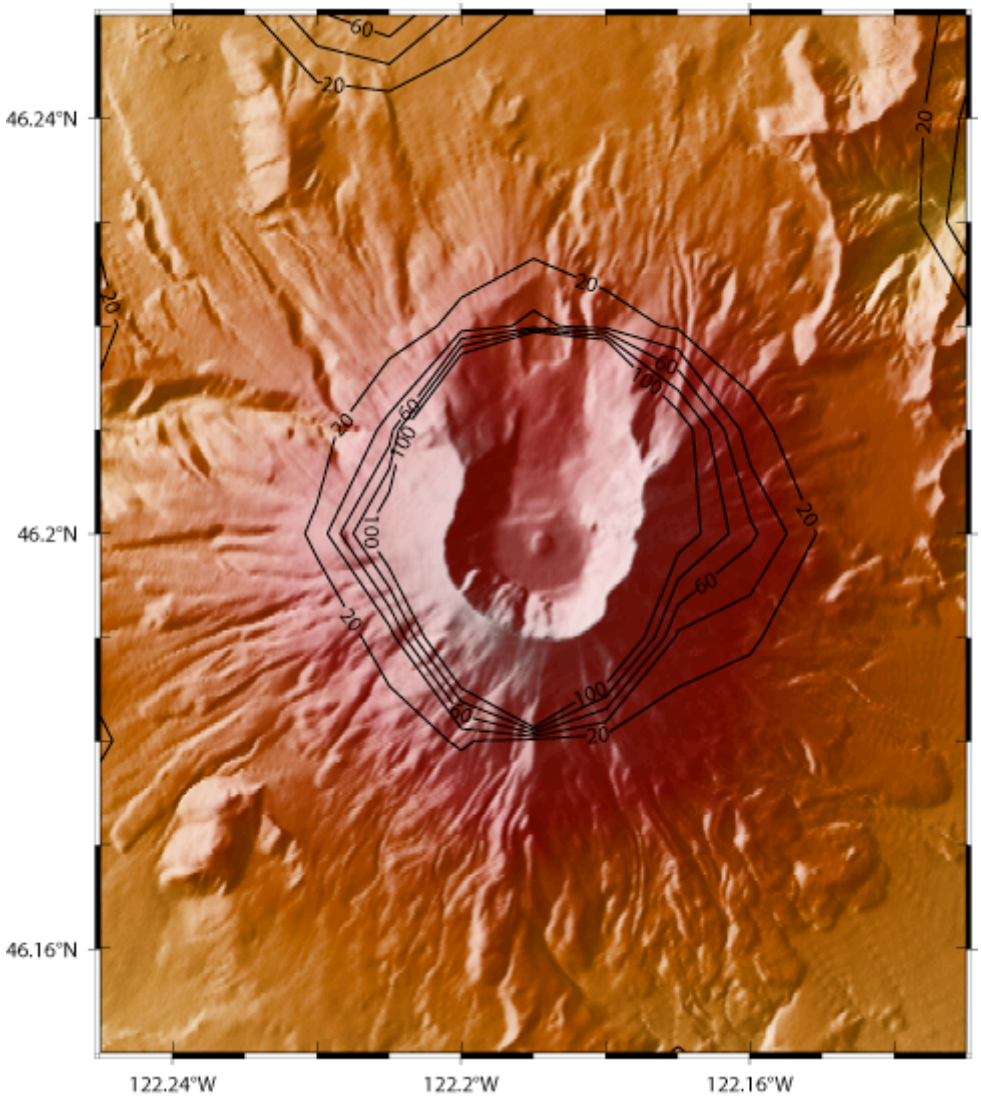

Figure 1.5: Epicenter density map at Mount St. Helens, Washington. Contoured seismicity includes the same earthquakes from Figure 1.4. To calculate the epicenter density, earthquake locations are binned within 0.001x0.001 degree squares and then contoured for density. Contour interval is 20 events. Maximum contour is 100 earthquakes. Background digital elevation map is from 1981, and thus the crater topography is no longer accurate.

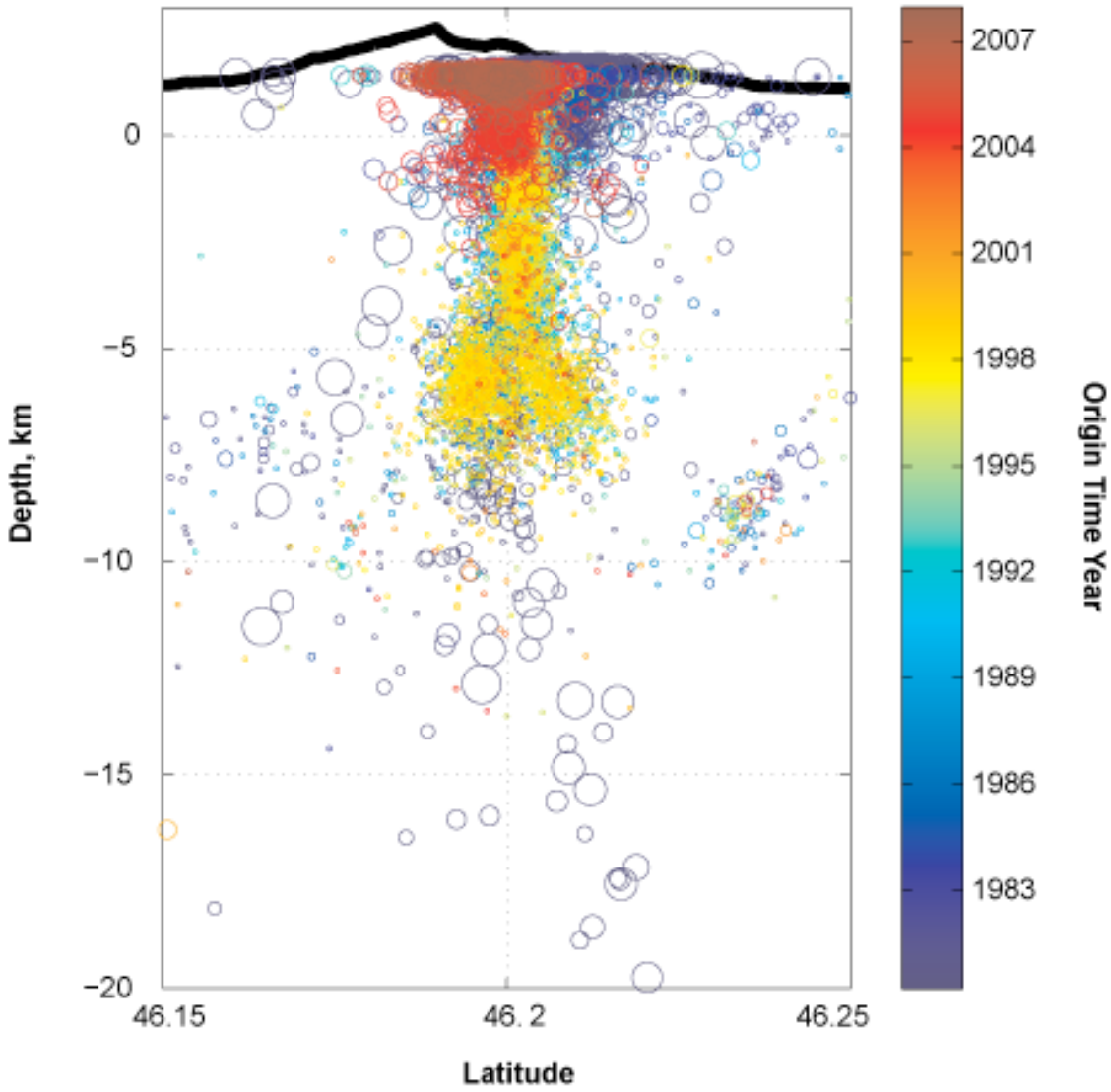

Figure 1.6: Cross-section of seismicity at Mount St. Helens. Earthquakes plotted here are the same as shown in Figure 1.4 and Figure 1.5. Earthquakes are sized based on their magnitude. Circles are color-coded sequentially.

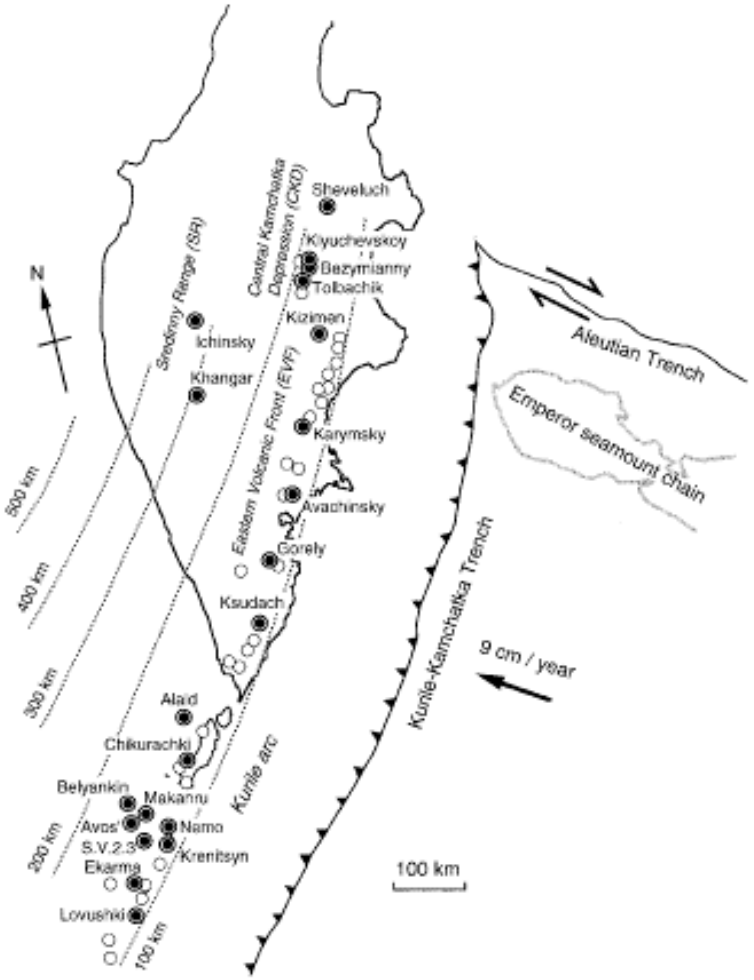

Figure 1.7: Regional tectonics of Kamchatka. Circles, white and dark, are active volcanoes. Light lines with kilometer labels are depth contours to the top of the subducting Pacific plate. The Klyuchevskoy Group lies near the extension of the Emperor Seamount Chain under Kamchatka. Figure from Ishikawa, 2001.

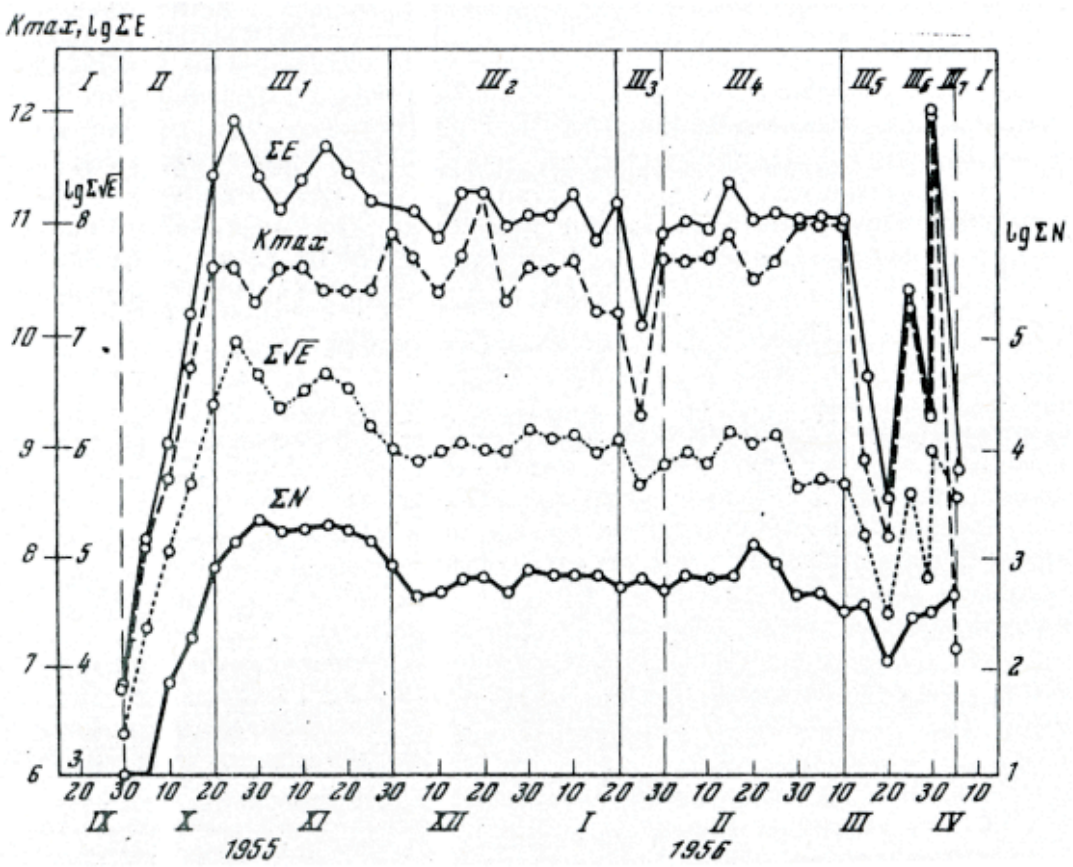

Figure 1.8: Seismic activity at Bezymianny volcano prior to the 1956 eruption. Roman numerals on the x-axis depict numeric months. ΣE is the sum of energy release each 5 days. Kmax refers to the maximum magnitude of earthquakes during each 5 day period. K can be converted to magnitude (M) using the following equation: M = (K-4.6)/1.5. A K of 10 corresponds to a M3.5 earthquake. $\Sigma\sqrt{E}$ is the sum of strain energy calculated every 5 days. ΣN is the number of earthquakes calculated every five days. All axes, except Kmax are presented on a logarithmic scale. Roman numerals refer to different phases of the eruption as defined by Tokarev (1981). Figure from Tokarev (1981).

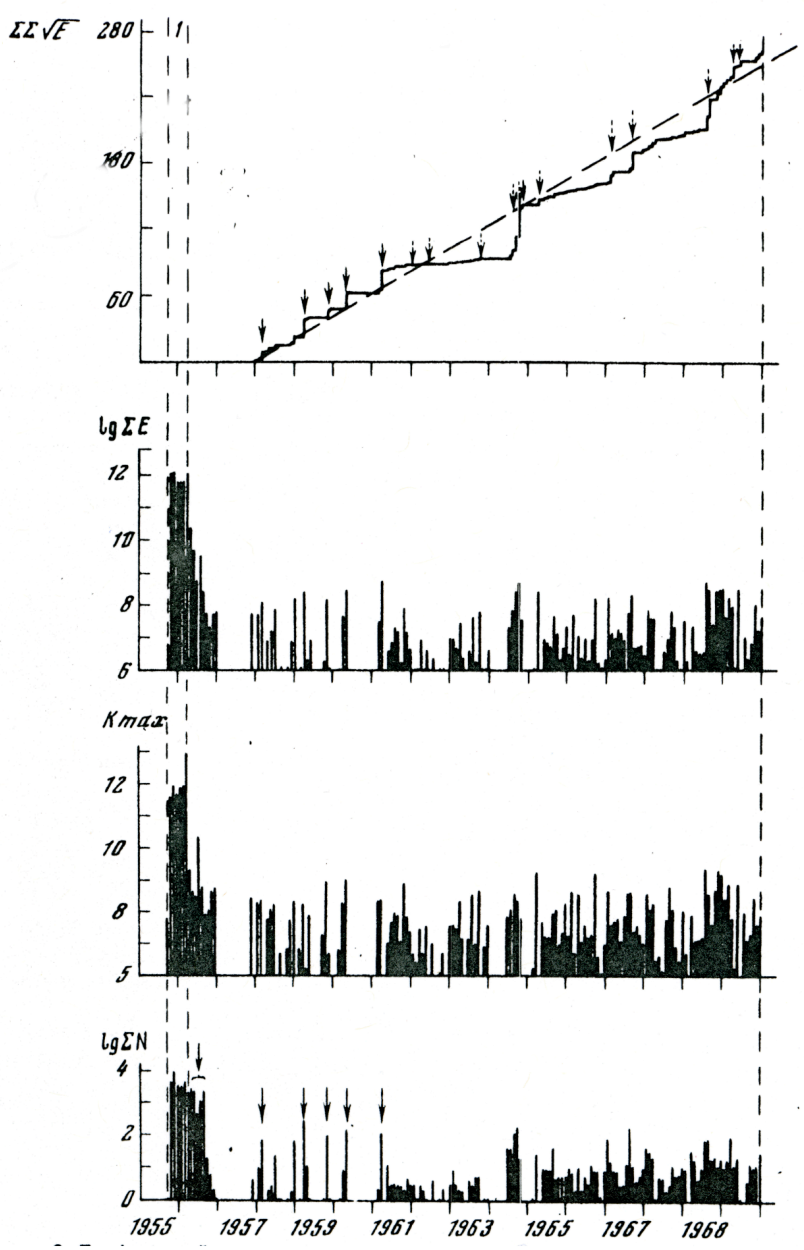

Figure 1.9: Post-1956 seismic activity at Bezymianny Volcano. All plots range from April 6, 1956 to December 31, 1970. Top plot: Cumulative strain energy calculated every 5 days starting Jan 1, 1957. Arrows refer to explosions. Middle top: Sum of energy released in five day intervals. Middle bottom: Maximum energy class (K) of each 5 day time period. An energy class of 8 corresponds to an earthquake of approximately M2. Bottom: Number of earthquakes calculated every 5 days. Catalog has detection threshold between M0.9 and M1.3. Arrows refer to discrete dome-forming eruptions. Figure from Tokarev (1981).

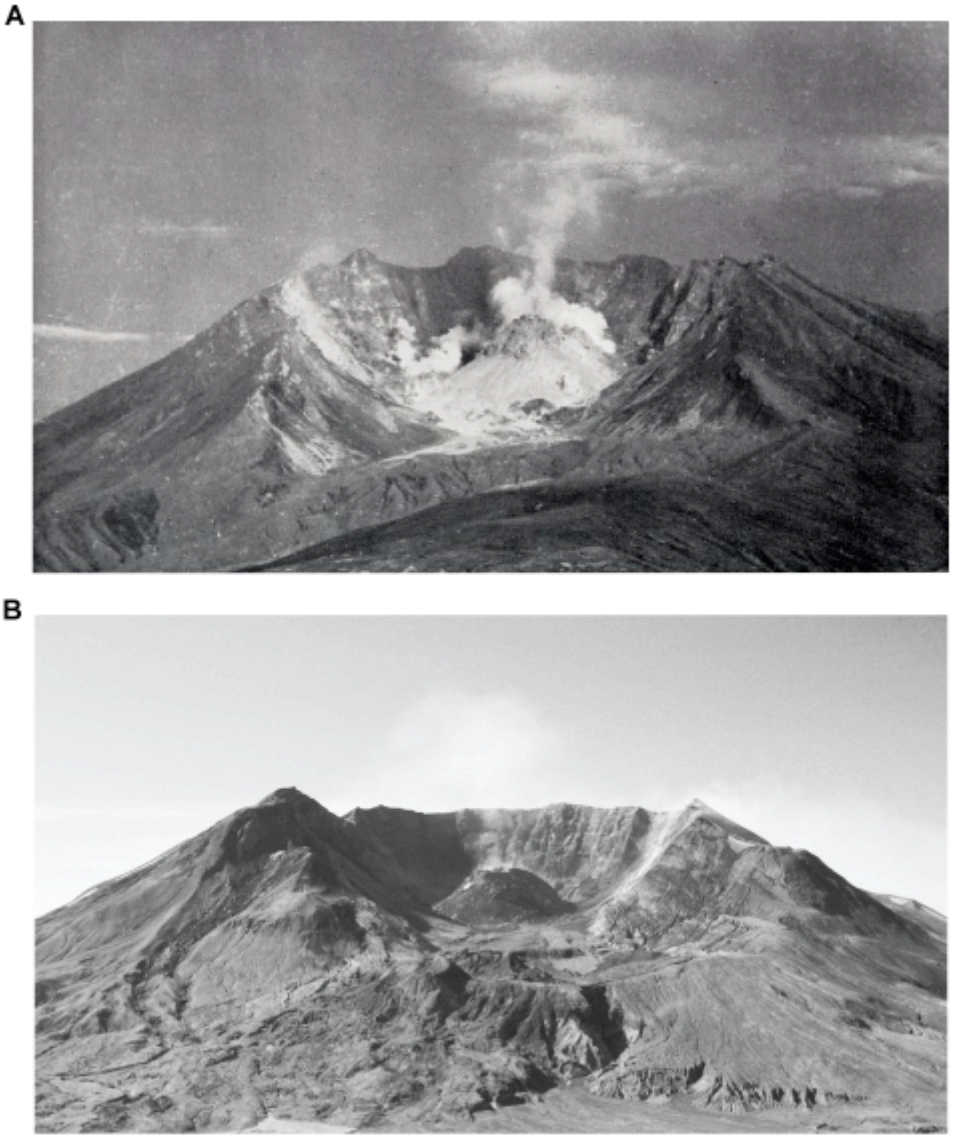

Figure 1.10: Comparison of dome extrusion rates. A. Photo of Bezymianny taken approximately 6 months after the edifice collapse [Gorshkov, 1959]. B. Photo of Mount St. Helens taken approximately 2 years and 5 months after the edifice collapse. Photo from Lynn Topinka, USGS. Craters at both volcanoes had approximately equivalent volumes in each picture.

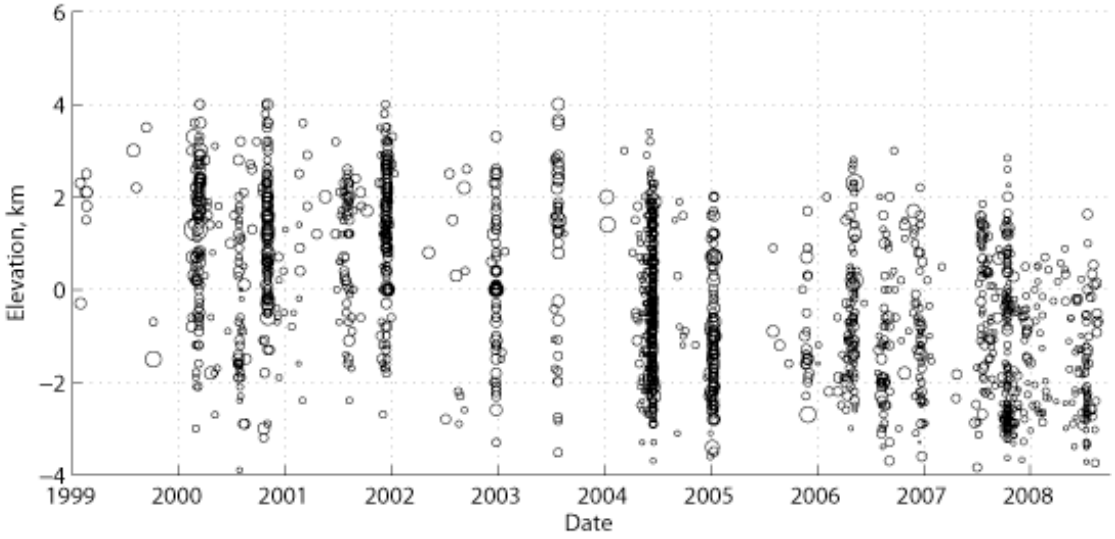

Figure 1.11: Time-depth plot of shallow seismicity underneath Bezymianny Volcano. Earthquakes are plotted as circles sized based on their magnitude using the same scale as the Figures 1.3 and 1.4. Eruptions are clearly denoted by vertical lines of earthquakes. An apparent deepening of earthquakes after 2004 corresponds to the addition of new stations closer to the volcano that better constrain the earthquake depths. The summit of Bezymianny lies at approximately 3 km elevation. An increase in the number of earthquakes after 2004 is likely due to the presence of closer stations as well.

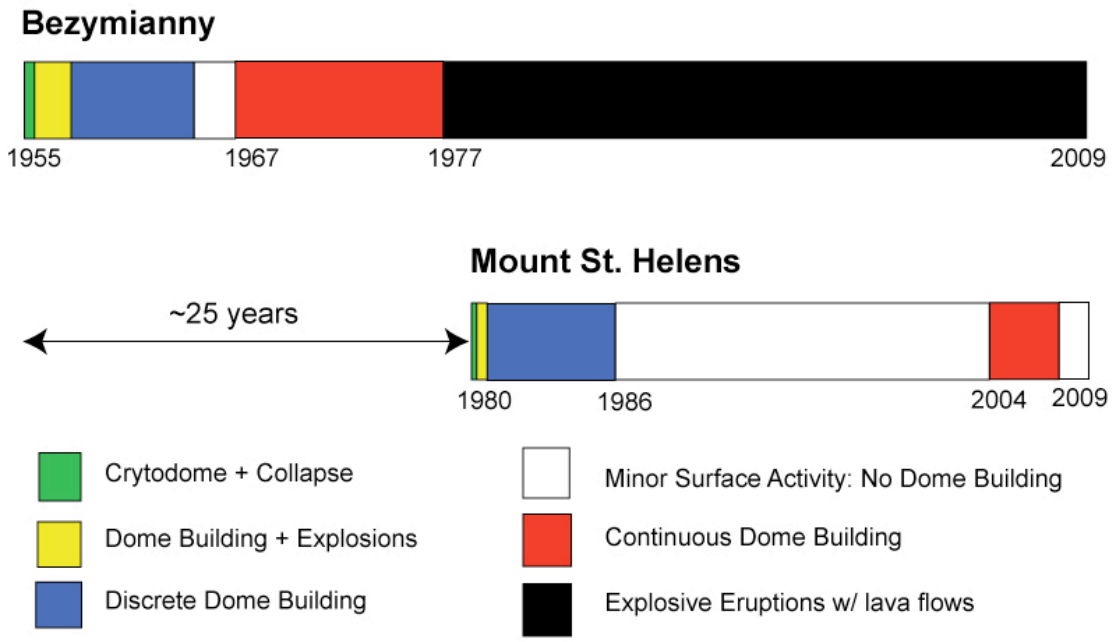

Figure 1.12: Graphical comparison of eruptive histories at Bezymianny and Mount St. Helens. Eruptive phases are plotted to scale on the same timeline. Different eruptive phases are plotted with different colors. See text for references of different time periods. While the individual phases have different lengths at different volcanoes, the sequence of eruptive phenomenon are the same.

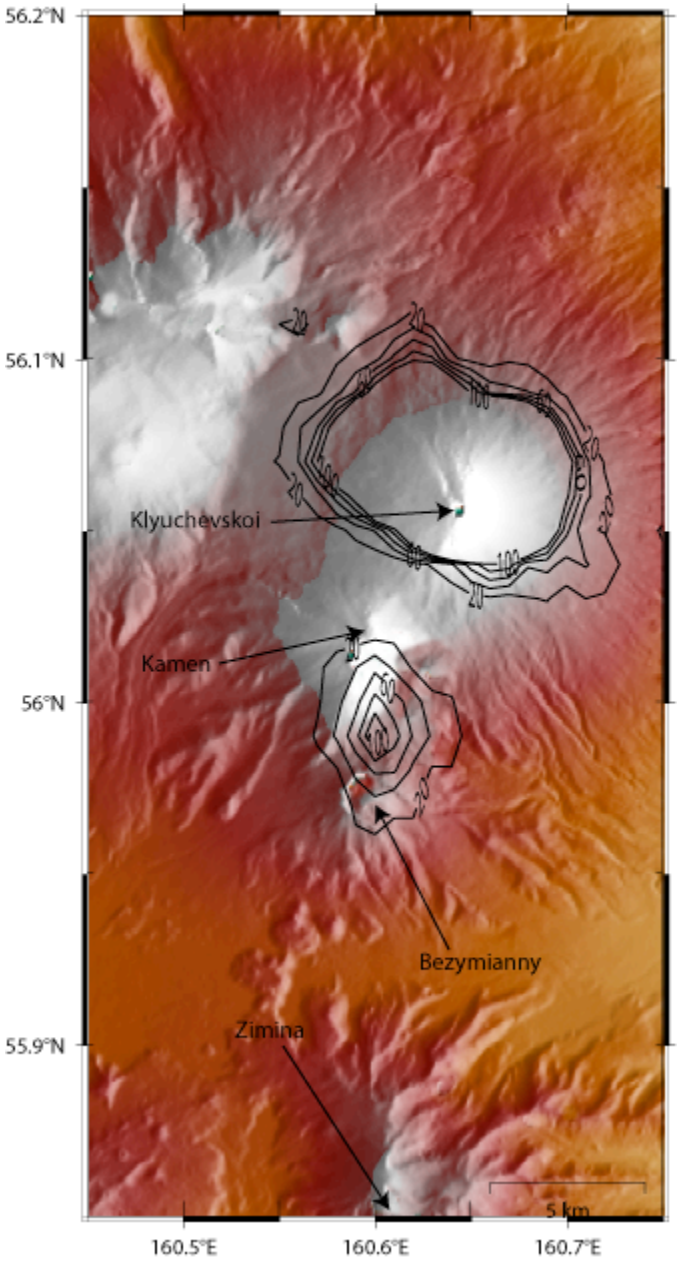

Figure 1.13: Epicenter density of the Klyuchevskoy Group using KBGS earthquake catalog between January 1, 2000 and August 1, 2007. Each earthquake within a 0.01x0.01 degree square is counted and then those values are contoured to represent density. The contour interval is 20 earthquakes, with a maximum contour of 100 earthquakes per 0.01 square degrees.

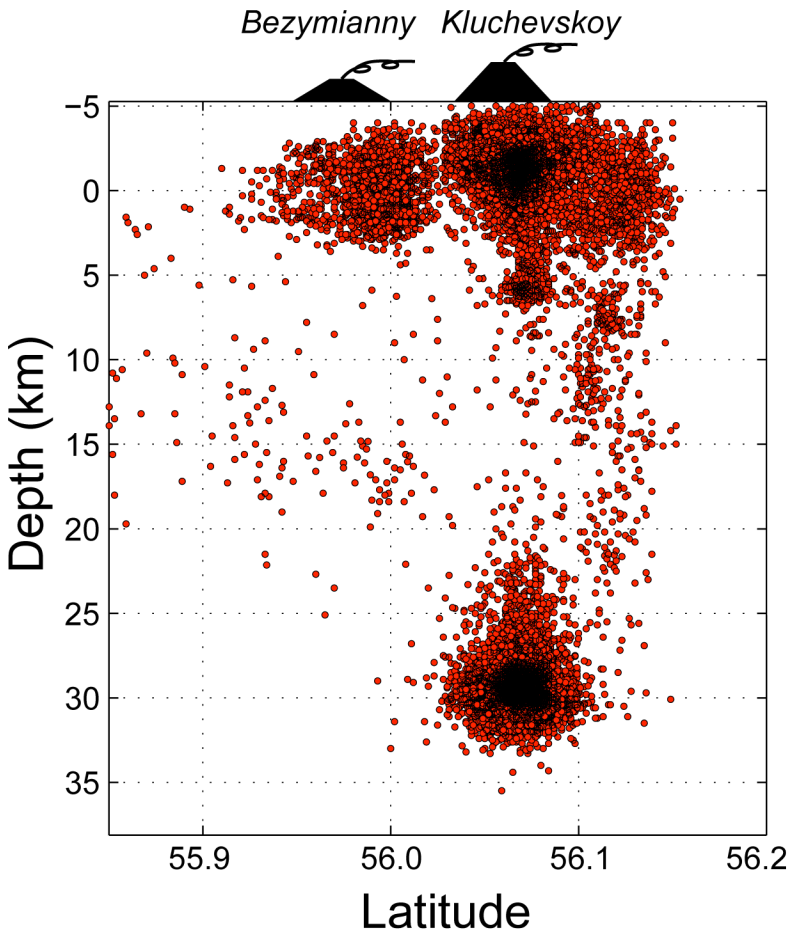

Figure 1.14: Cross-section of earthquakes in the Klyuchevskoy group. Earthquakes are from the KBGS earthquake catalog between 1999 and 2007. Figure courtesy of M. West.

II. Seismic Characteristics of Bezymianny Volcano, Russia

2.1 Introduction

In this chapter, I present the results of earthquake locations, report on multiplet behavior and analyze seismic signals associated with eruptions of Bezymianny in 2007. I have chosen these analyses because they are appropriate for the characteristics of the dataset and provide useful comparisons to data from Mount St. Helens. Interpretation of the results of these analyses also provides important, first-order information on the characteristics of the volcano that have not been well studied up until now. These characteristics provide a foundation for a direct and meaningful comparison between Mount St. Helens and Bezymianny Volcano. The results in this paper will also provide a basis for more sophisticated and thorough analyses of longer time series at Bezymianny.

Earthquake locations provide a basis for interpreting the tectonic setting and magmatic plumbing system of any volcano. The KBGS uses a regional network to locate seismicity within the Klyuchevskoy Group of volcanoes. Earthquake locations are available from the Kamchatkan Branch of Geophysical Services (KBGS) beginning in 2000 (Figure 1.11, Figure 1.13, Figure 1.14). Though the network has good coverage around the Klyuchevskoy Group, the sparse nature of the network near the edifice of Bezymianny leads to poor depth constraints and a catalog of completeness above M1 [S. Senyukov, pers. comm., 2007]. To better constrain the earthquakes below Bezymianny Volcano, the Partners in Education and Research (PIRE) installed a temporary network closer to the volcano [Thelen and Team, 2006]. This study utilizes data from both seismic networks to better understand the

distribution of earthquakes through the crust and to make better interpretations of the earthquake locations.

The average amplitude of a continuous seismic signal, called RSAM (Rectified Seismic Amplitude Monitor), is a useful parameter to grossly identify the duration of an eruption and the timing of large tremor or explosion signals [Endo and Murray, 1991]. Tracking the prominence of certain types of volcanic earthquakes, particularly low frequency earthquakes, is often useful to further characterize activity during eruptive and non-eruptive periods [Chouet, 1996]. Often the classifications of earthquakes at volcanoes are done manually, either in near-real time, or in post-processing. Tracking volcano tectonic, hybrid and low frequency earthquakes, as well as rockfall, is common on other volcanoes such as Soufriere Hills, Montserrat [Miller et al., 1998], Unzen Volcano, Japan [Umakoshi et al., 2008a] and Mount St. Helens [Moran et al., 2008; Malone et al., 1983], thus providing a direct point of comparison. Here, I classify the seismicity occurring within the active dome of Bezymianny prior to an eruption to look for patterns that may lead to a more accurate forecast and to understand the seismic signature of different volcanic phenomenon.

Multiplets, or earthquake families, are commonly observed in a variety of tectonic settings. Multiplets are observed during dome building eruptive sequences at volcanoes such as Mount St. Helens [Fremont and Malone, 1987] and Soufriere Hills [Rowe et al., 2004]. Likewise, multiplets are observed in tectonic settings such as the San Andreas Fault [Vidale et al., 1994] and Taiwan [Chen et al., 2007]. Because of their repetitive nature, these earthquakes suggest a stationary, non-destructive source; however, their actual cause in volcanic settings is uncertain. The

occurrence of repeating earthquakes in tectonic settings is believed to be associated with the repeated failure of fault asperities [Chen et al., 2007]. The sensitivity of earthquake families to changes in eruption dynamics is yet to be established. Bezymianny is an excellent candidate for testing the hypothesis that changes in eruption dynamics will result in changes in characteristics of earthquake families. Bezymianny often has multiple eruptions in a given year, and multiplets occurred prior to at least one previous eruption [West et al., 2007].

The analyses in this chapter largely focus on a 3 month sequence of eruptive activity between September 2007 and December 2007 for which high quality seismic data are available. The seismic activity and thermal anomalies between September 2007 and December 2007 are shown in Figure 2.15. There were 3 clear increases in seismic amplitude (Sept. 25, Oct. 14, Nov. 5) that correlated with confirmed eruptive activity. The September 25 eruption had minor pre-eruptive seismicity, no deep post-eruptive seismicity and a very small plume (Figure 2.15 and Figure 2.16; KBGS, 2007). No pyroclastic flow or ash deposit was preserved and thus it is interpreted that no juvenile material was involved in this small eruption. The October 14 eruption is more characteristic of the twice-yearly eruptions that have occurred at Bezymianny since 2000. The eruption had significant pre-eruptive seismicity and thermal anomalies, a pyroclastic flow that included juvenile material [T. Kayzar, pers. comm, 2009], and a large eruption plume [KBGS, 2007b]. Additionally, significant deep post-eruptive seismicity suggests that the magmatic source was below 4 km depth. The November 5 eruption had no pre-eruptive seismicity, and a pyroclastic flow that contained no juvenile material [KBGS, 2007c]. The event has been interpreted as a dome collapse [T. Kayzar, pers. comm., 2009].

2.2 Methods

2.2.1 Earthquake Locations

I present earthquake locations spanning a time period from September 2007, to August 2008. In late August 2007, three PIRE stations were installed on the edifice of Bezymianny volcano. Prior to August 2007, the nearest permanent station was nearly 8 km away. The addition of new edifice stations provides better depth constraints for shallow (< 5 km deep) earthquake locations. In late October 2007, the remainder of the PIRE network was installed around the volcano, establishing in total, an 8-station network of broadband seismometers (Figure 2.17). All 8 stations operated between October 2007, and August 2008, with few data gaps present. Up to 7 stations are used here because the data from BEZD was unavailable at the time of writing. To calculate absolute earthquake locations, I use the program SPONG, an adaption of FASTHYPO [Herrmann, 1979], which has been benchmarked against HYPOINVERSE [Klein, 1985], and is currently used, for routine earthquake locations at the Pacific Northwest Seismograph Network (PNSN). The velocity model used in this study for earthquake locations is currently used by the KBGS network and is shown in Table 2.1 [Senyukov, 2004].

At Bezymianny Volcano, I recalculated earthquake locations using two datasets. The first dataset is based on the KBGS catalog. The advantage of the KBGS network is the azimuthal coverage of the network around Bezymianny Volcano and the long time span that the catalog covers. If earthquake locations have quality phase picks on stations distributed around the crater using a reasonable velocity model, the resultant epicenters in the KBGS catalog should be well constrained.

Because the PIRE network is located closer to the volcanic edifice of Bezymianny than the KBGS network, the earthquake locations with supplemented phase picks from the PIRE network should have more accurate depths. To obtain the new phase picks, each earthquake in the KBGS catalog in the vicinity of Bezymianny was analyzed using PIRE network data. Relocations included the new PIRE network phase picks with the unchanged KBGS phase picks. Uncertainties in PIRE phase picks were generally less than 0.1 s. The uncertainty in the KBGS phase picks is unknown, however I assume for the purpose of the earthquake relocations that they are similar to the PIRE station phase picks and set them to a constant 0.1 s. Uncertainties in phase picks are highly dependent on the magnitude of the earthquake and clarity of the phase arrival (emergent vs. impulsive), however introducing a sliding scale of uncertainties into the KBGS phase picks without access to the original waveforms may unevenly and unnecessarily bias earthquake locations.

The second dataset of earthquake locations exclusively used the PIRE seismic network. The presence of stations on the edifice of Bezymianny Volcano allow for the detection and location of much smaller earthquakes than are in the KBGS catalog. Additionally, the earthquake locations that were calculated using the PIRE network alone have better depth constraints than earthquakes using only the KBGS network. The drawback to using exclusively the PIRE network is that there is a large gap in the coverage of the network to the north. This is where many of the epicenters from the KBGS catalog are located and thus special care was taken when considering earthquake locations to the north of the PIRE network. The disadvantage of both relocated datasets in this chapter is the short period of time that is covered.

As the PIRE network records more data, many more quality earthquake locations will become available.

Several sources of error exist when calculating earthquake locations. The first source of error lies in the accuracy of phase picks. Earthquakes with emergent phase arrivals often have more uncertainty than impulsive arrivals. Each phase pick made with PIRE stations was assigned a phase pick uncertainty based on the quality of the arrival. SPONG takes the uncertainty of the phase pick into account when calculating errors for the earthquake relocations. A second source of error can come from inaccuracies in the velocity model. The use of a 1-D model clearly introduces error, mostly in the determination of depths. This type of error is among the hardest to quantify because the 3-D variability in seismic wave speeds is not well characterized in this region and thus the absolute errors cannot readily be determined. An additional source of uncertainty can be introduced by the distribution of phase picks on stations around the hypocenter. If the focal depth of the earthquake exceeds the aperture of the array, than the earthquake depth may be poorly constrained. Alternatively, if phase picks are not well distributed on seismic stations around the source, artifacts in the earthquake epicenter can exist.

To quantify the errors introduced by the PIRE network geometry, I ran a simulation of earthquake locations around the network and calculated the difference between the original earthquake locations and the recalculated earthquake locations. First, I built a 3-D grid with 0.2 degree increment in latitude and longitude, and a 1 km increment in depth. For each grid point, synthetic travel times were calculated from each grid point to each station in the PIRE network. With the synthetic travel times at

each station, an earthquake location was calculated using the SPONG program. The distance between the original earthquake location at each grid point and the recalculated earthquake location using only PIRE stations is shown in the cross-sections in Figure 2.18. As expected, the errors are lowest directly under the network, extending in some cases to approximately 6.5 km depth (-4 km above sea level). Somewhat unintuitive is the extension of low errors to the north of the network. The SPONG code is especially good at locating earthquakes outside the network when compared to other location codes such as HYPOINVERSE [S. Malone, pers. comm., 2009]. It is important to note that these are only errors due to the configuration of the PIRE network, and does not incorporate other errors including errors in the velocity model, or errors in phase picks.

To further refine the absolute earthquake locations, I relocated a subset of earthquakes by differencing phase picks. This type of analysis often leads to more precise earthquake locations because phase differences are less sensitive to errors in the velocity model [Waldhauser and Ellsworth, 2000]. I used the double difference algorithm to carry out the relocations using only the manually picked phase differences because the similarity between most of the earthquakes in the KBGS catalog was not sufficient to warrant the use of cross-correlation derived lags.

Using phase pick differences instead of absolute phase arrivals reduces the error introduced from inaccuracies in the velocity model. Other sources of error present in standard earthquake locations still apply. Linear artifacts in phase-differenced earthquake locations can exist from a poor distribution of phase picks around the epicenter. To quantify this effect, we use a jackknife test [Efron and

Gong, 1983]. This method evaluates changes in the distribution of phase picks around an earthquake by removing one station at a time and relocating all of the earthquakes using the remaining phase picks from the reduced station set. For each station that is removed, a new phase-differenced earthquake location is calculated. To evaluate the results of the jackknife test, I calculated the distance between the final earthquake location using the full dataset and each earthquake location calculated with the jackknife test. Those distances gave an estimate of the effect that removing each station has on each final earthquake location. To get an average error due to poorly distributed phase picks, I plotted every distance calculated from each earthquake and draw an ellipse that encompasses 95% of the distances. An additional source of error inherent in earthquake locations is the selection of the initial location of each earthquake. In this study, the initial location of each earthquake was set to the absolute location calculated using the raw phase picks. This selection should significantly reduce the errors from choosing an incorrect initial location.

2.2.2 Automatic Event Classification Methods

In this study, I first used a short-term-average-to-long-term-average-ratio (STA/LTA) to determine initial triggers in the continuous data on stations BELO, BESA and BERG. Only edifice stations are used to emphasize the activity occurring at the shallowest levels in the dome. The continuous data was filtered between 2 and 12 Hz to accentuate the event arrival. When triggers at three stations were within 8 seconds of one another, an event is declared and forwarded on for further analysis.

Volcanic earthquakes are often classified based on frequency [Chouet, 1996]. In this study, I divided earthquakes into high-frequency, and low-frequency

earthquakes based on their spectra (Figure 2.19). Upon inspection of the spectra in Figure 2.19, there is a division at 5 Hz that can be used to help classify events automatically. By taking the ratio of the average of two short frequency bands, an event can be accurately characterized and tabulated [Buurman and West, in review]. In this study, I used a low-frequency band between 1 and 5 Hz, and a high-frequency band between 6 Hz and 10 Hz. The high-frequency classification only refers to observable energy above 5 Hz. Volcano-tectonic earthquakes are few at Bezymianny and the spectra of the events classified as high frequency are not similar to volcano-tectonic earthquakes in most cases. Due to the potential of high attenuation within the dome and edifice, it is not clear if the frequencies above 5 Hz are being reduced preferentially by the path. For each event, I calculated the spectra of a 13 second window around the trigger (3 seconds before, 10 seconds after) and calculated the ratio of the averages of the high-frequency band and low-frequency band. The frequency ratio was discarded if the maximum signal to noise ratio (SNR) of the event was less than 3. This was done to make sure that background noise in the signal is not contaminating the spectra. The noise average was calculated by taking the average absolute value of amplitudes of a 3 second window prior to the start time of the event. The average signal amplitude is calculated by finding the average absolute value of amplitude over a 3 second window, incrementing from the beginning of the record to the end of the record one sample at a time. The SNR at a given time is determined by the center time of the signal average divided by the noise average.

The frequency ratios were then averaged across stations to get the final frequency ratio for a given event. The duration for each event on each station was

calculated by finding the first point past the maximum amplitude of the event when the SNR dropped below 1.5. The durations of events are highly sensitive to station noise and site effects, and thus I used the median duration of the three stations to determine the final event duration. The use of the median minimized the effect of a single erroneous value.

In this study, I make a distinction between short duration signals and long duration signals. By analogy with signals seen at Mount St. Helens [Malone et al., 1983] and Soufriere Hills [Calder et al., 2005], high-frequency signals with long durations are classified as rockfall. No direct visual observations of rockfall have been correlated with seismic signals at Bezymianny though rockfalls from the lava dome have been observed. The duration delimiting rockfall from regular events is chosen deliberately so that only small- and intermediate-sized dome events are classified as high- or low-frequency events. The largest events that are locatable by the KBGS network have long durations. These events represent a small proportion of the overall seismicity and thus the inclusion of these events with the longer duration signals did not dramatically affect the final results.

There are several potential pitfalls in this type of analysis. The largest source of error in this type of analysis comes from local noise or electronic noise that contaminates the spectra. I considered events with signal to noise ratios over 3, which minimized the errors from noise contamination. Taking averages of the frequency ratio and duration also helps mediate this problem. Another source of error is strong regional or teleseismic earthquakes that often have spectra that mimic low-frequency events. Time periods with spikes in low frequency earthquake activity

were visually scanned for regional and teleseismic events, however they were generally few. Larger, locatable events from Bezymianny also may be classified as either rockfall or low-frequency long duration events (LFLDE) if their length exceeds 25 seconds. Most of the larger locatable events occur around the time of eruptions, when the counts of rockfall and LFLDEs are already high. Thus the effect of misidentified Bezymianny earthquakes is small. Nearby volcanic activity from Klyuchevskoy volcano could also contaminate the seismic record. The KBGS keeps regular records of the magnitude of completeness of the local catalog (a measure of background activity at the surrounding volcanoes) and the amplitude of tremor originating at Klyuchevskoy. I chose times when the magnitude of completeness and tremor amplitudes were low and thus contamination of the results presented here were minimized. Even so, it is hard to determine at what level tremor and other activity start to contaminate the results presented here. Contamination shows most obviously in the LFLDEs and low-frequency earthquakes, since higher frequencies are usually attenuated due to the path effects between Klyuchevskoy and Bezymianny.

2.2.3 Multiplet Methods

2.2.3.1 Data and Event Selection

To initially identify events, I considered multiple stations based on several criteria; 1) operational throughout the study period, 2) high signal to noise ratio, and 3) proximity to the dome. Each seismogram was initially filtered between 2 and 10 Hz to improve the signal to noise ratio. A STA/LTA was calculated on the Hilbert Transform for each waveform. If the STA/LTA exceeded 2.5 on three stations within 8 s, then the trigger was considered to be a real event. A nine second window,

including two seconds before the earliest trigger, was then extracted for further analysis. I used a relatively large window prior to the automatic pick because triggers are often observed to be later than the actual first arrival, specifically in cases where the arrival was emergent.

2.2.3.2 Multiplet Selection

After all of the events were selected for a certain day, each nine second event waveform was normalized and cross-correlated on each individual station. Cross-correlation is a measure of similarity commonly used to compare two waveforms (e.g. [Rowe et al., 2004; Poupinet et al., 1984; Dodge et al., 1995]. Cross-correlation was completed in the time domain because of its ability to recover large lags that might be introduced by an inaccurate automatic phase pick [Schaff et al., 2004]. Three stations (BELO, BERG and BESA) were used in this study. Nine-second windows were selected to increase the stability of the cross-correlation values and prevent cycle skipping, which is common with smaller time windows [Schaff et al., 2004]. I chose to partition analyses into day-long data segments (up to 1000 events during eruptive periods) because of available computer resources. The cross-correlation functions of some events have large side lobes, and thus some events are prone to cycle skipping. To ensure that we include only cross-correlations that have a distinct peak, we only include cross-correlation functions that have side lobes that are less than 0.707 of the main peak after Stephens and Chouet [2001].

After cross-correlation of every event against every other event, the result is an N X N matrix of cross correlation values for each station where N is the number of events. Following the method of Petersen [2007], I then find the mean cross-

correlation value of each row of the correlation matrix at a single station. In this study I use station BELO. The row with the highest average cross-correlation value is then searched for events that exceeded the normalized cross-correlation value threshold. I chose a cross-correlation threshold of 0.7 based on visual observations of similarity. Below that value, events could not be visually distinguished as being similar and higher values of the cross correlation threshold divided the events into smaller multiplets that appeared similar. Our understanding of multiplets is limited at best, therefore I try to keep events that look similar to the naked eye together and assume that they are due to similar source processes.

The events that exceed the cross-correlation threshold within the selected row of the cross-correlation matrix are then checked for similarity on the other stations (BESA and BERG). Any event within the row that exceeds the cross-correlation value threshold on 2 out of 3 stations is considered part of the same multiplet and removed from the cross-correlation matrix. After removal, the row with the highest average is again selected, and the same method as above is followed to extract subsequent multiplets until there are no rows (events) left.

2.2.3.3 Combining Days into a Continuous Catalog

To this point, I have compared all of the events within a given day, and grouped events that are highly similar on 2 or more stations. To get a catalog of multiplet occurrence, one must devise a scheme to combine each day of multiplets into a continuous record. This method must seek to reduce the number of events to compare so that the analysis does not exceed existing computing resources. Using event stacks of each multiplet can reduce the total number of events to compare and

many days of event stacks can be compared without running out of computing resources. To implement this, I discarded all of the events that are not similar to another event over the course of a day. I then stacked each event within the multiplet for each day, creating a set of stacks, one per multiplet. All stacks were amplitude-normalized and cross-correlated, creating an M x M matrix of cross-correlation values for each station where M is the total number of daily stacks. The M x M matrix includes all event stacks from each day during the entire study period. I used the same technique to identify similar stacks in the cross-correlation matrix that I used to identify similar events in the day-long individual event analysis. Stacks were considered similar and combined if the normalized cross-correlation threshold is 0.8 on two or more stations. The individual events of similar stacks were then combined to create one multiplet. Because the individual events within a stack do not perfectly correlate with the stack itself, I chose a higher cross-correlation threshold than in the individual event analysis. The intention is to keep a cross-correlation value between individual events of combined stacks at or above the cross-correlation threshold of the day-long individual analyses.

The analysis employed here attempts to produce a complete catalog, however during long time periods it is often unreasonable, given computing resources, to consider every event that occurs every day for several months. To reduce the computing load in combining multiplets across individual days, I only consider events that have repeated at least once on a given day. This opens the possibility that a multiplet that has an event once a day would not be detected using this method. It also suggests that a multiplet could be active at a low level before or after it was detected in this method, producing longer durations of multiplets than shown in this

analysis. While a multiplet that occurs once a day for a long time period may be useful to track changes in velocity [Gret et al., 2005], for the purposes of this study I wish to have better temporal resolution of changes within the volcano.

2.3 Earthquake Locations

The KBGS catalog between September 2006 and August 2007 contains 342 earthquakes around Bezymianny Volcano. Figure 2.20 shows the earthquake locations with added PIRE phase picks. Earthquakes are shown with at least 1 edifice station picked, 6 total phases and a Root Mean Square (RMS) residual of less than 0.5 s. No s-waves were used from the KBGS catalog because the s-wave phase picks could not be reliably identified on PIRE seismograms when PIRE and KBGS seismometers were collocated. The resulting catalog of well-located KBGS earthquakes with PIRE supplemental picks consists of 95 total earthquakes. Adding the additional PIRE stations resulted in a 21% improvement in the average error of the earthquakes within the relocated catalog (0.98 km to 0.77 km) and a 22% improvement in the average RMS of the residual of the earthquakes in the relocated catalog (0.32 s to 0.25 s). The average number of p-wave phase picks was 9.8 and the average gap was 124 degrees.

Absolute earthquake locations generally trend north-northeast, sub-parallel to the trend between Kamen and Klyuchevskoy volcanoes. In cross-section, the absolute earthquake locations have depths mostly between -2 and 2.5 km elevation above sea level (0 to 4.5 km deep). The trend in earthquake locations shows a near vertical or very steeply dipping structure. There is also a weak trend of deepening earthquake locations to the north of Bezymianny volcano. The orientation of

earthquake locations is not likely an artifact of the network configuration since the KBGS seismometers surround the earthquake epicenters to the north.

To locate smaller and shallower seismicity than is possible with the sparser and more distal KBGS network, I chose to analyze the seismicity during November 2007 using the PIRE network exclusively. I chose November 2007 because the full PIRE network was installed and there was only minor activity at nearby Klyuchevskoy. Earthquakes were chosen based on their size and impulsive phase arrivals. 138 earthquakes were initially located. Earthquake locations with 5 or more phase picks, an RMS of the residuals less than 0.5, and one edifice station pick are shown in Figure 2.20. Two example record sections are shown in Figure 2.21. The resulting 73 earthquakes in the PIRE relocated catalog have an average RMS error of 0.11 s an average number of phase picks of 5.8 and an average gap of 185 degrees.

Like the KBGS earthquake locations, the earthquake locations using only PIRE network stations showed distinct trends in epicenters to the north-northeast. Since the trends between the two sets of locations are similar, I am confident that the trends are not an artifact. Additionally, it is shown in Figure 2.18 that the earthquakes were all located in areas of relatively low errors due to network coverage. In addition to the north-northeast trend of epicenters, a cluster of seismicity to the east of the main cluster, between stations BELO and BERG, was detected at 4.5 km depth. More shallow seismicity was located using the PIRE network compared to the KBGS catalog.

To reduce relative earthquake location errors discussed above, I relocated both earthquake datasets with manually-picked phase differences using the HypoDD

program [Waldhauser and Ellsworth, 2000]. Earthquakes were selected that had 5 or more phase picks. Earthquake locations of the 121 relocated earthquakes are shown in Figure 2.22. Of the 121 earthquakes, 75% have 7 or more phase picks in the solution. As in the other datasets, there was a general orientation of epicenters to the north-northeast. These earthquake locations show more clustering than the other datasets, a characteristic often seen when comparing absolute locations to phase-differenced locations. The results of the jackknife tests for the high-resolution earthquakes are shown in Figure 2.23. Ellipses encompassing 95% of the errors due to a poor distribution of phase picks were 0.72 km, 0.76 km and 0.77 km in X, Y and Z directions, respectively. Jackknife errors considering only earthquakes with 7 or more picks were not significantly better than the earthquakes with 5 or more picks.

2.4 Automated Event Classification Results

The distribution of ratios for the month of October 2007 is shown in Figure 2.24. The parameters for classifying events are shown in Table 2.2. The cutoff between high and low frequency events was chosen near a shoulder in the histogram. An additional boundary could be drawn between low-frequency and high frequency events at a ratio of 0.2 or 0.25, however the physical basis for the distinction is not clear. The resultant events from these boundaries are broadly consistent with the classification of Power et al. (1994) and Lahr et al. (1994) . What I wish to emphasize in the current classification are events with noticeably more low-frequency energy than high-frequency energy.

Using ratios to classify event types, I analyzed the sequence of seismicity between September 1, 2007 and November 1, 2007 (Figure 2.25). Increased rates of

low-frequency earthquakes appeared prior to the September and October eruptions, however the peak in activity was after both eruptions. Large variations in the occurrence of low frequency earthquakes in November coincided with increased activity at Klyuchevskoy, and thus may reflect contamination of the record [S. Senyukov, pers. comm.., 2008]. High-frequency events significantly increased during the October eruption, and to a lesser extent, during the September eruption. The September and October eruptions both had peaks in rockfall activity, while the November eruption was relatively quiet. LFLDEs maintained a steady background rate through the September eruption, but increased dramatically prior to the October eruption. As with the low-frequency earthquakes, the LFLDEs have a peak in occurrence after the main October eruption. Also like the low-frequency earthquakes, the LFLDEs are highly variable in November, revealing possible contamination from volcanic activity at Klyuchevskoy.

To understand better how the energy of the dome seismicity was partitioned, I calculated the average amplitude of each event within each classification for September and October 2007 (Figure 2.26). Tracking the evolution of event amplitudes as a function of the type of event through time could reveal changes or trends in processes that may not be detected using all of the undifferentiated events together. I used the cumulative maximum amplitude as a proxy for energy release. At Bezymiany, the LFLDEs and low-frequency earthquakes have a significantly higher energy release than the rockfall or high-frequency events. Additionally, the October eruption produced the only significant departure from the background rate of energy release of all event types. A summary of observations of changes in the cumulative maximum amplitude can be seen in Table 2.3.

As with amplitude, changes in frequency of different event types through time can provide insight into the changes in processes at work under the volcano. I tracked the maximum frequency of each event type though time in Figure 2.27. The changes in maximum frequencies were much more subtle than the changes in maximum amplitudes. The most conspicuous change in the average maximum frequency occurred just prior the October 14 eruption. The average maximum frequency of low-frequency earthquakes and LFLDEs jumped from 2 to 3 Hz. The average maximum frequency of low-frequency earthquake and LFLDEs continued to rise after the October eruption to a value of nearly 4 Hz before it declined back to 2 Hz by November 1. A summary of observations of changes in the maximum frequency can be found in Table 2.3.

2.5 Multiplet Results

A continuous record of multiplet occurrence from September 1, 2007 to December 1, 2007 is shown in Figure 2.28. Many multiplets occurred during the study period. Nearby volcanoes Klyuchevskoy and Zimina are both seismically active and were capable of contributing multiplets to the dataset. To insure that only seismicity from Bezymianny was included, I looked at manually-picked phase differences between the three edifice stations (BELO, BESA, BERG). Formal locations for most of the study period were impossible because the full PIRE network was not installed until late October 2007. Manual phase picks were made on stations with quality arrivals, and synthetic times were calculated from each nearby volcanic center. The synthetic times were then differenced between stations to get characteristic phase differences. Multiplets with phase differences that were

consistent with locations at Klyuchevskoy or Zimina, or that could not be picked on all three stations were discarded. Over 30% of the initial multiplet catalog was discarded. Nearly all of the discarded multiplets occurred in November 2007 because of increasing activity at Klyuchevskoy. The removal of multiplets did not drastically affect the overall trends in the multiplet timeline.

Using the full PIRE network to analyze individual event locations of multiplets in late October and November produced a range of depths from 0.5 km to 6 km depth in areas consistent with earthquake locations from Figure 2.20 and Figure 2.22. Many multiplets had quality arrivals only on the edifice stations. Most times these events did not have phase arrivals that were identifiable on enough stations to get a quality location, however the lack of observations on stations outside the edifice suggested a location in the upper 1-2 km of the edifice. Though not many multiplets were able to be formally and precisely located, there was weak tendency of shorter duration multiplets at shallower depths (less than 2 km) compared to deeper multiplets, which had longer durations.

With a catalog of multiplet occurrence, it is possible to quantify several characteristics of the earthquake families to determine how they changed during the three eruptions that occurred during the study period. The average amplitude and standard deviation around the average of each multiplet is shown in Figure 2.29. The average of the maximum amplitudes of each multiplet was unchanged through the September eruption. Prior to and after the October eruption, the average amplitudes of the multiplets increased to values higher than at any other time during the study period. The average amplitudes of the multiplets then decayed to relatively low

values throughout the end of October and November. The November eruption does not obviously affect the average amplitudes of the multiplets. The standard deviation of the maximum amplitudes of the events within each multiplet, a measure of variability in amplitudes within the multiplet, showed similar patterns to the average maximum amplitudes.

In Figure 2.28, the lifespan, or duration of each multiplet, clearly changed. This observation is quantified in Figure 2.30. In general, multiplets had durations of about 2 weeks (e^{14} seconds). There was a clear break from this pattern prior to and during the October 14 eruption. After the October 14 eruption, durations increased slowly to durations observed in September and November.

The number of contemporary multiplets also changed through the study period (Figure 2.31). The number of contemporary multiplets increased through the September eruption, and then drops prior to the October eruption. After the October eruption, the number of concurrent multiplets again increased through the November eruption to between 10 and 12 different multiplets occurring at the same time.

The multiplet proportion of total seismicity (MPTS) is generally between 10 and 20% (Figure 2.31). Trends in the MPTS followed trends in the number of contemporary multiplets. With such a low overall proportion of total seismicity, individual multiplets would be hard, if not impossible to track manually. Prior to the October eruption, the proportion of overall seismicity that consisted of multiplets dropped significantly. The fraction of overall seismicity made up by multiplets also decreased prior to the September eruption, although the significance of the drop is questionable.

It is also clear that some multiplets continued through the September and November eruptions, while no multiplet that occurred prior to the October eruption reoccurs after the eruption (Figure 2.32). This suggests a fundamental change occurred in the multiplet source area during the October eruption. Whatever multiplet source or sources that existed prior to the eruption were destroyed. During the September and November eruptions, either the eruptions were not strong enough to destroy the source areas, or the multiplet source area was deeper than the source depth of the eruption.

Many factors could lead to different results and trends in the behavior of multiplets. The October eruption has the largest average seismic amplitude of any time during the study period. Thus, it is possible that the increased seismicity could have produced events with overlapping codas, which may have interfered with the detection of multiplets. The requirement of a 0.7 cross-correlation coefficient across a nine-second window has the potential to be susceptible to interference, much more so than a shorter time window. To test if the multiplets that stopped prior to the October eruption were obscured during the increased levels of seismicity, I looked for multiplets using much shorter windows and only a single station. First I stacked a single multiplet and cut out the largest amplitude 3 second window on station BELO. I used the north channel of the seismometer, since the largest amplitudes are likely s-waves, or surface waves. I then cross-correlated the three second window against several days of continuous data prior to the October eruption. A potential trigger is declared when the 3 second stack is similar to the continuous data at a 0.7 cross-correlation coefficient. During this analysis only a handful of triggers were found outside the declared bounds of the multiplets in Figure 2.28. It is also possible, with a

short window, that the interference pattern between two overlapping events or simply random noise could mimic the snippet of multiplet used in the cross-correlation. Updating the multiplet catalog with this much more liberally defined set of multiplets did not significantly change the results or trends of the analysis so the events were discarded from further consideration. In conclusion, the change from long duration multiplets to short duration multiplets prior to the October eruption is real and not due to interference because of increased seismicity.

2.6 Discussion

2.6.1 Earthquake Locations

Using different earthquake datasets, station configurations and earthquake location techniques, I showed the dominant pattern in earthquake locations was a north-northeast trending lineament with a vertical or steeply east-dipping orientation (Figure 2.20, Figure 2.22; [Balesta et al., 1976-77]). An attractive explanation is that the earthquakes are occurring along some type of preexisting fracture or fault structure. Magma often utilizes existing weaknesses in the crust to get to the surface, and the relative ease of moving magma along a fault structure as opposed to homogeneous crust could help explain the frequency and size of eruptions at Bezymianny [Costa et al., 2007].

The presence of a northward trending fault is also supported by the GPS network installed at Bezymianny by the PIRE group. Preliminary results of long time series reveal a contraction of monuments around Bezymianny toward a north-south line [J. Freymueller, pers. comm., 2008]. Results also show a peak in the subsidence

across the proposed fault. The pattern is similar to dike-like patterns of deformation at other volcanoes.

Other fault zones have been identified within the Klyuchevskoy Group. Based on a combination of magnetotellurics and gravity, a large north-northeast trending topographic high exists in the Cretaceous-age and crystalline bedrock centered about 5 km to the west of Bezymianny (Figure 2.33; [Balesta et al., 1976-77]). The Cretaceous basement is approximately 1.5 km deep (~ 1 km elevation asl), and the crystalline basement is located at about 4 km deep (~-1.5 km elevation asl) in the vicinity of Bezymianny. The feature is interpreted as a deep seated fault that assists magma to the surface. In the east-west cross-sections, the localization of seismicity between -1 km elevation and 1 km elevation could be reflecting stress concentrations in the Cretaceous-age basement. It is not clear if the seismicity on the fault proposed here is the same one suggested by Balesta et al. (1976-77) or another sub-parallel, related fault structure.

The presence of seismicity that extends very clearly from Bezymianny toward Kamen volcano is an intriguing result considering Kamen has had no historical eruptions. It has been active in the Holocene, though its dissected morphology suggests that it has been quiecent for some time. If the earthquakes are responding to magma movement, then it is possible that Bezymianny is using part of the same plumbing system that previously fed eruptions at Kamen Volcano.

There exists an intriguing earthquake-free zone directly underneath Bezymianny volcano in the higher resolution earthquake locations (Figure 2.22). Earthquake-free zones have been interpreted as indicating the presence of magma

below the surface [Weaver et al., 1983]. Fluid inclusions in the rims of plagioclases erupted from recent eruptions requires the presence of a small, shallow magma chamber [P. Izbekov, pers. comm., 2009]. The position of this earthquake-free zone also coincides with preliminary depths given by the fluid inclusions. The earthquake-free zone is highly speculative given the potential errors in the earthquake locations, and the relatively low number of earthquakes present in the analysis.

2.6.2 Seismological characteristics of volcanic phenomenon

The eruptive sequence between September 1 and December 1 contained several different types of observed phenomenon. By utilizing the differences in the September, October and November eruptions, insight into the relationship of seismicity to the processes that were present is possible. The number of rockfalls increased prior to the September and October eruptions. Rockfalls, when proven to be rate dependent, has been shown as a proxy for extrusion at Soufriere Hills Volcano, Montserrat [Calder et al., 2005]. There is no evidence for extrusion during the September eruption, however it is possible that the rockfalls could reflect increased deformation from endogenous dome growth or hydrothermal interaction. At Bezymianny, the dome within the crater has grown quite large over 50 years of extrusion (Figure 2.34). The dome is at or near the angle of repose over much of its surface and thus a minor steepening of the surface of the dome would result in increased rockfall. Rockfalls may also be formed through more dynamic processes such as degassing and extrusion of unstable flows or lobes. The rapid decrease in rockfalls after the eruption in September suggests that the deformation source was immediately removed as a result of the small plume that was observed [KBGS, 2007a]. There were no direct observations of the dome immediately prior to the

September or October eruption, thus it is not clear if the extrusion of a cold and progressively degrading plug was responsible for the observed patterns in rockfalls prior to the September and October eruptions, as described in other eruptions at Bezymianny by Belousov et al. [2007]. The more gradual decrease in rockfalls after the October eruption, suggests that the increased deformation of the dome continued after the eruption. The pressure that led to the increased deformation could have slowly bled off by the extrusion of lava after the eruption, or it could reflect endogenous growth of the dome.

The LFLDE signals were among the strongest signals during the study period. LFLDEs are a combination of tremor, and low-frequency events that immediately precede rockfalls. In the later case, a low frequency event occurs at the beginning of a rockfall signal, suggesting a coupled relationship (Figure 2.35). Such coupled events have been identified at Soufriere Hills, Montserrat where the long period portion was identified as violent gas escape from the dome that accompanied rockfall [Luckett et al., 2008]. Prior to the October eruption, the number, average amplitude and maximum frequency of LFLDEs increased dramatically. After the eruption, the number, average amplitude and maximum frequency decayed over the course of two weeks to background levels. This behavior suggests a rapid influx of gas into the dome, presumably from juvenile material making its way to the surface from depth. This is consistent with the observation of juvenile material in the pyroclastic flows of the October eruption. If the number or cumulative amplitudes of LFLDEs are used as a proxy for gas influx into the dome, then the October eruption included more gas than the September eruption, an observation supported by the relative heights of the observed eruption plumes.

The occurrence of multiplets, low-frequency and high-frequency events during the October eruption provided insight into the seismic signature of lava flow emplacement. The multiplets that were present after the October eruption had shorter durations, and fewer concurrent multiplets than eruptions in September and November. Peaks in the number of low-frequency and high-frequency events occurred several hours after the October eruption (Figure 2.36, Figure 2.37). In contrast, the September eruption, which had no lava flow, had a relatively high number of low-frequency earthquakes, but no obvious peaks. Similarly, the occurrence of high-frequency earthquakes was unchanged during the September eruption. Most striking was the increase in maximum frequency of low- and high-frequency events prior to the October eruption. The frequencies slowly decayed to background levels after the eruption. Since the October eruption had a lava flow and the September eruption did not, the higher frequency, higher amplitude low-frequency and high-frequency events are likely recording the ascent of magma. The peak in numbers of low- and high-frequency events after the initial explosive eruption in October 2007 may indicate the beginning of the flow on the surface as the volcanic system was opened. The slow decay in the numbers of events, average amplitude and maximum frequency is likely a reflection of the overpressure gradually declining. The durations and number of contemporary multiplets also increased slowly to values seen in September 2007. The timing and duration of the lava flow is speculative as no observations of the lava flow emplacement were made until days after the October 2007 eruption.

2.6.3 Conceptual Model

The patterns in the characteristics of multiplets outlined above, give insight into the multiplet source area. Multiplets imply a stable and repeatable source process over the time that they are active [Geller and Mueller, 1980]. Here I assume that earthquakes, multiplets or not, are happening at the edges of a conduit, or along cracks peripheral to the conduit (Figure 2.38). Between large eruptions (background periods), magma and the associated gases move relatively slowly through the conduit. Between eruptions, there is measurable SO_2 emitted from the dome [T. Lopez, pers. comm. 2008]. The presence of passive degassing between eruptions necessitates the convection of magma to low pressures within the magmatic conduit [Shinohara, 2008]. The resultant small and stable stress and pressure gradients generated by the escaping gases produces a relatively stable source region for the production of repeating earthquakes. This environment results in relatively long duration multiplets since large stresses are not reorienting or destroying sources. Many different source areas may be active at any one time if the geometry of the multiplet source area is dendritic and stresses or pressures are being diffused in a broad region. Member events of the multiplets will be small and of similar size. Prior to a large eruption, pressure builds in the conduit system, forcing a faster and more chaotic flow of magma, as more gas escapes into the outer conduit and surrounding crust. This pre-and syn-eruptive environment is more dynamic than background levels, and produces higher stress or pressure gradients. Conceptually, multiplet sequences will have shorter durations and there will be fewer contemporary multiplets, since the chaotic nature of the area around the pre-eruptive conduit will produce constantly changing volatile pathways. A reduction in the number of

contemporary multiplets may also occur, as the dynamic stresses are concentrated to a small area such as a constriction in a conduit. Such a concentration of stress or pressure may occur in an impermeable section of the conduit where volatiles cannot escape into the area surrounding the conduit. As the volatile pathways change, different cracks are favored for failure, and thus short duration multiplets occur only sporadically. Higher stress or pressure gradients during pre-eruptive periods will also generate larger earthquakes with sizes that reflect the chaotic nature of the forcing stress. The result is higher amplitude earthquakes with more variability.

2.6.4 Application of the Conceptual Model and Event Observations

If the conceptual model and observation of event types is applied to the September, October and November eruptions, something can be learned about the eruptive processes at Bezymianny during this time period. I treat the multiplets and occurrence of event types separately because the multiplets make up less than 30% of the overall seismicity during the study period. Since the multiplets are a low percentage of the overall seismicity, the patterns in event types may be caused by a different process than is responsible for the development of multiplets.

During the September eruption, there was no obvious change in the multiplet parameters. Only a minor amount of pre-eruptive seismicity was present in the form of high-frequency events, rockfall (Figure 2.25) and LFLDEs (Figure 2.26), and no deep post-eruption seismicity was present (Figure 2.16). The eruption had a small ash cloud (2 km high) and did not produce a pyroclastic flow [KBGS, 2007a]. Given its seismic characteristics and small size, it is clear that the eruption involved only the very shallowest part of the conduit and dome, evidently above any active multiplet

source area. The eruption was not strong enough to significantly alter the multiplet source area, since many multiplets continued unchanged through the eruption (Figure 2.32).

During the October eruption, all of the multiplet parameters changed significantly prior to and after the eruption. The multiplet amplitudes increased and had more variability. The durations and number of concurrent multiplets decreased significantly. No multiplet prior to the eruption was found after the eruption, suggesting an irreversible change in the multiplet source area during the explosive phase. Observations of the explosion itself reveal a 7 km high plume and a pyroclastic flow with juvenile material within it [KBGS, 2007b]. The eruption also had significant pre-eruptive seismicity outside the occurrence of multiplets. Low-frequency earthquakes, high-frequency earthquakes, rockfall and LFLDEs all increased prior to the eruption (Figure 2.36). With reference to the cumulative moment release, the rockfall and LFLDEs were particularly productive prior to the October eruption (Figure 2.37). Deep post-eruptive seismicity was also present (Figure 2.16). The evidence above leads to the conclusion that the October explosion and subsequent lava flow sourced a deeper part of the conduit than the September eruption, presumably deeper than the multiplet source area. This deep and energetic source affected the multiplet characteristics studied here, and permanently changed the region around the conduit, preventing any multiplet occurring prior to the explosion to reoccur after the explosion.

After the October explosion, there was a slow increase in the duration and number of concurrent multiplets, and a decrease in the amplitude and variability of

multiplets. The multiplet source area was returning to a background state similar to times in September and early October. This change in multiplet parameters coincided with high occurrences of low-frequency earthquakes, high-frequency earthquakes and LFLDEs. The cumulative amplitude release of low-frequency events and LFLDEs after the explosion in October is particularly high and gradually decays to background rates by the end of October. I interpret this slow return to background levels in multiplet parameters and moment release to decreasing flow within the conduit and a gradual return to a more stable environment within the conduit. The surface expression, if observed, would have been a slowing of the rate of extrusion of lava at the surface.

The November eruption did not obviously affect the multiplet characteristics and no individual multiplet was affected by the eruption. There was a lack of significant pre-eruptive seismicity, and no juvenile material was found in the eruptive deposit. No ash cloud was reported though there was a large thermal anomaly [KBGS, 2007c]. Local scientists interpret the November event as a dome collapse [P. Izbekov, pers. comm., 2008]. This interpretation is consistent with the unchanged patterns in multiplet characteristics if the dome collapse was strictly a shallow process and did not extend deeper into the conduit and multiplet source region or if the perturbation in the shallow conduit was not strong enough to disrupt this region.

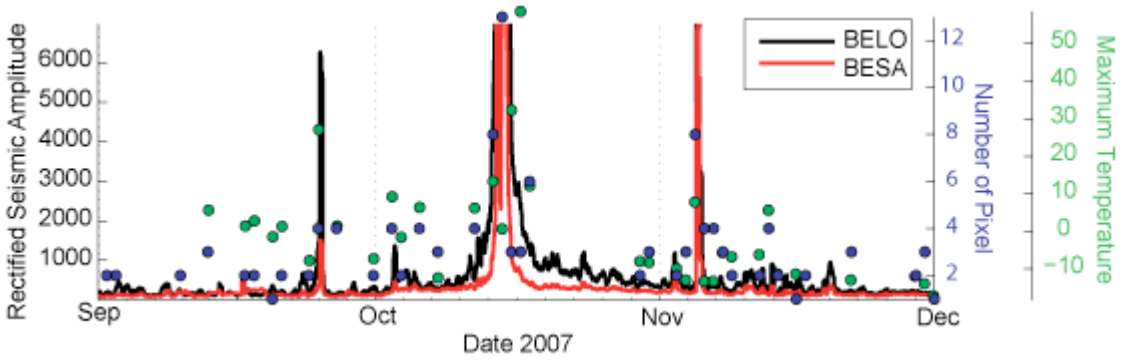

Figure 2.15: Eruption chronology between September 1, 2007 and December 1, 2007. The rectified seismic amplitude (counts) is shown as black and red lines for stations BELO and BESA, respectively. To convert to nm/s, multiply by 2.980235. Blue dots are the size (number of pixels) of the thermal anomaly on the dome of Bezymianny and green dots are the maximum temperature of the anomaly. Thermal information is from the AVHRR platform on the NOAA 17 and NOAA 18 satellites. Each pixel is 1 km across.

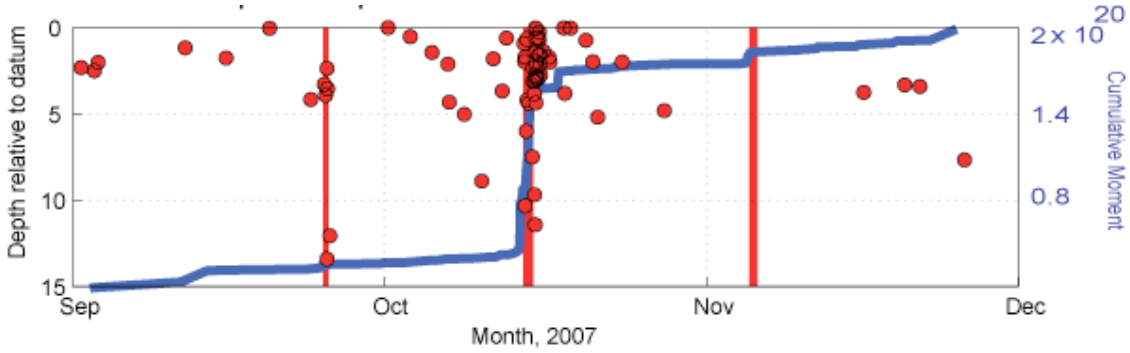

Figure 2.16: Earthquake depths and cumulative moment release between September 1, 2007 and December 1, 2007. Red dots are earthquake depths from the KBGS earthquake catalog. The blue line is the cumulative moment release, calculated from the magnitude of the earthquakes plotted. The moment release during the October eruption is approximately equivalent to a magnitude 2.4 earthquake. The other eruptions have a negligible moment release compared to the October eruption.

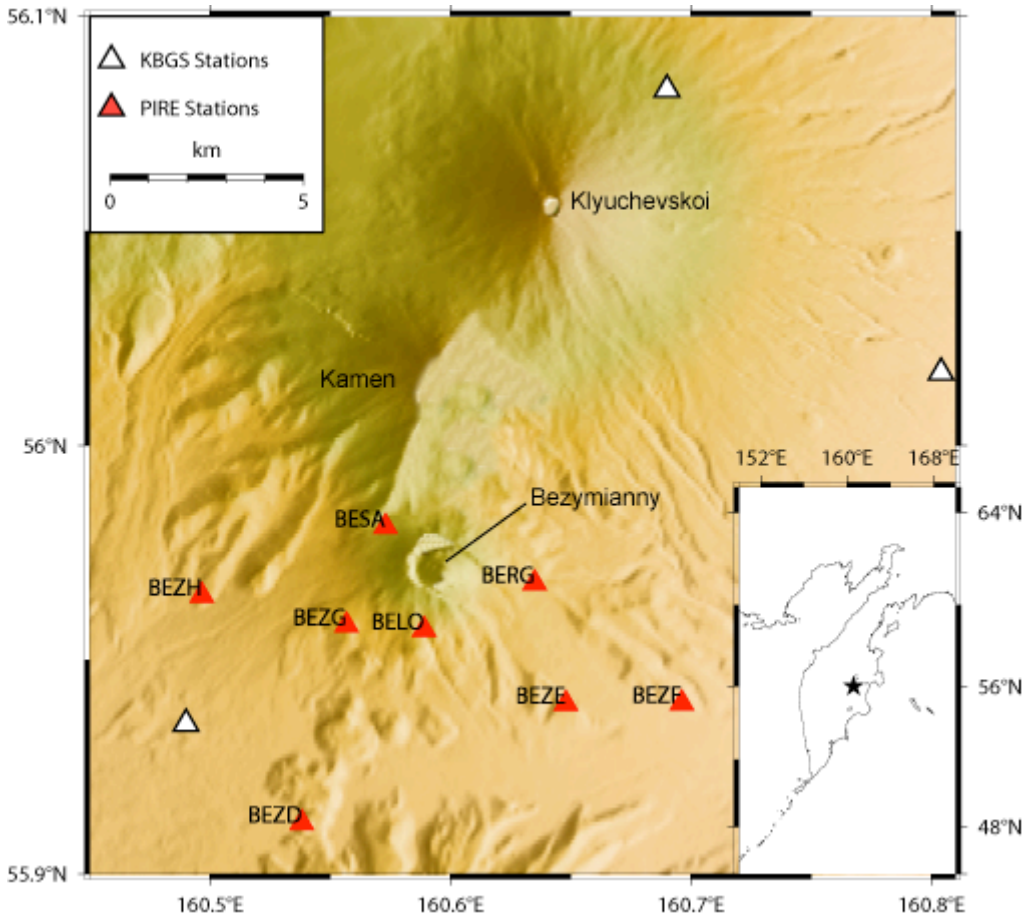

Figure 2.17: Seismometer network map at Bezymianny Volcano. Labels without triangles are volcanic edifices in the immediate area. Other stations in the KBGS network exist outside the map limits, providing good azimuthal coverage for larger events. Inset map: Regional map of Kamchatka, Russia. Bezymianny volcano is shown with a black star.

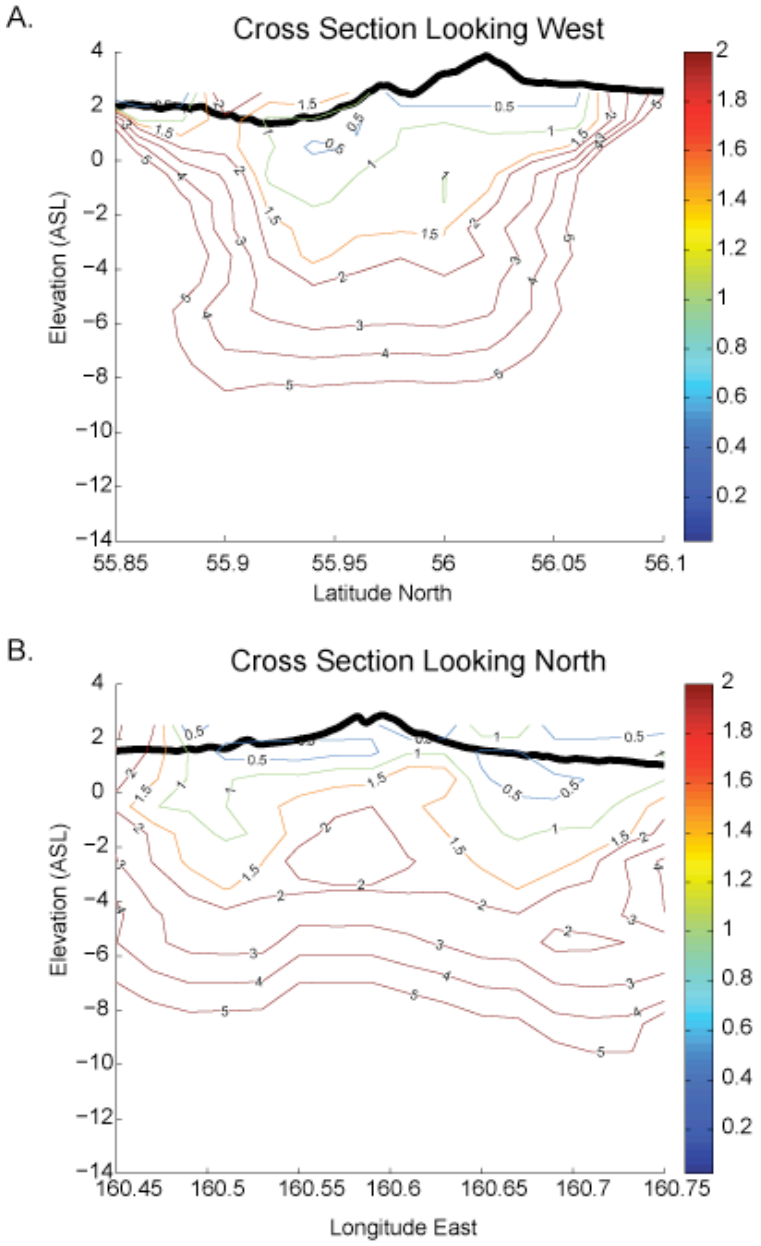

Figure 2.18: Results of sensitivity tests of PIRE network. The distance in kilometers between the original synthetic earthquake location (grid point) and the relocated earthquake location is contoured on the plots above. Contours above 5 km are not shown. The dark black line is the elevation profile along the cross-section. The summit of Bezymianny is approximately 2.5 km high. A. Cross section of location errors looking West. Bezymianny is located at 55.97 degrees latitude. The highest point in the cross-section is the summit of Kamen Volcano. B. Cross-section looking north.

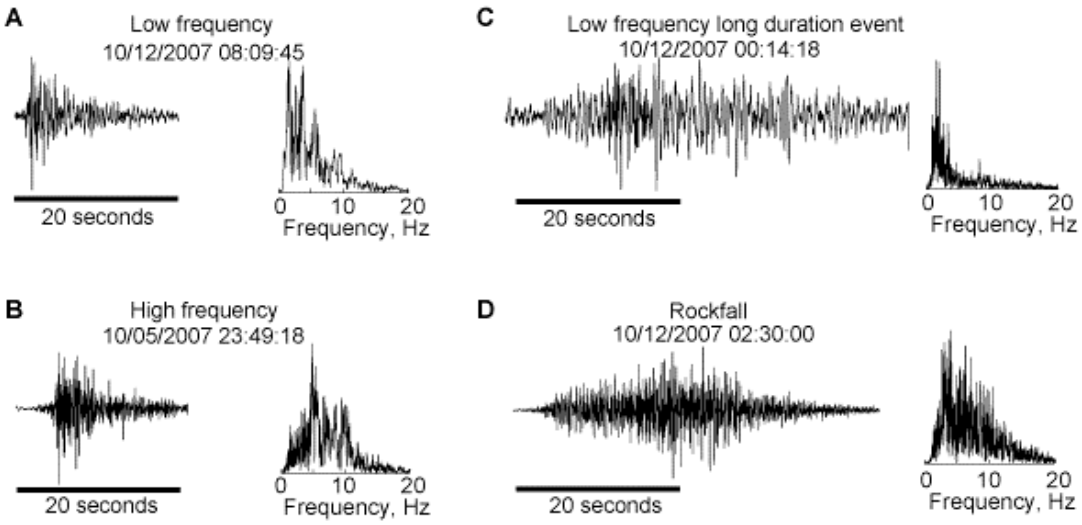

Figure 2.19: Waveform definitions used for ratio analysis at Bezymianny Volcano. For each pane, the waveform is shown on the left and the power spectrum is shown on the right. All waveforms have been filtered between 1 and 20 Hz.

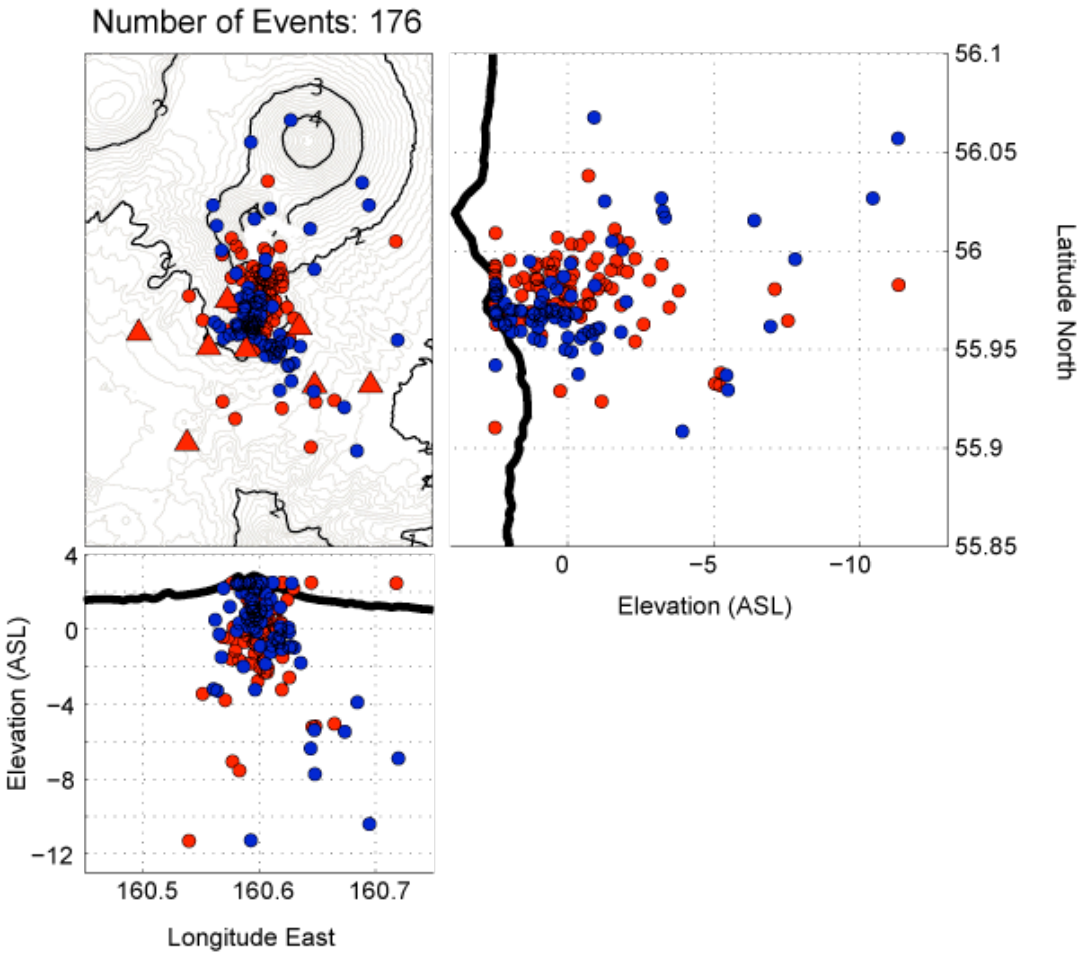

Figure 2.20: Absolute earthquake locations from Bezymianny Volcano. Upper Left: Map view of absolute earthquake locations of KBGS catalog locations with added PIRE picks (red circles), and earthquake locations using only the PIRE network (blue circles). Elevation contours are from the digital elevation map in Figure 2.17. Dark contours are at 1 km intervals, and labels are in kilometers. Lower Left: East-West cross section of earthquake locations. Dark line is elevation profile along cross-sectional line. Upper Right: North-South cross section. Cross-sectional views are constructed as if folding up the edges of a three-dimensional cube. No vertical exaggeration in either cross-section.

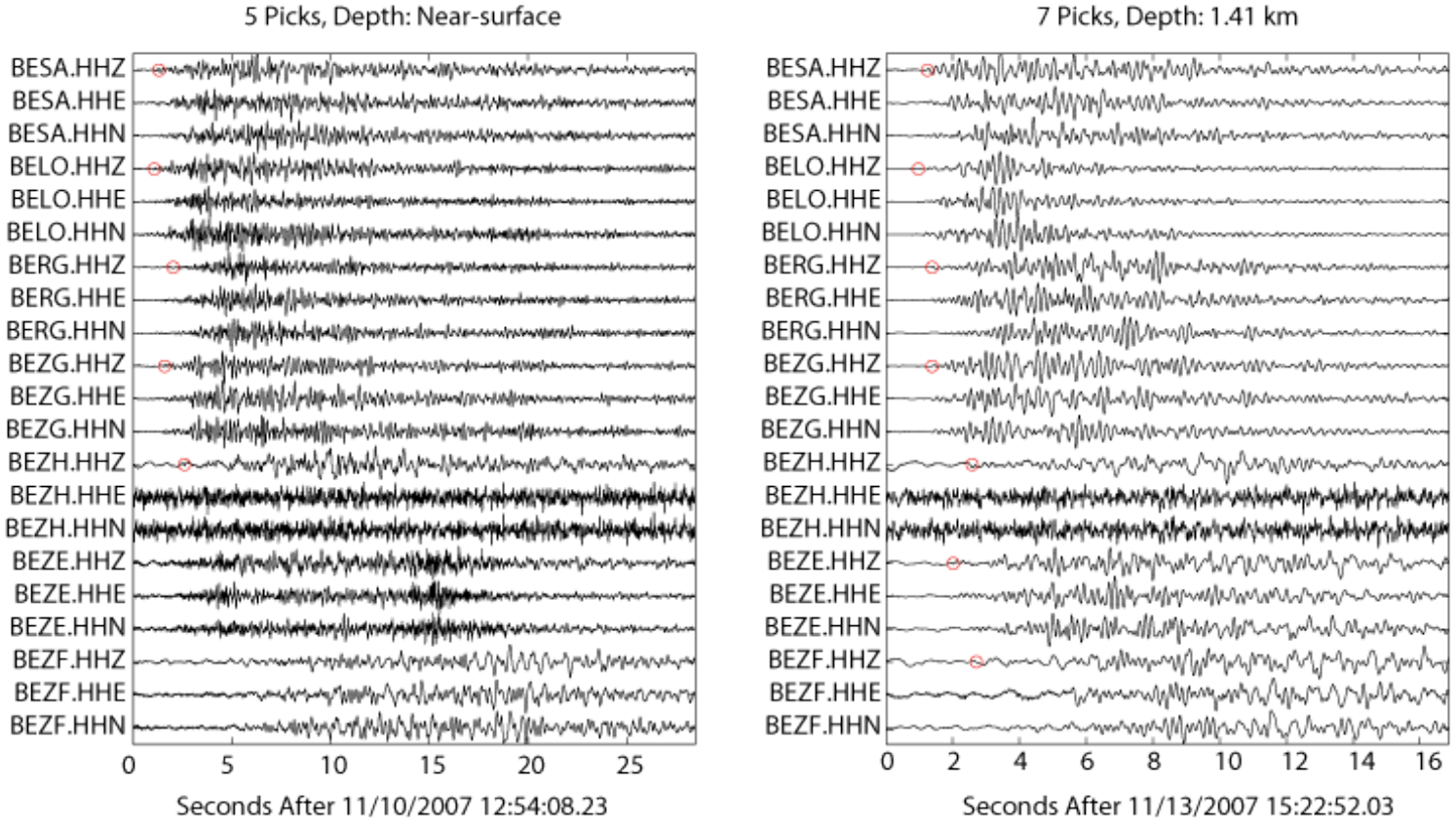

Figure 2.21: Representative record sections on PIRE stations. Records have been filtered between 1 and 20 Hz. Channel names are shown on the y-axis of each plot. Station locations can be found in Figure 2.17. Phase picks are shown with red circles. S-waves were generally not recognizable.

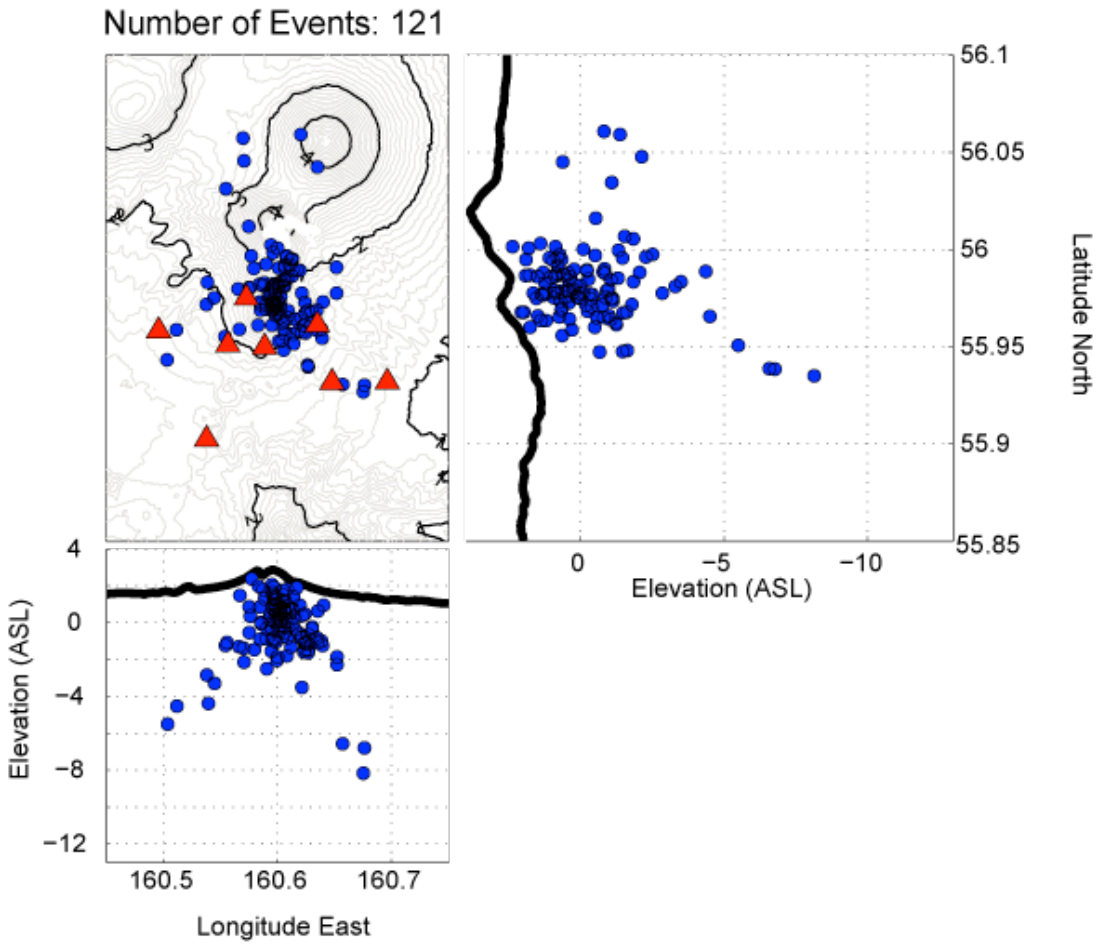

Figure 2.22: Earthquake locations at Bezymianny using differential travel times. Symbols and axes are the same as Figure 2.20.

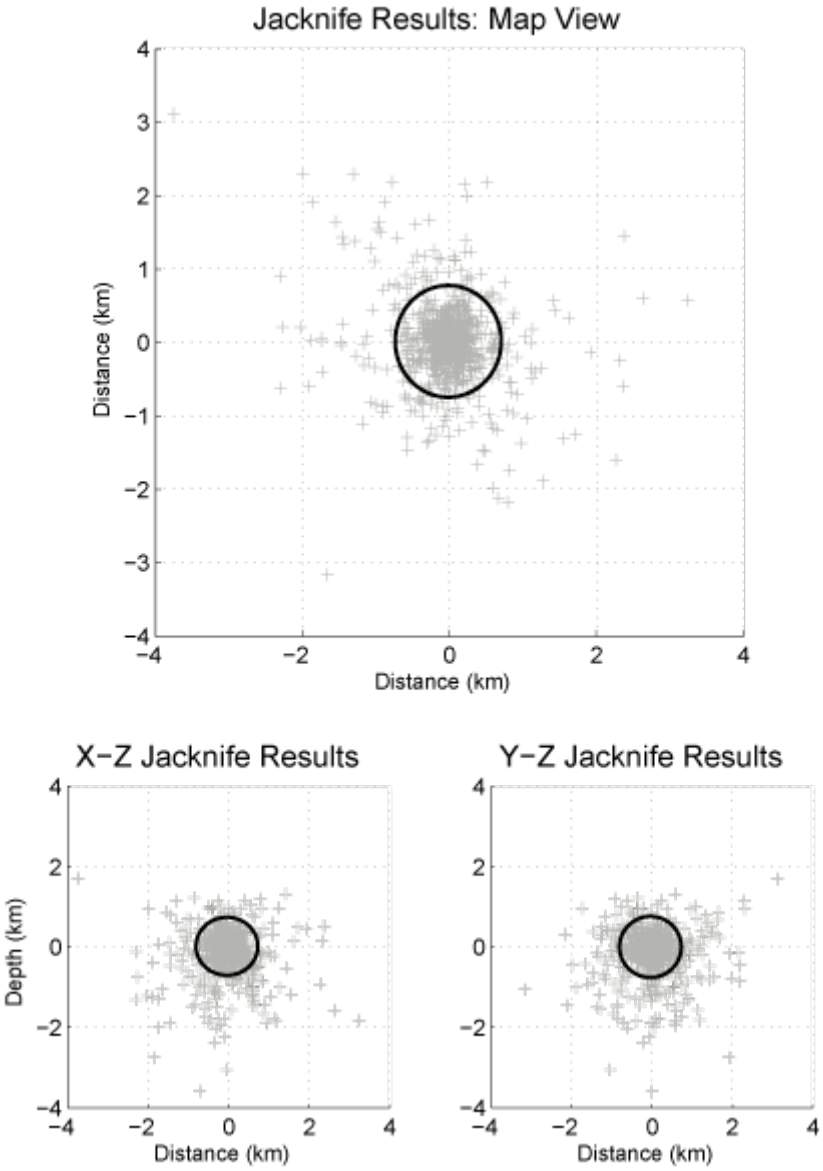

Figure 2.23: Results of jackknife analysis of earthquake locations calculated with differential times. Each gray cross represents the difference between the original earthquake location calculated with all of the stations and the earthquake location calculated without a single station. The black ellipse in each plot encompass 95% of the data points for a given projection.

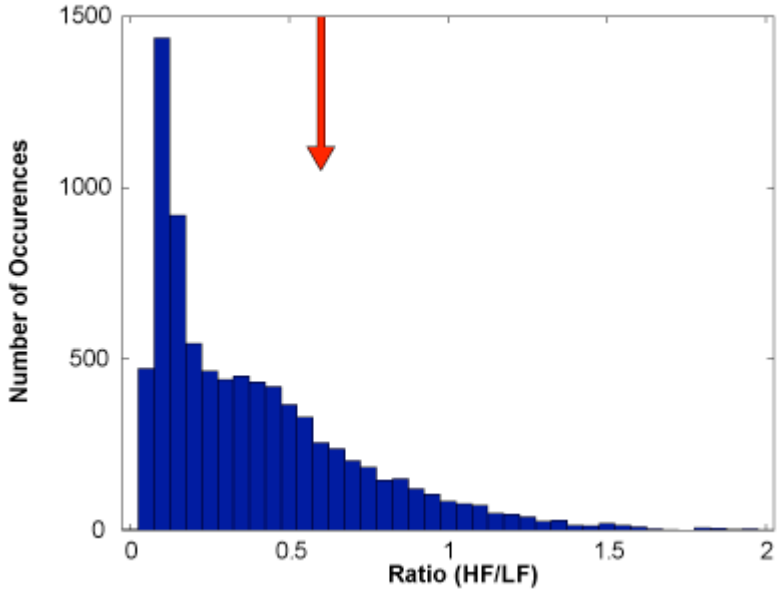

Figure 2.24: Histogram of average ratios from all analyzed events. Bins are centered at 0.05 intervals. The red arrow shows the division between “low-frequency” and “high-frequency” events.

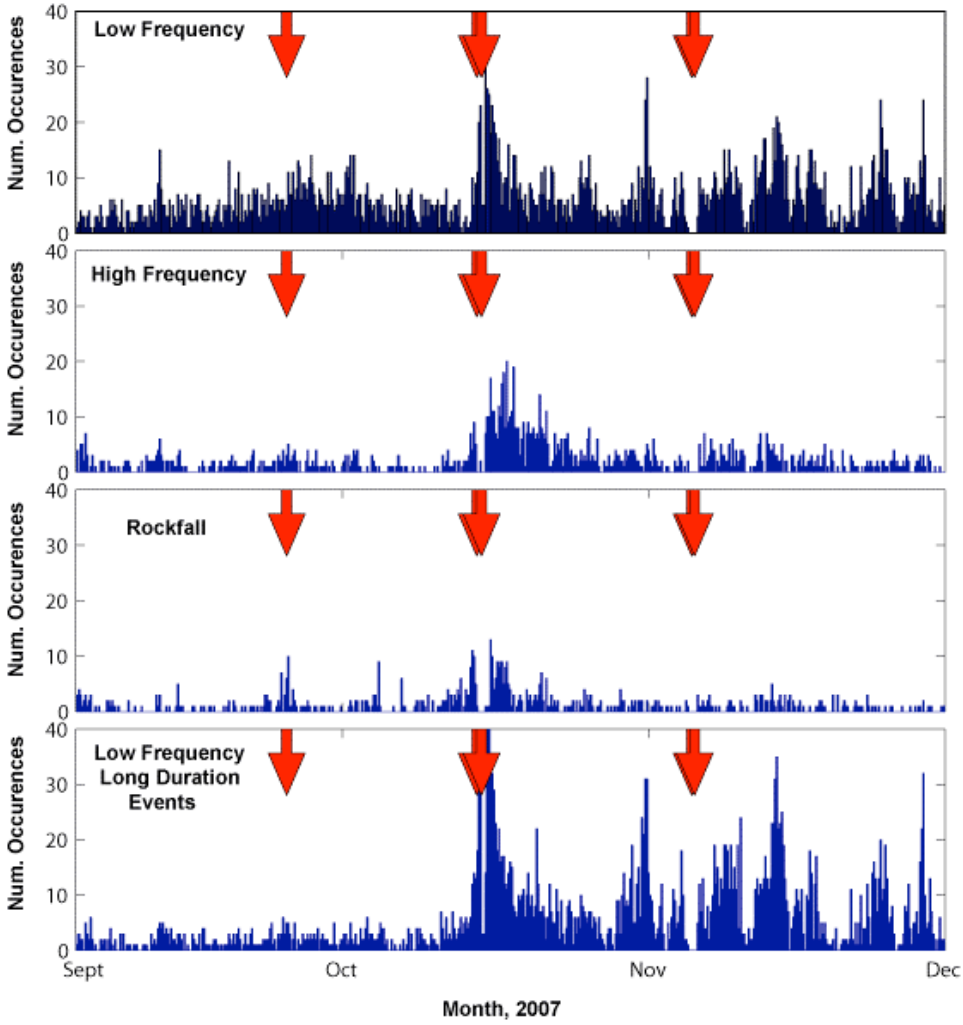

Figure 2.25: Event occurrence with time at Bezymianny Volcano. Blue bars represent the occurrence of a given event type calculated every 4 hours. Red arrows are explosion times. Gaps in the occurrence of all event types after eruptions reflects continuous tremor, which is not tabulated as part of this study.

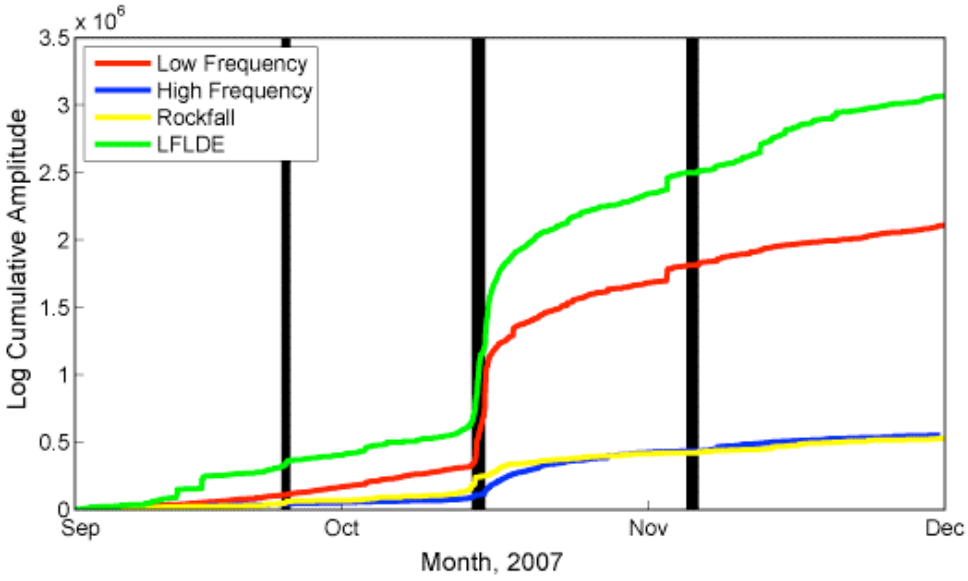

Figure 2.26: Cumulative amplitude release of event types at Bezymianny Volcano. Black lines are eruption times.

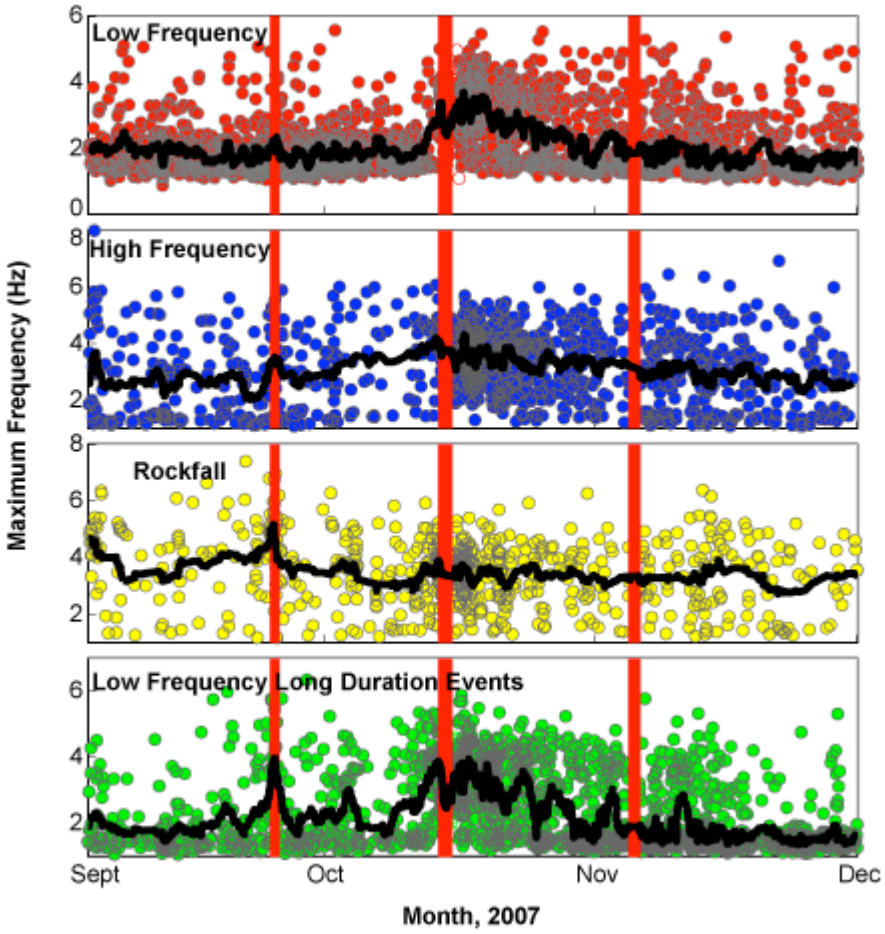

Figure 2.27: Maximum frequency of classified events with time, Bezymianny Volcano. Each event is shown as a colored circle in its respective category. The black line is a 10-event running average. Red lines are eruptions.

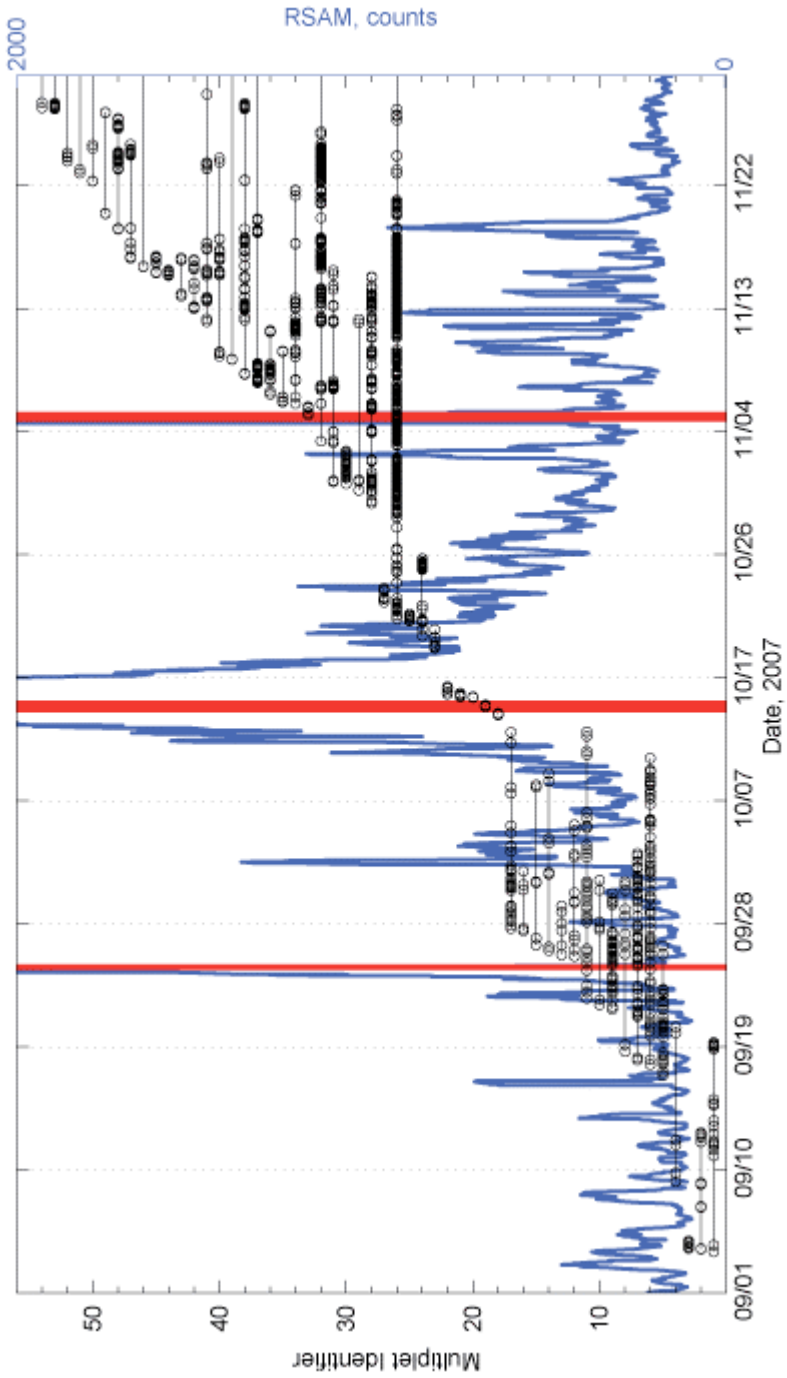

Figure 2.28: Multiplet timeline from September 1, 2007 to December 1, 2007. Each black dot is an earthquake; black dots that lie on the same line are part of the same multiplet. The blue line is the rectified seismic amplitude on station BELO. Vertical red lines are confirmed eruptions. Only multiplets with 5 or more events are included.

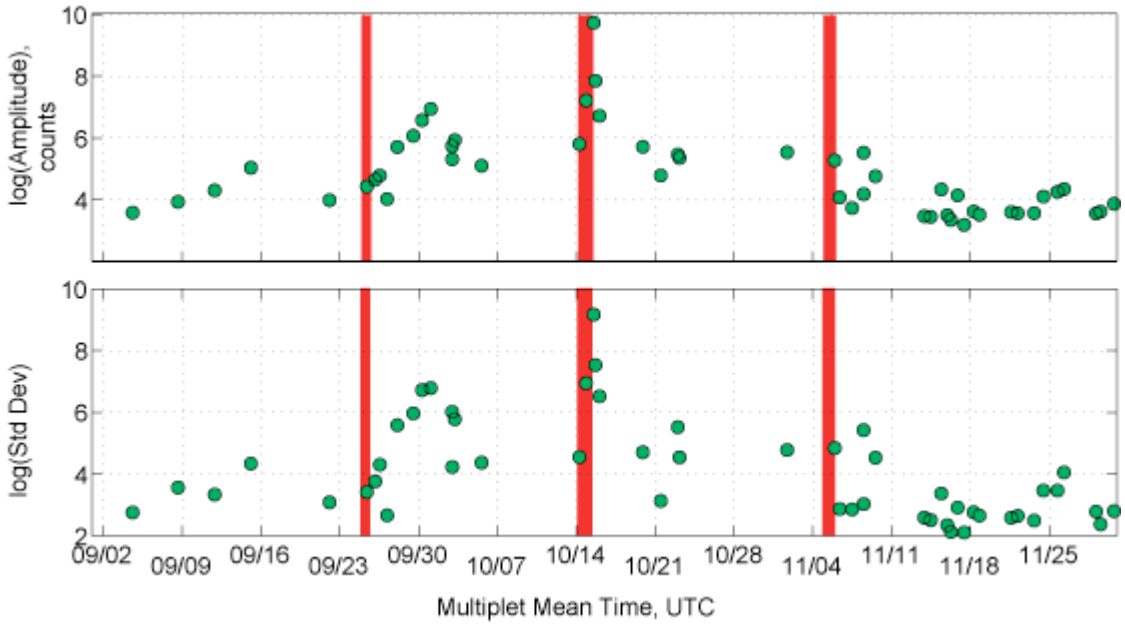

Figure 2.29: Average amplitude and standard deviation around the average amplitude of multiplets. Each green dot represents one multiplet in Figure 2.28. Each multiplet is plotted at its mean time, or the time halfway between the first and the last event. Red lines are eruptions. The average amplitude is calculated using the mean of the maximum amplitude of each event that makes up the multiplet. The standard deviation is the standard deviation of the maximum amplitudes within a multiplet.

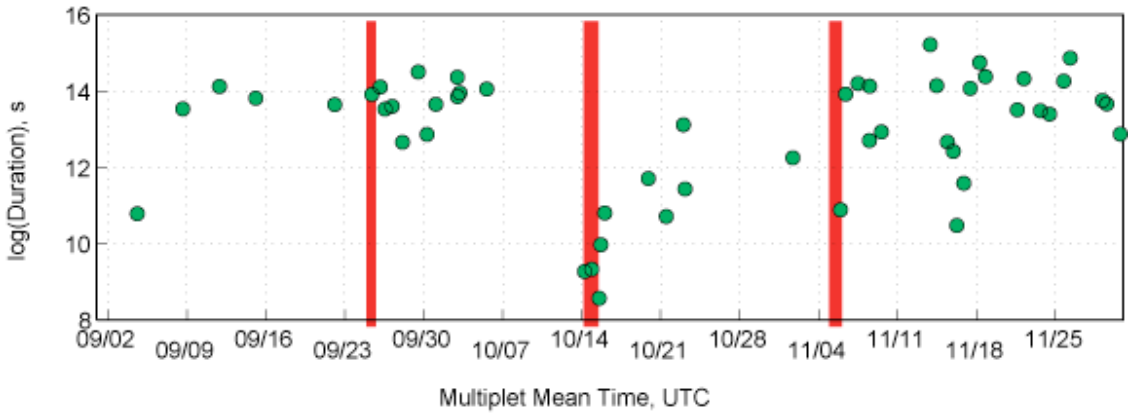

Figure 2.30: Duration of multiplets at Bezymianny Volcano. Each green dot is the duration a multiplets plotted in Figure 2.28. The duration is the time, in seconds between the first and last event in a given multiplet. As in Figure 2.29, each multiplet is plotted with its mean time. Red lines are eruptions.

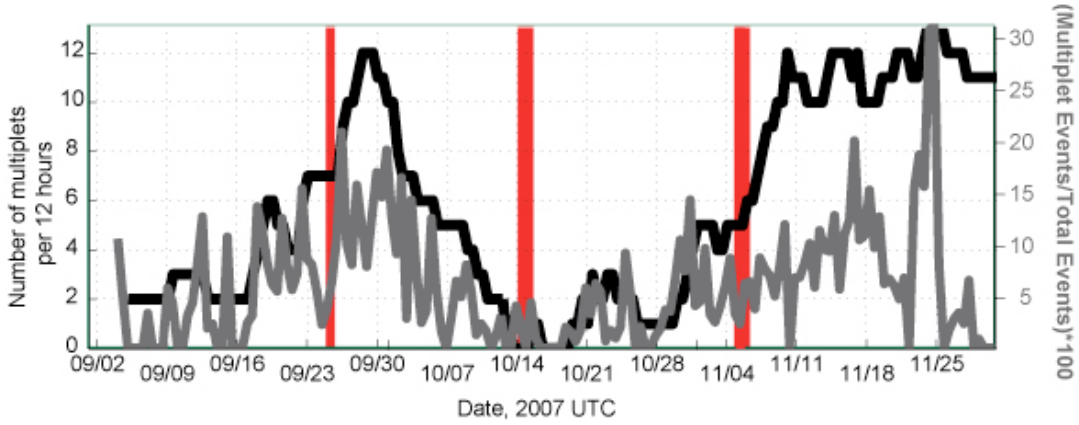

Figure 2.31: Number of contemporary multiplets at Bezymianny Volcano. The black line is the number of concurrent multiplets calculated every 12 hours. The gray line is the proportion of total seismicity that consists of multiplets. The proportion is calculated 12 hours. The left y-axis refers to the number of contemporary multiplets. Red lines are eruptions.

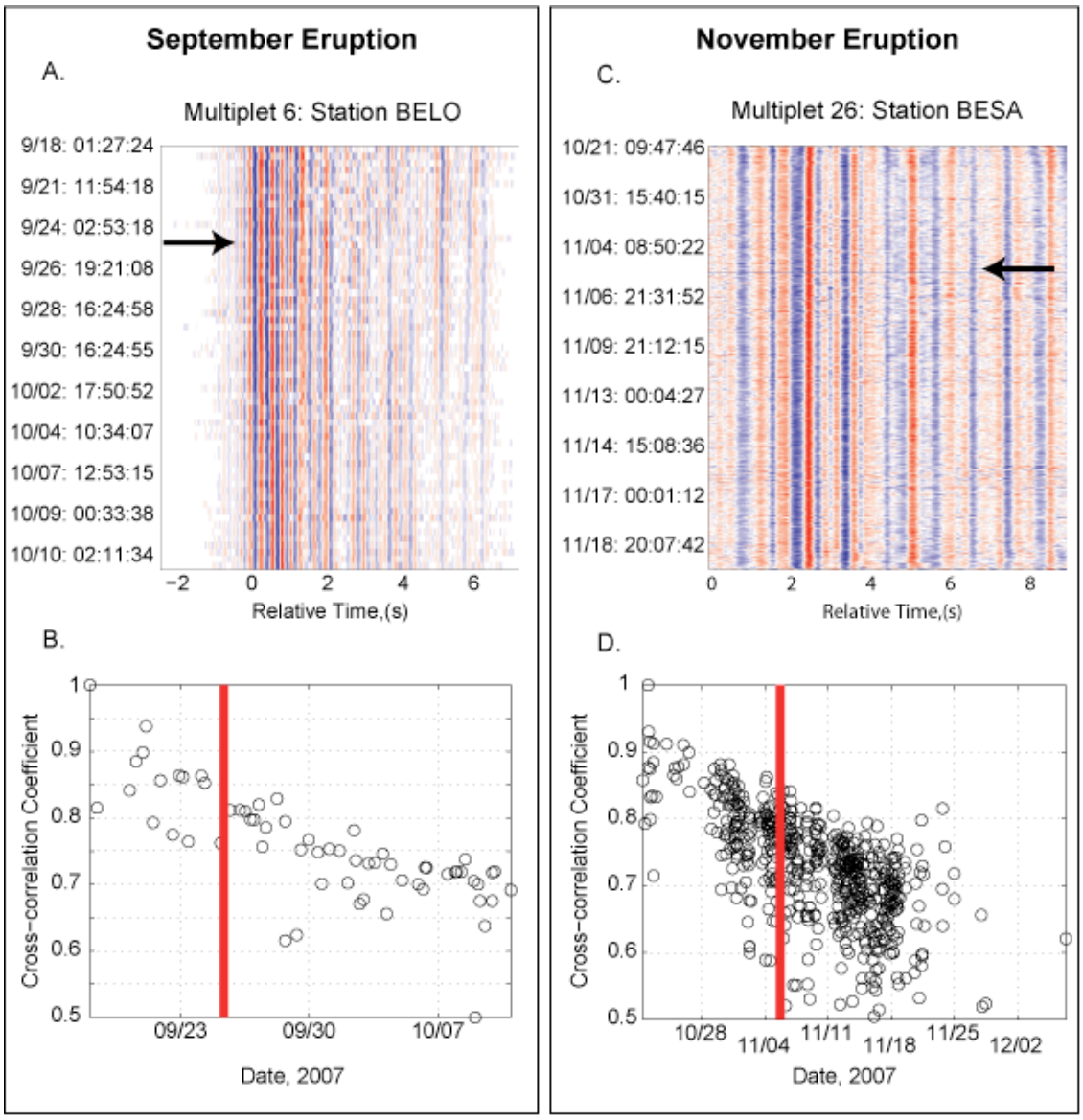

Figure 2.32: Multiplet behavior during September and November eruptions. A.) Record section of events from multiplet 6 (Figure 2.28) recorded on station BELO. The multiplet consists of 62 events. Times on the right are absolute start time of the record. The black arrow shows the approximate time of the eruption. B.) Cross-correlation coefficient of the first event in multiplet 6 to every other event with time. Red line represents the time of the September eruption. C.) Record section of events from multiplet 26 on station BESA. The multiplet contains 562 events. Labels and arrows are same as A. D.) Cross-correlation coefficient of third event in multiplet 26 compared with all other events on station BESA.

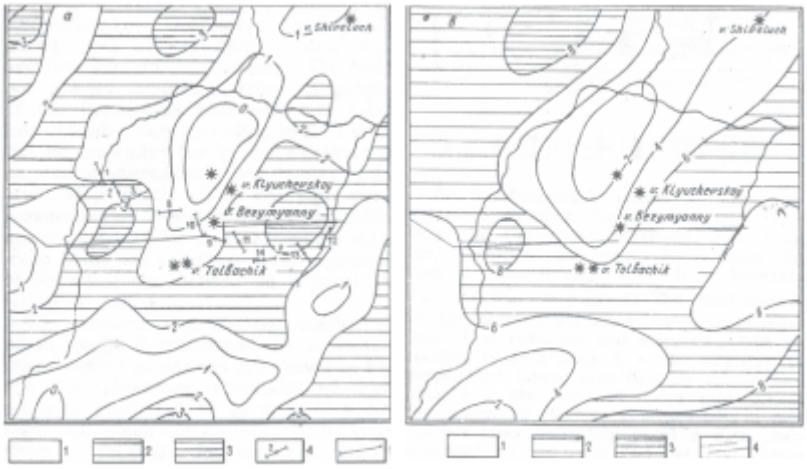

Figure 2.33: Topography of basement material under Bezymianny Volcano, Russia. Left: Depth to Cretaceous basement. 1: From 0 to 2 km; 2: from 2 to 3 km; 3: more than 3 km; 4: directions of maxima of impedance diagrams from magnetotelluric data; 5: deep seismic sounding profiles. Right: Depth to Crystalline basement. 1: Less than 6 km; 2: from 6 to 8 km; 3: more than 8 km; 4: deep seismic sounding profiles. Figure from Balesta, 1976.

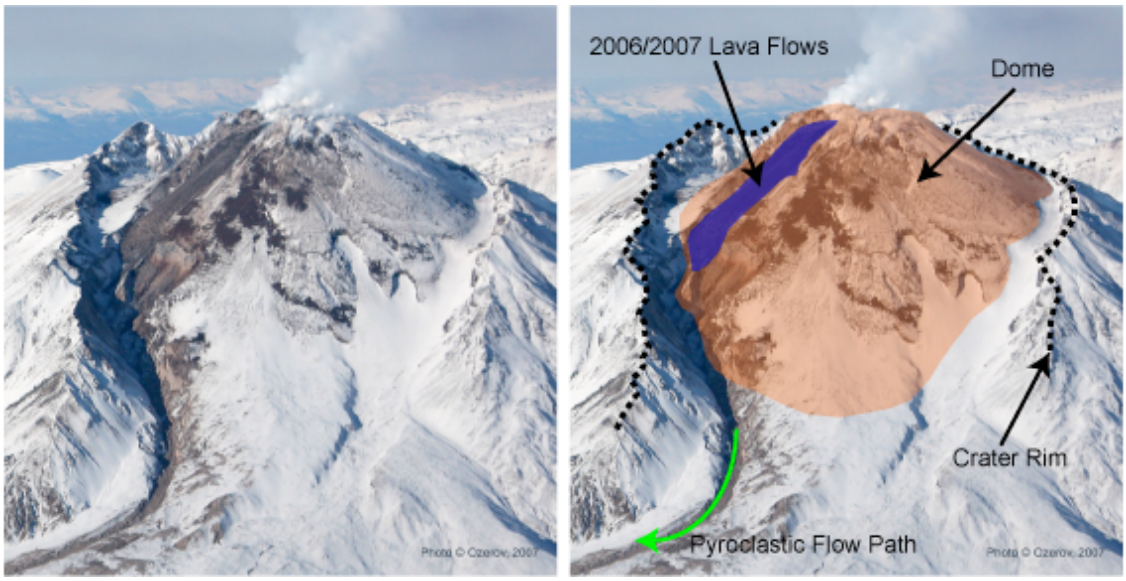

Figure 2.34: Dome morphology of Bezymianny Volcano. Photo is the same on the left and right except for annotations. Photo was taken on November 8, 2007. The summit of the dome (orange) is higher than any point on the rim (dotted line). Photo courtesy of Alexi Ozerov.

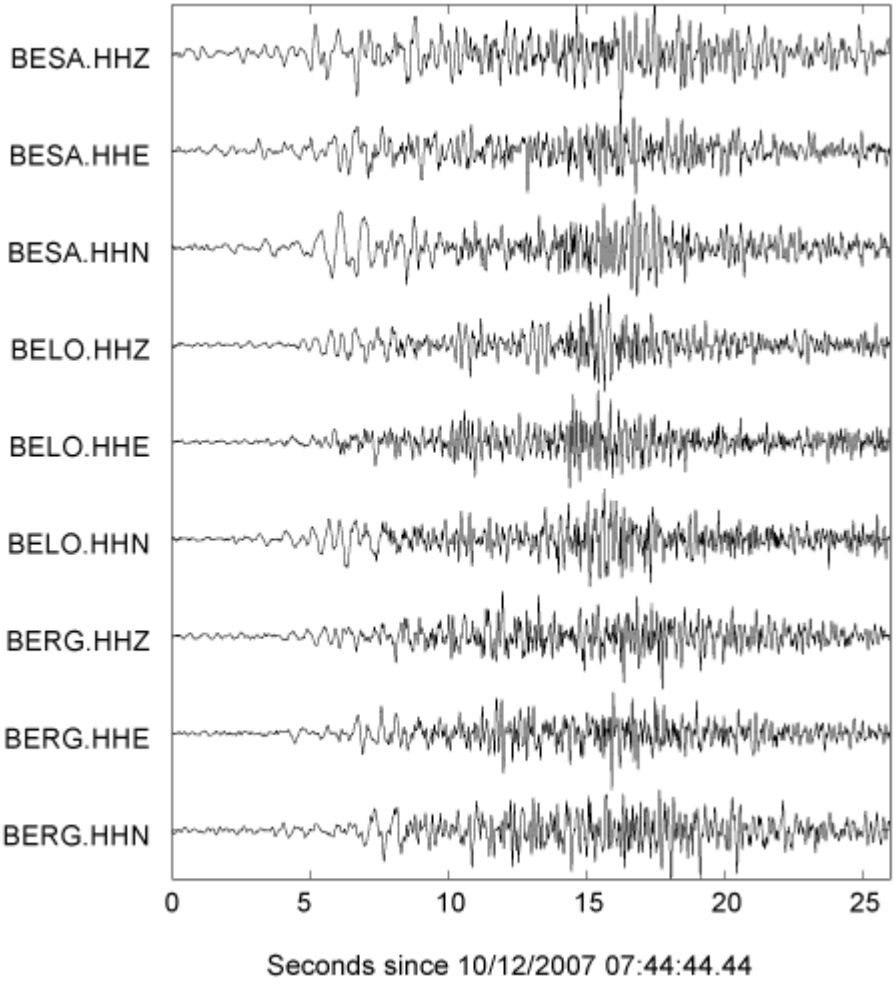

Figure 2.35: Record section of example LFLDE. Channel names are on the y-axis. The signal begins with a low frequency signal which is particularly strong on the horizontal channels. The signal is then dominated by a higher frequency and high amplitude signal, that is interpreted by analogy to Mount St. Helens as a rockfall.

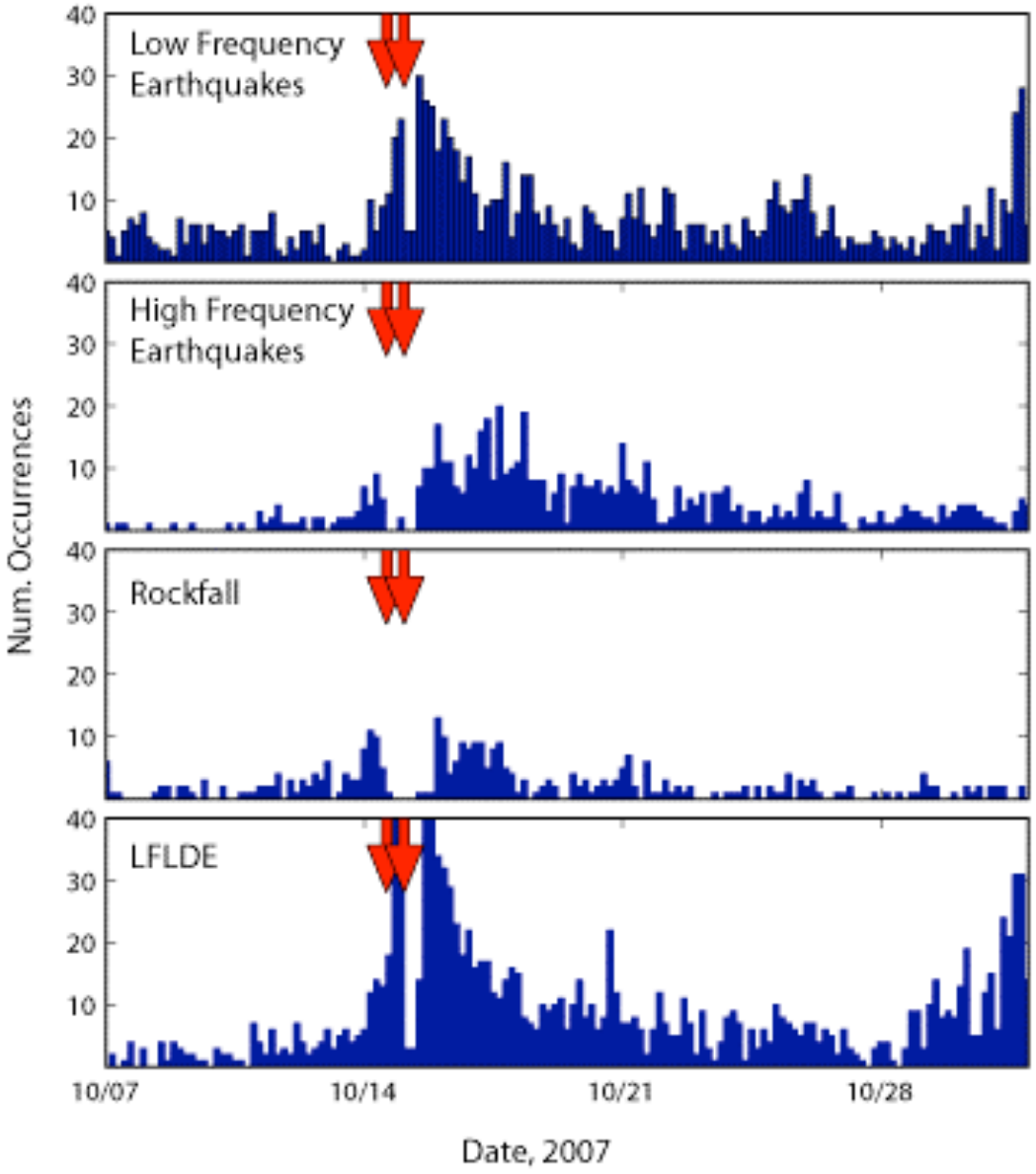

Figure 2.36: Close up of event occurrence during the October 2007 eruption. See Figure 2.25 for specifics of plots. Blue bars represent the occurrence of a given event type calculated every 4 hours. Red arrows are explosion times. Gaps in the occurrence of all event types after eruptions reflects continuous tremor, which is not tabulated as part of this study.

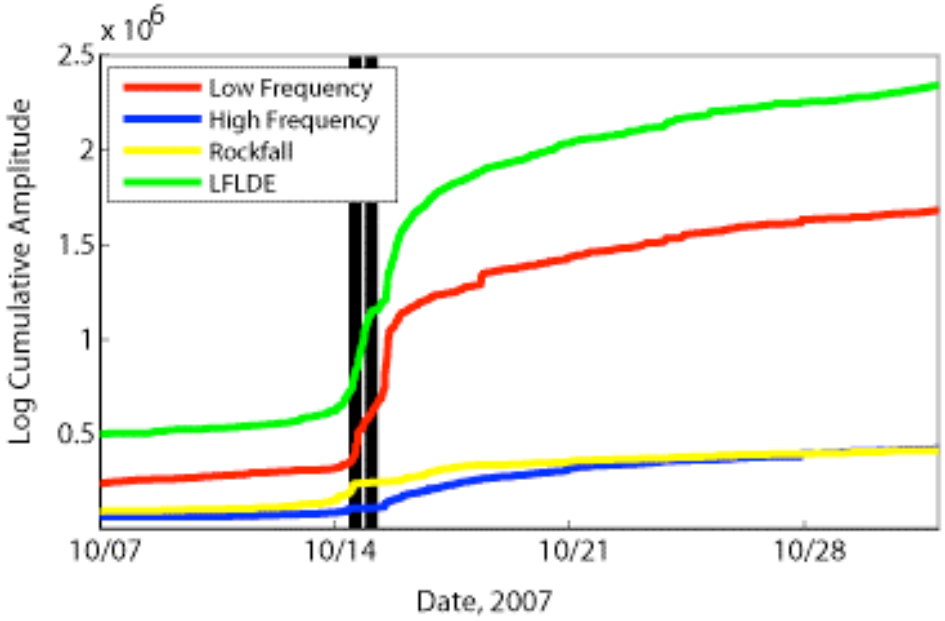

Figure 2.37: Close up of cumulative maximum amplitude. Black lines are eruptions.

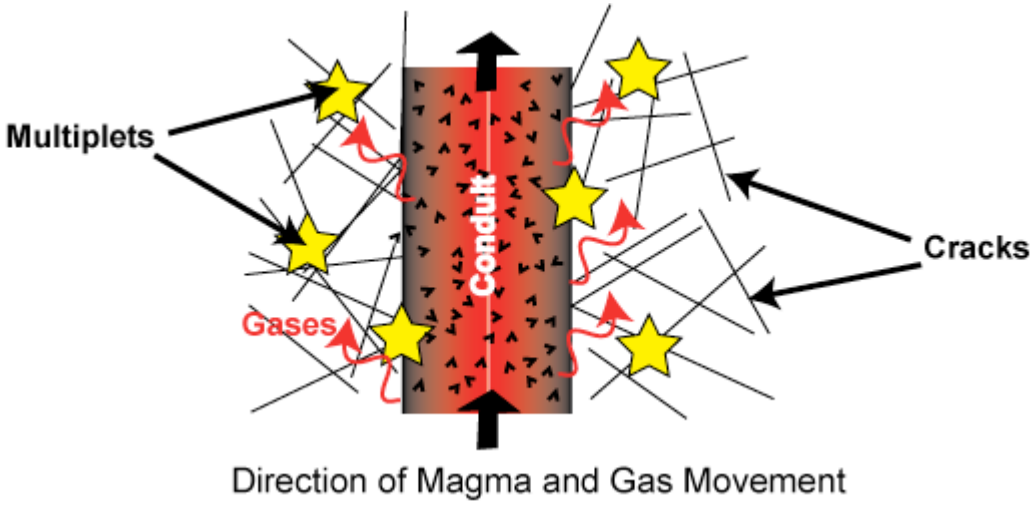

Figure 2.38: Conceptual model of multiplets at Bezymianny. Multiplet source area is represented by yellow stars. Cracks are thin black lines. Gases, shown conceptually, escape through the conduit walls. The direction of gas and magma movement is shown with the thick black arrows.

Table 2.1: Velocity model used in earthquake location analysis. The datum (zero depth) is at 2.5 km elevation.

Depth (km)	P-wave Velocity (km/s)
0.0	2.95
2.5	3.2
4.5	4.3
6.5	6.1
11.5	6.3
21.0	6.8
31.0	7.7

Table 2.2: Parameters for classification of events at Bezymianny Volcano.

Classification	Frequency Ratio (High / Low)	Duration (s)
Low-Frequency	<= 0.6	< 25
High-Frequency	> 0.6	< 25
Rockfall	> 0.6	> 25
Low Frequency Long Duration Events	<= 0.6	> 25

Table 2.3: Table summarizing observations of ratio analysis at Bezymianny volcano. A "#" sign means number, "Amp." stands for amplitude, "Cum." stands for cumulative, "n/c" stands for no change and "AMF" refers to the average maximum frequency.

	Eruption				
	Sept. 25, 2007		**Oct. 14, 2007**		**Nov. 5, 2007**
Observation	**Pre-eruption**	**Post-eruption**	**Pre-eruption**	**Post-eruption**	
# of Low Frequency	n/c	Minor peak 2 days after eruption, slow decay	Up, 12 hours prior	Peak 12 hours after eruption, slow decay	contaminated
# of High Frequency	n/c	n/c	Up, 24 hours prior	Peak 3 days after eruption, slow decay	Minor increase after eruption
# of Rockfall	Up, 14 hours prior, peak at eruption	Rapid decrease	Up 4 days prior	4 day decrease to background	n/c
# of LFLDE	n/c	n/c	Up 3.5 days prior	Peak at eruption, slow decay after eruption	contaminated
Cumulative Amp. Low Frequency	n/c	n/c	Broad increase starting Oct.1, rapid increase 1+ days prior	Rapid decrease 2 days after eruption, broad decrease until Nov. 1	contaminated
Cumulative Amp. High Frequency	Minor increase	n/c	Broad increase starting Oct.1, rapid increase with eruption	Rapid decrease after eruption, slow decrease until Nov. 1	n/c

Table 2.3 continued

Cumulative Amp. Rockfall	Small increase	n/c	Increase 3 days prior	Decrease to background 4 days after	n/c
Cumulative Amp. LFLDE	Small increase	n/c	Increase 2.5 days prior	Rapid decrease after eruption, slow decrease until Nov. 1	contaminated
AMF Low Frequency	n/c	n/c	Increase 2 days prior	Peak 4 days after eruption, slow decay to background by Nov. 1	contaminated
AMF High Frequency	n/c	n/c	Broad increase	Broad decrease	n/c
AMF Rockfall	Abrupt increase w/ eruption	Abrupt decrease w/ end of eruption	Slow decrease?	n/c	n/c
AMF LFLDE	Abrupt increase w/ eruption	Abrupt decrease w/ end of eruption	Small increase 6 days prior, larger increase 3 days prior	Slow decrease after eruption to Nov. 1	contaminated

III. Seismic Characteristics at Mount St. Helens, Washington

Mount St. Helens is one of the most heavily studied volcanoes in the world. It possesses one of the densest seismic networks of any volcano in the United States. Thus the history between 1980 and 2000 is well documented in the peer-reviewed record. The most recent eruption between 2004 and 2008 now has a large volume of published papers dealing with many aspects of this eruption [Sherrod et al., 2008]. One paper, Thelen et al. (2008) , describe in detail the absolute locations and relative locations of a subset of earthquakes between September 23, 2004 and November 30, 2004. Additionally, Thelen et al. (2008) describes the occurrence and behavior of multiplets during the same time period. This paper is included in its final form as Appendix A of this dissertation. Additional analysis and results in this chapter either supplement the analysis and results in Appendix A, or are completed to aid in the comparison of Mount St. Helens and Bezymianny Volcano.

3.1 Multiplets during the 1980-1986 eruption at Mount St. Helens

The 1980-1986 eruption at Mount St. Helens provides an excellent opportunity to search for the occurrence of multiplets during many different types of activity, from cryptodome emplacement, to explosive activity, to discrete dome forming activity. The occurrence of multiplets in a volcanic environment was first published at Mount St. Helens by Malone and Fremont [1987] . These authors studied in detail multiplets occurring during eruptions in 1983 and 1984, and commented on their increased occurrence as the discrete dome building phase continued.

3.1.2 Methods

Prior to 2000, little continuous seismic data was stored for Mount St. Helens due to limitations in disk size and cost. Thus, the 1980-1987 record of seismicity is made up of larger events automatically triggered and located by the PNSN. Clearly, the dataset is not a comprehensive record of seismicity between 1980 and 1987. However it is complete enough to look for the relative abundance of multiplets in a variety of volcanic stages. In this study, I used all of the triggered events at Mount St. Helens between 1980 and 1987. This included both located events along with events that did not have enough phase picks to be located.

Event start times were based on one of three criteria in descending order of preference:

1) The mean P-wave arrival time of stations selected in the analysis (e.g. SHW, HSR, JUN).
2) If there were no manual picks, an automatic sta/lta picker was used to generate a pick.
3) If no sta/lta pick was generated because of an emergent arrival, a pick was assigned at 2 seconds prior to the maximum amplitude.

Each station selected for the analysis was then cut at 1 second prior to the pick time and 7 seconds after the pick time and cross-correlated against every other event during the given year.

Multiplets were selected based on the same criteria as the multiplet search at Bezymianny Volcano in Section 2.2.2.2. As at Bezymianny, the cross-correlation threshold was set to 0.7 and the event had to be similar at the cross-correlation

threshold on two stations. Each year was considered independently. It is important to note that by considering a year at a time, this analysis will pick up additional multiplets compared to the Bezymianny multiplet analysis. In the Bezymianny analysis, I considered only a day at a time when cross-correlating, and removed events families with fewer than 2 events in a given day (orphans). Since I consider an entire year when cross-correlating in this analysis, single events within a multiplet may occur over the several months without any two events occurring on the same day.

While some stations are consistent across years, the seismic network at Mount St. Helens was rapidly changing, and in most cases, the station configuration between years was different. Stations were selected based on their proximity to the volcano and consistent data quality. The stations used for each year of the analysis are shown in Figure 3.39 and Table 3.4.

3.1.3 1980-1986 Multiplet Results

Multiplets were widespread throughout the eruptions from 1980 to 1986 (Figure 3.40). In 1980, there was weak development of multiplets, particularly with respect to the number of events that were in the catalog. Prior to the May 18 eruption, all multiplets had less than 20 events and an event rate of 1-2 events per day or less. The initial emplacement of the crytodome was accompanied by increased seismicity, however the existing seismic network immediately around the volcano was off-scale for most events. An additional search for multiplets using a close station set (SHW, LMW, LVP, MTM, RAN, BFW, COW) appropriate for the initial buildup of the eruption did not reveal any additional multiplets during that period

of time. Many of the closest stations soon became clipped and thus a different station set is used to search for multiplets during all of 1980. Most of the multiplets during 1980 occurred after the May 18 eruption in the form of deep high-frequency earthquakes. Few multiplets occurred through the smaller explosive eruptions in the remainder of 1980.

Multiplets between 1982 and 1987 were numerous, however not every eruption was preceded by multiplets. The March 19, 1982 eruption was the first event that clearly showed precursory multiplet activity. Interestingly, the multiplets were not as vigorous after the eruption. In 1983, continuous dome building occurred for almost a year; however multiplets only occurred during a period of increased seismicity between March and July, 1983. Eruptions in 1985 and 1986 showed much more organized multiplet development. Multiplets were generally confined to periods around eruptions when earthquake rates were high, and vigorous multiplets generally do not continue between eruptions.

3.1.4. Discussion of 1980-1986 Multiplets

It is difficult to gauge how complete the triggered record is from 1980 to 1987. The catalog is more complete when the activity is low and only a few events are occurring per day. When activity is significantly higher, the catalog completeness degrades. Many small events were intentionally left out by PNSN analysts because they did not record on a significant number of stations, or had emergent arrivals. While the catalog is not complete, the catalog is probably representative of the seismicity between the 1980 and 1986 eruptions when interpreting the results below [S. Malone, pers. comm., 2009].

The most conspicuous expression of multiplet development was after the eruption on May 18, 1980. This seismicity, attributed to decompression and readjustment of the magma plumbing system [Barker and Malone, 1991; Moran, 1994], plummeted to depths as deep as 16 km (Figure 1.4). Multiplets during this time period consisted of high-frequency events. The development of multiplets suggests that the readjustment of the magma chamber and conduit occurred along a few discrete faults throughout the crust, not over random discontinuities.

The eruption in March 1982 was unique within the discrete dome building phase. The buildup to the eruption was two weeks long and consisted of both deep and shallow earthquakes [Weaver et al., 1983; Swanson et al., 1983]. This was also the first significant occurrence of precursory multiplets at Mount St. Helens. The dome building eruption was accompanied by an explosion, the largest since the explosions in 1980. The presence of deep seismicity and explosive activity suggests that the eruption was accompanied by fresh, gaseous magma. Multiplet development, in concert with the overall seismicity, was weaker during dome building after the eruption. The presence of dominantly precursory multiplets suggests that their occurrence was related to the additional gases accompanying the eruption. After the explosion, exogenous dome growth continued for 3 weeks with very-low levels of associated seismicity [Swanson and Holcomb, 1990]. Also after the explosion, the rate of SO_2 doubled from pre-eruptive levels suggesting an open system after the eruption [CVO and PNSN, 2007]. I infer that the lack of seismicity and multiplet development after the 1982 eruption was related to the opening of the conduit system to volatile lost. If the system was opened after the explosion, the

gases were able to escape relatively aseismically and without the generation of earthquakes or multiplets.

The continuous dome forming eruption beginning in 1983 represents a break in behavior and seismic characteristics of the volcano from activity before and after [Neri and Malone, 1989]. The continuous extrusion lasted for nearly a year, however multiplet development is only strong between March 1983 and July 1983. This time period coincides with the extrusion of a spine at the surface. The causal relationship between the spine and multiplet development strongly suggests that the multiplets during this time period are associated with the viscosity of the extruding magma in the shallow conduit. In this case, the seismicity was likely due either to shear along the edges of the extruding plug (i.e. Neuberg et al., [2006]), or failure of the viscous plug itself (i.e. Massol and Jaupart [2009]). Alternatively, the viscous state of the plug may facilitate the concentrated flow of exsolved gases. Gas flow into the surrounding crust is facilitated in high permeability areas, such as tensile cracks in the extruding plug. If the tensile cracks in the plug are formed in response to the quenching of microlite along a depth-dependent boundary (i.e. [Neuberg et al., 2006]), then the gas will escape into the same cracks at that depth and a multiplet will form.

After the discrete eruptions resumed in 1984, they became more seismically energetic with time [Neri and Malone, 1989]. This was attributed to more resistance to dome building at the surface, perhaps from the increased load of the extruded dome [Taisne and Jaupart, 2008]. The SiO_2 content of the magmas extruded increased from 62% to 64% between 1980 and 1986 [Pallister et al., 1992]. The increase likely contributed dramatically to increasing viscosity of the magmas with time. Extrusion was both endogenous and exogenous, although eruptions after 1983

contained a much larger component of endogenous dome growth compared to earlier eruptions [Swanson and Holcomb, 1990]. The exogenous growth was in the form of lobes. There was a shift in textures from scoriaceous to smooth as dome building progressed from 1980 to 1986 [Anderson and Fink, 1990]. This shift was interpreted as evidence of more complete degassing of magma in the shallow conduit later in the discrete dome-building phases. SO_2 output also dropped throughout the discrete dome-building phase which means that the extruded magma had less gas to exsolve [Swanson and Holcomb, 1990]. A combination of higher silica content and the additional loss of volatiles would make for a more viscous magma in the shallow conduit and could have contributed to the enhanced generation of multiplets between 1984 and 1986. Though not explicitly calculated here, multiplets could be identified by eye after the 1983 continuous eruption, suggesting a higher MPTS than previous eruptions [Fremont and Malone, 1987].

3.2 Interpretation of Upper Crustal Seismicity

After the dome forming eruption in 1986, a concentration of seismicity developed at 2 km below the dome (Figure 1.4). This band of seismicity was located at approximately the same depth as the deepest seismicity seen during and just prior to the dome-forming eruptions between 1980-1986 and 2004-2008. During the 1980-1986 eruptions, patterns in deformation led to the inference of a magma chamber at a depth that is coincident with the shallow band of seismicity [Chadwick et al., 1988b]. The b-values of the earthquakes within this band were also high (~1.5), indicating the presence of gases or magma [Wiemer and McNutt, 1997]. The depths at, and deeper than, the band of seismicity were not active during times of continuous extrusion,

such as 1983-1984 and 2004 to 2008. After dome-building ceased in 2008, deeper seismicity was once again present.

The concentration of seismicity at 2.3 km depth is approximately coincident with the transition from granitic bedrock to edifice material at Mount St. Helens, determined from gravity measurements and seismic tomography [Waite and Moran, 2009; Williams et al., 1987]. The Young's modulus is a measure of stiffness of a material. A large variation in Young's modulus between discontinuous layers, such as the boundary between edifice and bedrock, can act to arrest dikes and concentrate tensile stresses into the stiffer unit [Gudmundsson and Brenner, 2004]. The effect may be to pond magma or volatiles within the unit with the high Young's modulus. For magma to reach the surface, the tensile stress field above the chamber must encourage dike emplacement at all depths above the magma source. Thus for an eruption at Mount St. Helens, the tensile stress field must extend into the edifice material above the stiffer granitic bedrock. This may be accomplished through the progressive emplacement of dikes through the boundary [Gudmundsson and Brenner, 2004]. The stress field imparted by individual dikes through the boundary acts to change the initial stress field and gradually creates a zone of tensile stresses through the boundary that promotes the emplacement of dikes to the surface. The formation of dikes through the boundary may be reflected in the concentration of seismicity at 2.3 km depth.

The lack of deformation after 1991 and the initial deflation of the deep magma chamber in September, 2004, suggests that the deep magma chamber was pressurized since at least 1991 [Iverson et al., 2006; Lisowski et al., 2008]. Additional swarms of earthquakes occurred above the 7 km deep magma chamber in 1994 and

1997, suggesting ongoing pressurization of the region between 2 and 8 km depth (Figure 1.4; [Musumeci et al., 2002]). The time interval from 1991 to 2004 may reflect the time that it took to create a stress field that promoted dike emplacement and magma ascent at the mechanical boundary between the bedrock and the edifice. Magma rose to within a kilometer of the surface aseismically immediately prior to the 2004 eruption, which suggests that no stress concentration was present at the mechanical boundary just prior to 2004 (Appendix A, Figure 3A).

It is most likely that the concentrated stresses at the 2.3 km deep boundary were imparted by gases from a magma source in the deeper chamber. A low-velocity zone exists in this region with velocity perturbations up to 5.5% [Waite and Moran, 2009]. If this zone is filled with magma, this magnitude of the perturbation suggests that the crust consists of 5% or more magma by volume [Waite and Moran, 2009]. During the 2004-2008 eruption at Mount St. Helens, there was no petrologic evidence for magma source depths shallower than 5 km [Pallister et al., 2008]. Additionally, in the late 1980s, several phreatic explosions occurred with no juvenile material [Mastin, 1994]. These explosions pointed to the presence of a significant exsolved gas phase under the volcano at depth [Mastin, 1994]. Gas has a significantly lower seismic velocity than magma suggesting that only a small amount of gases (<5% of total volume) must be present within the low velocity zone to get the observed 5.5% velocity perturbation. Gases may have come from the cooling of the stagnant plug within the 1980-1986 conduit [Mastin, 1994], however the presence of passive degassing of CO_2 in 1998 [Gerlach et al., 2008] may suggest convection of magma within the conduit [Shinohara, 2008]. Convection of silicic melts within a conduit are possible in conduits with diameters between 5 and 20 m [Witter, 2003], which is far

smaller than a conduit diameter of 50-55 m estimated during the 1980 eruption at Mount St. Helens [Scandone and Malone, 1985]. In the case of convection within the conduit, shear along the edges of the conduit produce enough permeability for gases to escape into the surrounding crust at depths of up to 3 km [Okumura et al., 2009]. This escape of gas and storage of gas in cracks within the crust surrounding the conduit could explain the low-velocity zone below 2.3 km depth and the presence of a free gas phase at depth. A similar concentration of seismicity to that seen at Mount St. Helens exists underneath Augustine Volcano, Alaska at the presumed transition between bedrock and edifice [J. Power, pers. comm., 2009]. As at Mount St. Helens from 1980-1986, the concentration of shallow seismicity at Augustine volcano was co-located with the source of deformation prior to its 2006 eruption [Cervelli et al., 2006].

3.3 Automated analysis of 2004 Mount St. Helens eruption

The 2004 eruption of Mount St. Helens was highly seismogenic and quickly exceeded the capacity of the PNSN to conduct manual analysis of each event. The PNSN quickly switched to locating only a subset of representative seismicity and relied more on automated analysis such as Real-Time Seismic Amplitude Measurement (RSAM) [Endo and Murray, 1991; Qamar et al., 2008]. Moran et al. [2008] and Thelen et al. [2008]conducted an analysis of the seismicity between 2004 and 2005 at Mount St. Helens. The automatic analysis presented here was largely guided by the results in those studies. I reanalyze the seismicity between September 2004 and November 2004 in order to facilitate a direct comparison between the latest eruptions at Bezymianny and Mount St. Helens.

3.3.1 Methods

To automatically classify events, I relied on the ratio between the mean of two frequency bands. This analysis follows closely the methods of Section 2.3. Automatic picks were made using a STA/LTA picker. Events were selected when picks existed on three or more stations within 5 seconds of each other. For each event, 6 seconds were cut before the event and 10 seconds after the event. The Fourier Transform of the entire record was then calculated. Bands of seismicity from 1 to 5 Hz and from 12 to 18 Hz were averaged and then a ratio of the mean high frequency energy to the mean low frequency energy was calculated. The bands were selected based on the dominant frequencies that were present in the high and low frequency events [Moran et al., 2008]. The frequency ratio was the main discriminate for classifying events. Ratios on each station were only accepted if the signal to noise ratio of the record exceeds 5. The ratios on three stations (HSR, SHW and SOS) were averaged to get the final ratio (see Appendix A, Figure 2 for station map). Cutoffs were determined from the visual inspection of many hundreds of events and generally followed the standards of Moran et al. [2008] and Thelen et al. [2008]. A representative set of event spectra can be found in Appendix A, Figure 5. Maximum amplitudes of each event were calculated by taking the largest maximum amplitude on the stations that had a signal to noise ratio over 5.

This analysis differs from the ratio analysis at Bezymianny in several ways. Different frequency bands were used in this analysis to exploit the dominant frequency bands present. In most cases, the frequency band from 6 to 10 Hz also had energy during the high frequency events, especially with respect to the 1 to 5 Hz band, but the best discriminator was still the 12 to 18 Hz frequency band. In this analysis, I also chose not to track rockfall or low-frequency long-duration events

(LFLDE) because visual inspection of long duration signals were most often large-magnitude events, or bursts of events with overlapping codas. Generally rockfall signals were not common until later in the eruptive sequence when the dome was larger and more unstable. The LFLDEs found at Bezymianny had no analogue at Mount St. Helens during the 2004-2008 eruption.

3.3.2 Ratio analysis results

The results of the ratio analysis are shown in Figure 3.41. Generally, the prominent type of seismicity shifted from high-frequency events during the precursory swarm starting on September 23 to hybrid seismicity prior to the explosions, to low-frequency events during dome-building. Except for the transition between swarms on September 25, the amount of high frequency energy (high-frequency and hybrid earthquakes) decreased gradually until the first extrusion of magma on October 11, 2004. High-frequency earthquakes occurred rarely after the first explosion and hybrid earthquakes occurred rarely after the first extrusion of magma. These results are similar to observations made by Moran et al. [2008].

The evolution of amplitudes with time reveals how the seismic energy was partitioned (Figure 3.42). Here I used the cumulative maximum amplitude as a proxy for moment rate. Initially, the rate of high-frequency earthquake energy release was high, however it was soon eclipsed by the energy release of both hybrids and low-frequency earthquakes. The energy release of hybrids flattened out soon after the October 5 explosion. The energy release of low-frequency events was initially high and constant until the first extrusion of lava on October 11. After the start of

extrusion, the rate of energy release of low-frequency earthquakes decreased, and maintained a relatively constant rate through the end of the study period.

3.3.2 Ratio analysis discussion

The gradual evolution of frequency content during the beginning stages of the 2004 eruption gives insight into the state of the conduit. The presence of high frequency energy prior to extrusion shows that the high-frequency earthquakes were directly related to the breakup of a solidified plug. After September 25, 2004, the high-frequency earthquakes were also accompanied by more low-frequency energy, which was manifested by the presence of hybrid and low-frequency seismicity. The shift in the frequency character of the shallow seismicity from high to low frequencies was commonly seen during the discrete dome forming phase between 1980 and 1986 [Malone et al., 1983].

The sudden switch from only high-frequency events to high-frequency events with hybrid and low-frequency events can be explained two ways. The first is that the hybrid and low-frequency events were happening at a shallower level in the conduit and thus the low-frequency energy was due solely to attenuation. While there was evidence for a 200 m shallowing of earthquake locations ([Moran et al., 2008]; Appendix A, Figure 7), the small shift in source location is unlikely to change the character of the waveform so drastically.

The second explanation assumes that the low-frequency energy represented a different type of source process. Low-frequency events are usually explained by

invoking resonance in a fluid or gas filled crack [Chouet, 1996]. Hybrid events represent a combination of both high-frequency and low-frequency source types. In other words, hybrid events involve shear failure in the presence of a resonator. The initial presence of only high-frequency energy followed by a minor hiatus and then a dramatic increase in high-frequency, hybrid and low-frequency events may best be explained by a top-down process. The first phase was the initial breaking of the bottom of the plug through shear processes. The manifestation was the exclusive presence of high-frequency seismicity. No low-frequency or hybrid earthquakes were occurring, suggesting that there was no significant gas phase within the shallow edifice that was able to sustain resonance. The breaking of the plug decompressed the underlying plumbing system and allowed gas flow up the conduit. An exsolved gas phase is likely present at depths below 2.3 km (see Section 3.2) and the shear within the ascending magma would increase permeability, allowing the gases to move into the shallow edifice faster than the magma [Okumura et al., 2009].

The hiatus in activity on September 25 represented the time between the end of the initial breakup period, and the transport of gas from depth. As gas pressure increased under the dome, breakup of the plug continued, now with the added presence of gases, creating both hybrid and low-frequency events. Magmatic gases were not detected until after the first explosion on October 1 suggesting a closed system existed [Gerlach et al., 2008]. Such a closed system is proposed to occur in the presence of a large dome as the weight of the dome closes shallow cracks [Taisne and Jaupart, 2008].

The breakup of the deep plug may have been initiated by increased pore pressure from abnormally heavy rainfall that was present in the crater in mid-September [Iverson et al., 2006]. A similar mechanism was proposed by Mastin et al. [1994] for the 1989 to 1991 phreatic explosions . Large amounts of rain were also found to trigger dome collapse and pyroclastic flows at Soufriere Hills, Montserrat [Matthews et al., 2002]. There have been large rainfall events within the crater prior to September 2004 that did not lead to an eruption. If intense rainfall really triggered the eruption, then the magmatic system below the dome must have been poised for an eruption [Iverson et al., 2006]. The seismicity cluster at 2.3 km depth stopped when seismicity associated with the 2004-2008 eruption started (Figure 1.4). This suggests that the stresses at mechanical boundary between edifice and bedrock at 2.3 km depth were homogenous and incapable of creating earthquakes. The homogenous stress field at this boundary was no longer a barrier to flow and allowed magma and volatile flux from the chamber to the surface.

The absence of high-frequency and hybrid earthquakes after dome extrusion started is suggestive that the high-frequency energy in both types of events was related to the breakup of the plug and the opening of the conduit system. Low frequency events dominated, both in numbers and in energy released. The rate of energy release was notably lower after dome extrusion started, also suggesting a fundamental change in the state of the pressure source driving the seismicity. Clearly, once the conduit was opened, the shear fracturing required to break up the plug was no longer present, and thus the high-frequency and hybrid earthquakes ceased. Gases were consistently detected for the first time beginning October 7, also suggesting an opening of the conduit system [Gerlach et al., 2008].

3.4 Re-analysis of 2004 multiplets

Here I re-analyze the occurrence and behavior of repeating earthquake sequences, called multiplets, between September 23, 2004 and October 31, 2004. The analysis is done in a manner consistent with the multiplet analysis done at Bezymianny in Chapter 2. This was done to better make a comparison between the two systems.

3.4.1 Multiplet Methods

At Mount St. Helens, I use two separate station sets due to the limited dynamic range of the short period stations of the permanent network. The first set is from stations within 5 km of the dome (HSR, SHW, SOS, called near-field; Appendix A, Figure 2). During the strongest seismicity, these stations often clipped, or were saturated for a time. Clipping degrades the cross-correlation coefficient, thus altering the classification of multiplets. As the amplitude of signals decreased and low frequency earthquakes became dominant after the October 5 explosion, the triggering parameters used for the vent-clearing phase began to miss events. To reduce the effects of clipping filtering should be minimized, however to aid in noise reduction and automatic detection of events, filtering should be used. To satisfy both criteria, two different runs were completed, one with filtering and one without. Filtering is also not needed when the signal to noise of events is very high, such as between September 23, 2004, to October 11, 2004. During the time period after October 5, 2004, an additional run was completed with adjusted triggering parameters. This run, hereafter called the filtered set, included many more small events than the near-field set. Events between September 25 and October 11 often overlapped, further degrading the cross-correlations and desensitizing the triggering algorithm. During these times,

the same multiplet analysis as the near-field run was performed on stations 10-15 km away from the dome that were not saturated (TDL, ELK, CDF, called far-field; Appendix A, Figure 2). The events recorded at 10-15 km distances are a larger-magnitude subset of the overall seismicity. A summary of the characteristics of each multiplet run is shown in Table 3.5.

The parameters used here to define multiplets are intentionally similar to the runs at Bezymianny volcano. A trigger is declared when the STA/LTA exceeds 2.5 (2.0 for the filtered set) on three stations within 5 seconds of each other. Triggers are calculated using 6 stations at a variety of distances. The same triggers are used for the near-field, filtered and far-field sets. Two events are considered similar when they have a cross-correlation value of 0.7 or higher on two out of three stations. Cross-correlations are calculated on unfiltered data in the near- and far-field dataset and on filtered data in the filtered dataset.

3.4.2 Multiplet Results

The time series of multiplet occurrence using the close and far stations is shown in Figure 3.43 and Figure 3.44, respectively. The filtered set is shown in Figure 3.45. The results presented here are broadly similar to the results in Appendix A. There are some differences however. In Appendix A, only a single station is used during a particular time period for triggers and for finding multiplets. The use of multiple stations in the analysis in this section provided for more robust triggering and multiplet analysis because interference from sources of noise local to a particular station are minimized. Further, a cross-correlation cutoff of 0.8 was used in Appendix A. This cross-correlation coefficient was chosen because the emphasis in Appendix

A was on earthquake locations, and more reliable lags are possible with higher cross-correlation coefficients. In this analysis, the emphasis is on the characterization of the source, and thus, a cross-correlation cutoff of 0.7 groups many sources together while maintaining similarity. A 0.7 cross-correlation coefficient is also consistent with the multiplet analysis on Bezymianny and will allow for a direct comparison of multiplet behavior. Despite these differences, the multiplet analysis in Appendix A shows similar behavior in the initial swarm between September 23 and September 26. The analysis in this section also shows significantly longer duration multiplets once dome growth began, as in Appendix A.

Throughout the study period, a remarkable number of multiplets were present. Between September 23, 2004, and September 26, 2004, the multiplet proportion of total seismicity (MPTS) increased to as high as 72% (Figure 3.46). The multiplets were distributed over up to 19 different families at the same time. This diversity would have made it near impossible to identify multiplets manually (Figure 3.47). As seismicity began to surge again on September 26, 2004, the MPTS, number of contemporary multiplets and average amplitude of multiplets increased abruptly (Figure 3.47, Figure 3.48). The duration of multiplets measured on the near-field stations did not significantly change from September 23 to September 26, however there was the suggestion of an increase in multiplet durations in the larger amplitude multiplets measured on the far-field stations (Figure 3.49).

Immediately after a peak in MPTS on September 26, 2004, the MPTS decreased, both on near- and far-field stations up until the first explosion on October 1 (Figure 3.46). During the same time period, the number of contemporaneous

multiplets increased, as did the average maximum amplitude. Unlike the results presented in Appendix A, some multiplets were reactivated after the first explosion. This is because the cross-correlation coefficient threshold used in the current analysis was lower (0.7) than that in the analysis in Appendix A (0.8). The results are consistent with a small change in location of the multiplet or structure around the multiplet source area after the October 1 explosion. Such a change could potentially de-correlate at the 0.8 threshold, while maintaining similarity at the 0.7 threshold. This is an important distinction from the annihilation of the multiplet source area during the October 2007 eruption at Bezymianny and has important implications for determining the strength of an explosion. Many new multiplets began after the eruption on October 1 suggesting that some new and different sources were favored by the altered stress state present after the October 1 explosion.

Another significant change in the occurrence of multiplets was temporally associated with the tremor episode on October 2, 2004 19:17 UTC (Figure 3.44). Immediately after the tremor, many multiplets stopped, while many others started for the first time. The other instances of tremor and the other explosions that occurred in October 2004, did not obviously affect the start or stop time of multiplets, although the number of contemporaneous multiplets, the average amplitude, and the multiplet duration, as observed on far field stations, decreased from the first period of tremor through the last explosion of 2004. Interestingly, the MPTS, number of contemporary multiplets and the amplitude of the multiplets decreased dramatically after the October 5 eruption.

A transition occurred in the seismicity between the last explosion on October 5 and the first extrusion of magma on the surface on October 11, 2004 [Vallance et al., 2008]. The RSAM values waxed and waned during this time, with peaks in activity on October 7, 2004 and October 9, 2004. RSAM levels, in general, were lower during this time than during the explosive period between October 1 and October 5. The MPTS was generally high, between 50% and 85%, and the number of contemporaneous multiplets was relatively low (Figure 3.46, Figure 3.47). The average maximum amplitude of multiplets, MPTS and number of contemporary multiplets observed on far-field stations generally followed trends in the RSAM values (Figure 3.44). The duration of individual multiplets did not significantly change throughout this time period (Figure 3.49).

Dome extrusion began on October 11, 2004 [Vallance et al., 2008]. The RSAM values, once extrusion started, were quite low compared to the time period between September 27, and October 10, 2004 (Figure 3.43). Three phases of dome building were present [Vallance et al., 2008]. Multiplets often continued across these dome building phases (Figure 3.43, Figure 3.45). During this period, the MPTS varied between 40% and 90% and the number of contemporary multiplets varies between 2 and 23 on the near-field set, and between 7 and 63 on the filtered set. The most distinctive feature of this phase is the presence of long duration multiplets, in some cases over 2 weeks long (Figure 3.48). This is similar to the results in Appendix A Figure 11, which shows much longer duration multiplets occurring once dome forming begins compared to earlier in the earthquake sequence. Amplitudes also became more consistent between multiplets and less variable within multiplets as dome forming continued.

The three dome building phases had different multiplet behavior. The first dome building phase, corresponding to the extrusion of Spine 1, had low MPTS, a relatively low number of contemporaneous multiplets and a high degree of variability between multiplets and within multiplets. The second dome building phase, corresponding to the extrusion of Spine 2, had a high MPTS, with a number of contemporary multiplets that was consistent with the first dome building episode. Amplitudes between contemporaneous multiplets were very stable and had low relative variability within multiplets. The third dome phase started with a dramatic decrease in MPTS, which then increased until the end of the study period. The number of contemporary multiplets also increased dramatically. Multiplet amplitudes were similar in value to the second dome building phase. A larger number of long-duration multiplets were present during the third phase of dome building. The transition between the second and third phases of dome growth also coincided with a decline in the rate of new multiplet development (Figure 3.45). This rate is measured by the slope of the line that connects the first event of each multiplet.

3.4.3 Discussion of Behavior of Multiplets

The multiplet analyses here, and in Appendix A, clearly show that the multiplets are affected by changes in the conduit that change the surface expression of volcanic activity. The results of the multiplet analysis are interpreted in reference to the basic model proposed in Figure 2.24. Prior to the explosions on October 1, 2004, the average amplitude of multiplets increased significantly, while the MPTS declined from September 26 until October 1. After the first explosion all seismicity ceased, including the multiplets, for more than 3 hours [Moran et al., 2008]. This behavior strongly suggests that the driving force behind the multiplets was a pressure

source associated with the intrusion of magma that initially increased, driving up the amplitudes prior to the first eruption, then dropping significantly after the first eruption. The drop in pressure was significant enough to stop all seismicity for 3 hours. The decrease in MPTS prior to the first explosion can be explained if the increase in pressure led to more and more chaotic and forceful release of gases in the upper 1 km of the crust. Such a chaotic environment is relatively less stable and would not be conducive to generating as many multiplets. Alternatively, the interference of different overlapping seismograms could have contributed to an apparent decrease in the MPTS. This problem was less important on the far-field stations which recorded only a subset of the largest events, yet show the same decrease in MPTS.

Prior to the October 1 explosion, the number of contemporaneous hybrid and low-frequency multiplets also increased on both near- and far-field stations. This is an important constraint on what was occurring within and around the conduit. Consider a solid plug being pushed to the surface from a depth of 1 km, which was the deepest limit of seismicity prior to the October 1 eruption (Appendix A, Figure 3b). Shallow lateral degassing of the magma within the conduit is facilitated by a pressure gradient established by zones of high vesicularity at the edges of the conduit [Massol and Jaupart, 2009]. Gas will initially escape from the conduit through cracks that are optimally oriented with respect to the local stress field. Each crack is a potentially repeatable seismic source as the gas that moves through the crack drives the effective normal stress to zero.

The repeated injection of gas into the same crack (seismic source) is what causes the multiplet in this scenario. As pressure builds below the cap, cracks that are less optimally oriented with respect to the local stress field are incorporated as

sources of potential seismicity. As more gas-filled cracks are incorporated, a higher number of contemporaneous multiplets have the potential to occur. As pressure builds the area that is influenced by stresses due to degassing of the plug gets larger and larger, thus incorporating more potential seismic sources. This reasoning assumes a homogenous distribution of cracks above 1 km. Alternatively, the increased number of concurrent multiplets could be explained by the ascent of the plug into more fractured media as it approached the surface, incorporating more potentially repeatable seismic sources.

Steam-filled cracks were found to be a plausible source mechanism for the generation of repeated low-frequency events later in the dome forming eruption, and it is likely still applicable to events occurring prior to the October 1 eruption [Waite et al., 2008]. It is important to note that not every fracture will generate a multiplet. A fracture can be irreversibly changed if gas is so forcefully driven into the crack that the crack sustains permanent strain. Additionally, cracks that exist further and further from the plug will be affected only when the pressure is high and the permeability between the conduit and the crack is kept high. Such cracks would likely not be part of a multiplet since the pressure gradient is lower further from the plug, and thus gases can move aseismically. Clearly, the generation of multiplets due to repeated gas injection is more efficient in the presence of a closed system where large overpressures are allowed to build. In an open system, gases can escape more efficiently, and the pressures around the conduit are lower, producing less seismic activity as a result.

The continuation of several multiplets after the October 1, 2004, explosion suggests that the explosion irreversibly destroyed some multiplet sources, while

preserving others. The tremor episode on October 2, 2004, represents one of the strongest continuous signals of the entire eruptive episode. Most multiplets ceased after the tremor episode with new families starting afterward (Figure 3.44). This could be an example of a large pressure source causing permanent strain in a set of multiplet-generating cracks. After the high-pressure source had dissipated, the same cracks still generated multiplets, however the multiplets were different than before because the source geometry or local stress state changed. As the explosions continued through October 5, the amplitude, number of contemporaneous multiplets and MPTS all slowly declined, which is consistent with a decrease in the pressure source as the plumbing system gradually opened up after October 5.

After the October 5 explosion, the RSAM dropped dramatically. The multiplets that were active before and during the October 5 explosion ceased soon after the explosion and an entirely new set of multiplets began when seismicity increased on October 6. This period of time also marks the prominence of low-frequency events over hybrid events (Figure 3.41; [Moran et al., 2008]). All of these factors suggest a different state of the plumbing system and a different dominant source for the seismicity. If RSAM values are used as a proxy for pressure within the plumbing system, than the pressure within the plumbing system was far less during the dome forming phase than during the vent-clearing phase. It is reasonable to believe, at these low seismic levels with a dome smoothly extruding out of the vent, that the plumbing system is relatively open. This is supported by an increase in gas output after the dome building began compared to the eruptive phase [Iverson et al., 2006; Gerlach et al., 2008].

During the dome building phase, multiplet amplitudes were generally low, and multiplet lifespans of some multiplets were longer ([Thelen et al., 2008]; Figure 3.49). While the same mechanism of multiplet generation through gas-filled cracks proposed during the vent-clearing phase of the 2004-2008 eruption was still applicable during this time period [Waite et al., 2008], the pressures in the shallow edifice was less, and the resonating crack mechanism is not likely to be as seismically efficient in the presence of an open system.

Fault gouge formed a smooth carapace on the outside of the extruding plug beginning in October 2004. This strongly suggests the presence of shear slip along the outside of the hardened plug [Iverson et al., 2006; Cashman et al., 2008]. The gouge properties are also velocity-weakening, a necessary condition for the generation of earthquakes along a shear boundary [Moore et al., 2008]. This type of source has been explored by many authors [Iverson et al., 2006; Neuberg et al., 2006; Pallister et al., 2008; Goto, 1999; Voight et al., 1999; Harrington and Brodsky, 2007]. A model of slip along the edges of an extruding plug was shown to be a plausible explanation for the highly regular recurrence intervals of multiplets during dome building at Mount St. Helens [Iverson et al., 2006]. This source process provides for a stable and repeatable source over an extended time period. Assuming shear slip, the small amplitudes of the multiplets suggests that in order to move the plug toward the surface, multiple slip patches must be present at any one time. This has the potential to create the many simultaneous, low amplitude multiplets that are seen during this time period (Figure 3.43,Figure 3.48). Throughout the study period, there is ample evidence for the presence of multiple different seismic sources occurring contemporaneously. Prior to the October 1, 2004, eruption, there was a

high-amplitude, high-frequency subset of seismicity that was clearly separate from the relatively low-amplitude, lower-frequency seismicity that was occurring at the same time (Figure 3.50). At this point in volcano science it is difficult to delimit different low-frequency sources, such as conduit resonance or crack resonance, even within well-constrained dataset such as the seismic dataset at Mount St. Helens. Analysis of earthquakes at Mount St. Helens during the 2004-2008 eruption has revealed both shearing around a conduit [Iverson et al., 2006; Harrington and Brodsky, 2007] and crack resonance [Waite and Moran, 2009] as viable sources. Given the number of earthquakes and earthquake multiplets, it is likely that both sources could exist simultaneously, however at Mount St. Helens, the relative proportions of each source type is unknown.

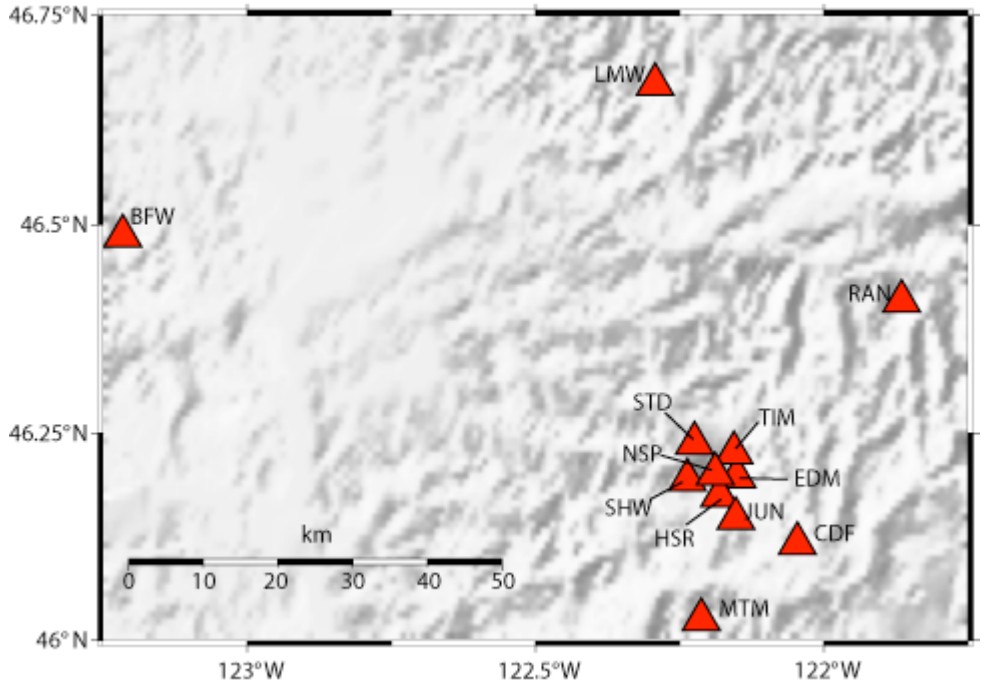

Figure 3.39: Map of stations used in the 1980-1986 multiplet analysis. Mount St. Helens is located at the concentration of stations. Station YEL is not shown because its location is indistinguishable from NSP at this scale. A more detailed map of the stations around Mount St. Helens is found in Appendix A, Figure 2.

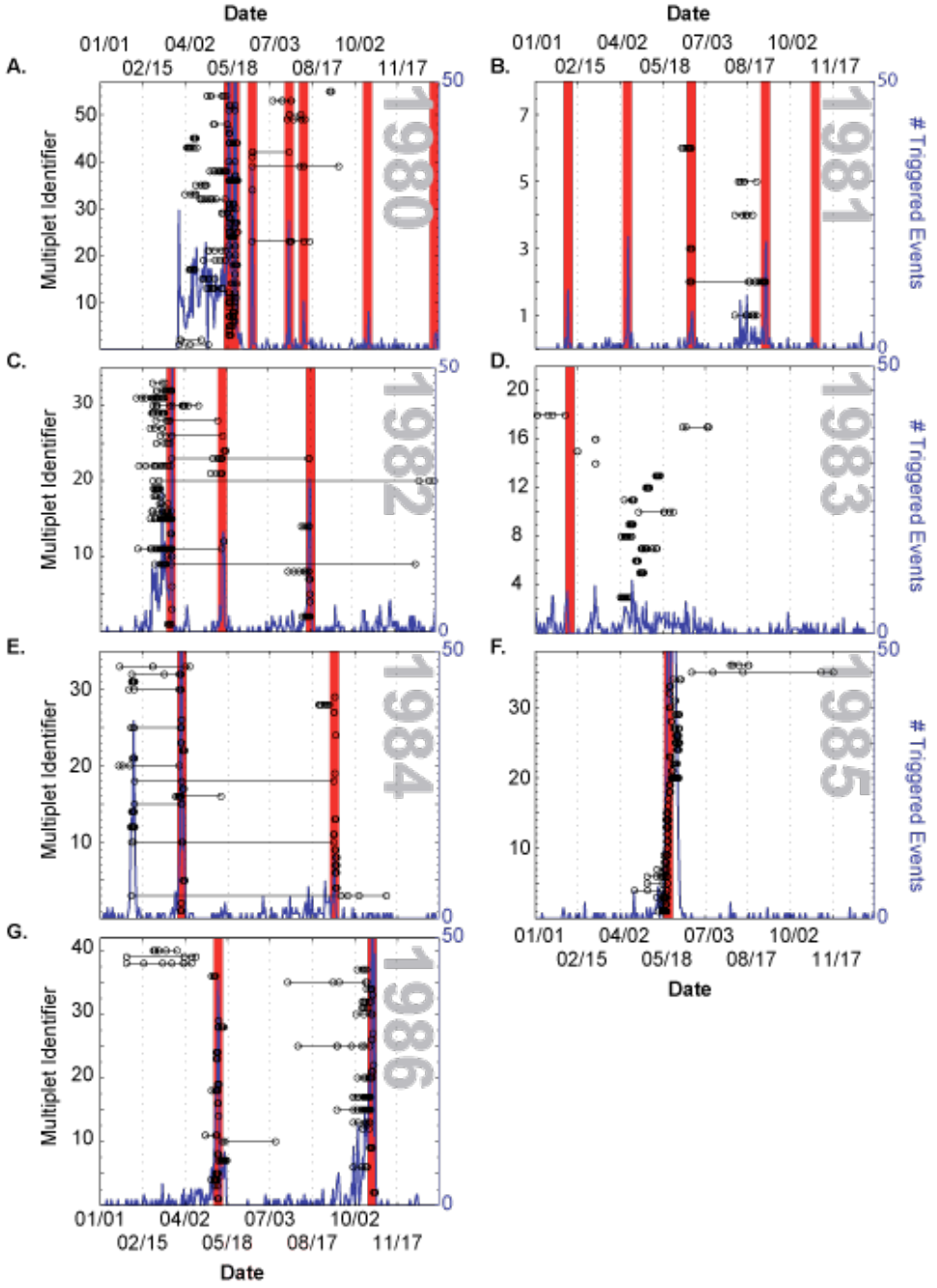

Figure 3.40: Multiplet timeline for Mount St. Helens between 1980 and 1987. Only multiplets with more than 5 events are shown. Black circles are earthquakes, circles on the same horizontal line are part of a multiplet. The blue line is the number of triggered events in the PNSN catalog per day. Red lines are eruptions as defined by Mullineaux and Crandell [1981] and Swanson and Holcomb [1990].

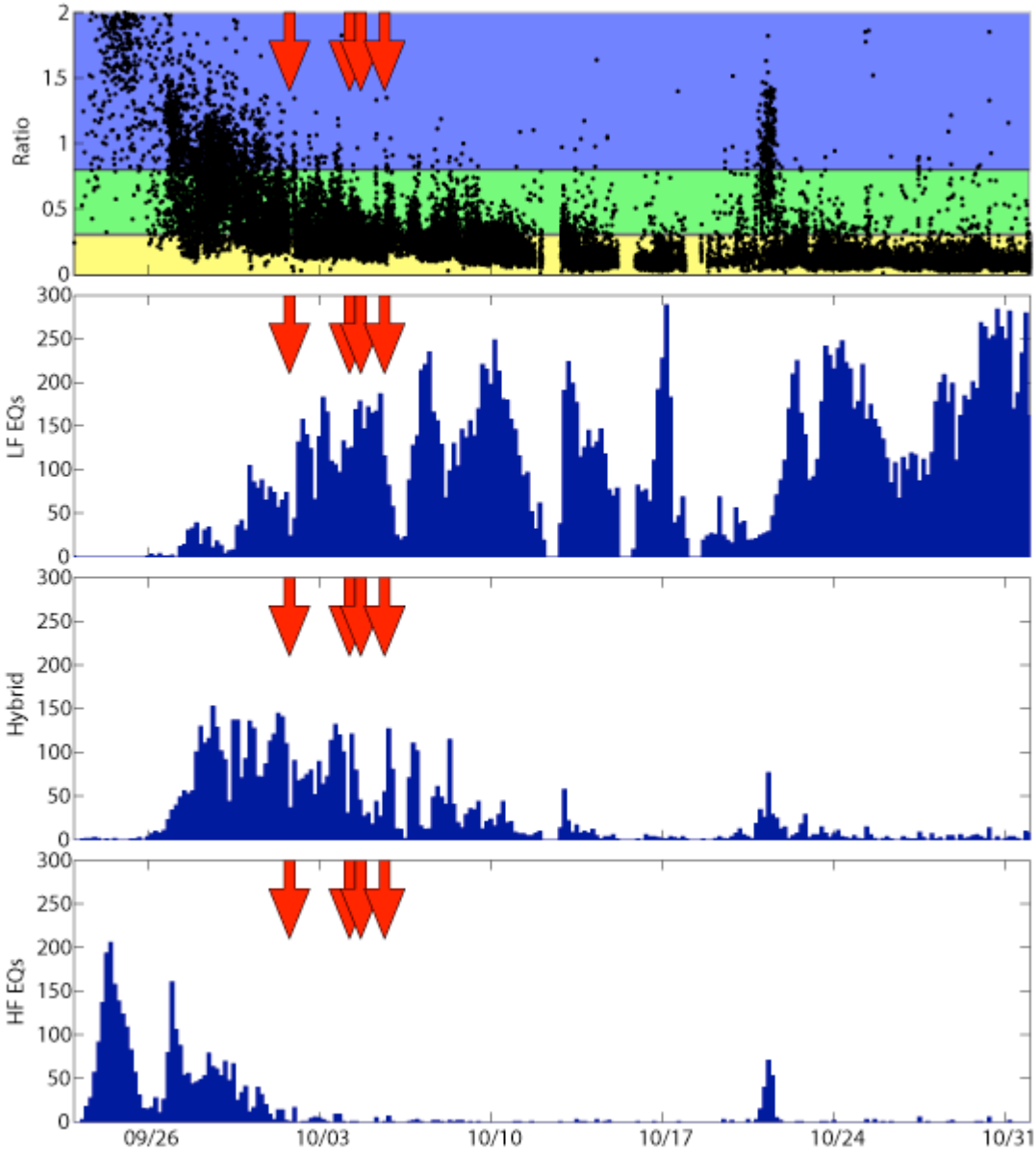

Figure 3.41: Results of ratio analysis at Mount St. Helens between September 23, 2004 and November 1, 2004. Top panel: Raw frequency ratios with cutoffs shown in different colored boxes. The blue box shows the range of high-frequency events, the green box shows hybrid events, and the yellow box shows the range of ratios encompassing the low-frequency events. Lower panels: Histograms of occurrence of different event types each 4 hours based on the cutoffs in the top panel. Red arrows are explosions. 3 gaps in events occur between October 10 and October 24 (most obvious in top pane) are due to gaps in data. A spike in activity on October 21 is due to noise in the data present on all channels, not real events.

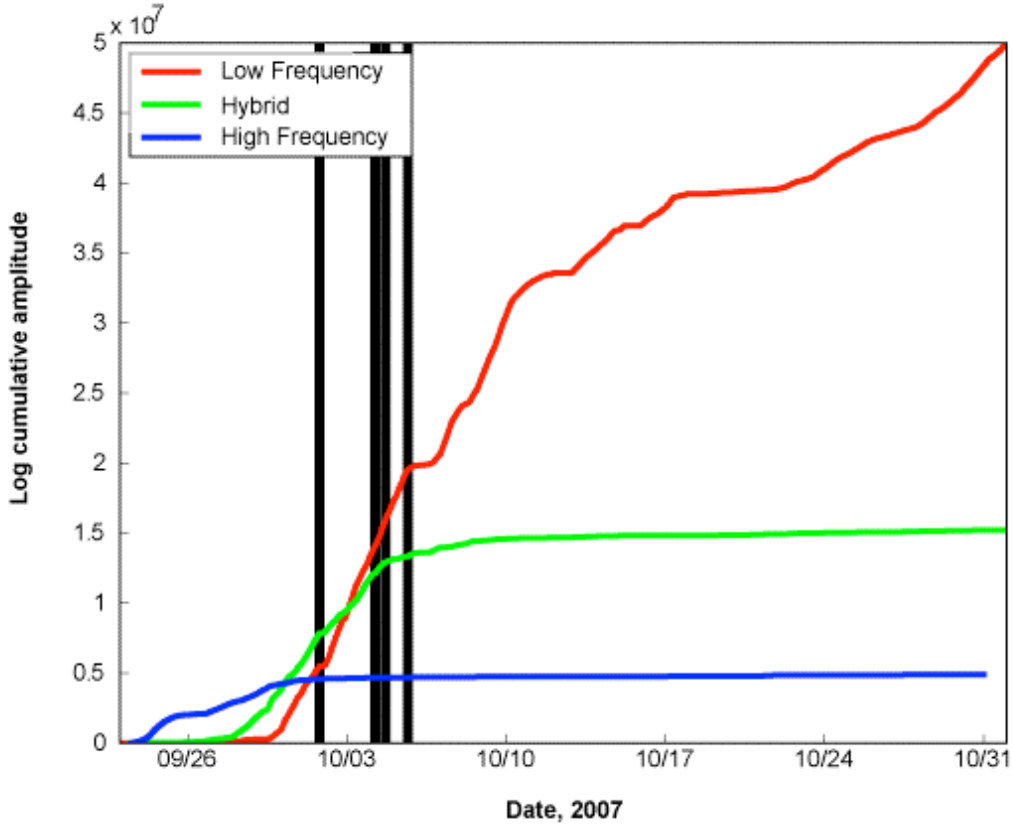

Figure 3.42: Cumulative amplitude of events occurring at Mount St. Helens between September 23, 2004 and November 1, 2004. The cumulative amplitude was calculated by summing the average maximum amplitudes (see section 3.2.1). Vertical lines represent explosions.

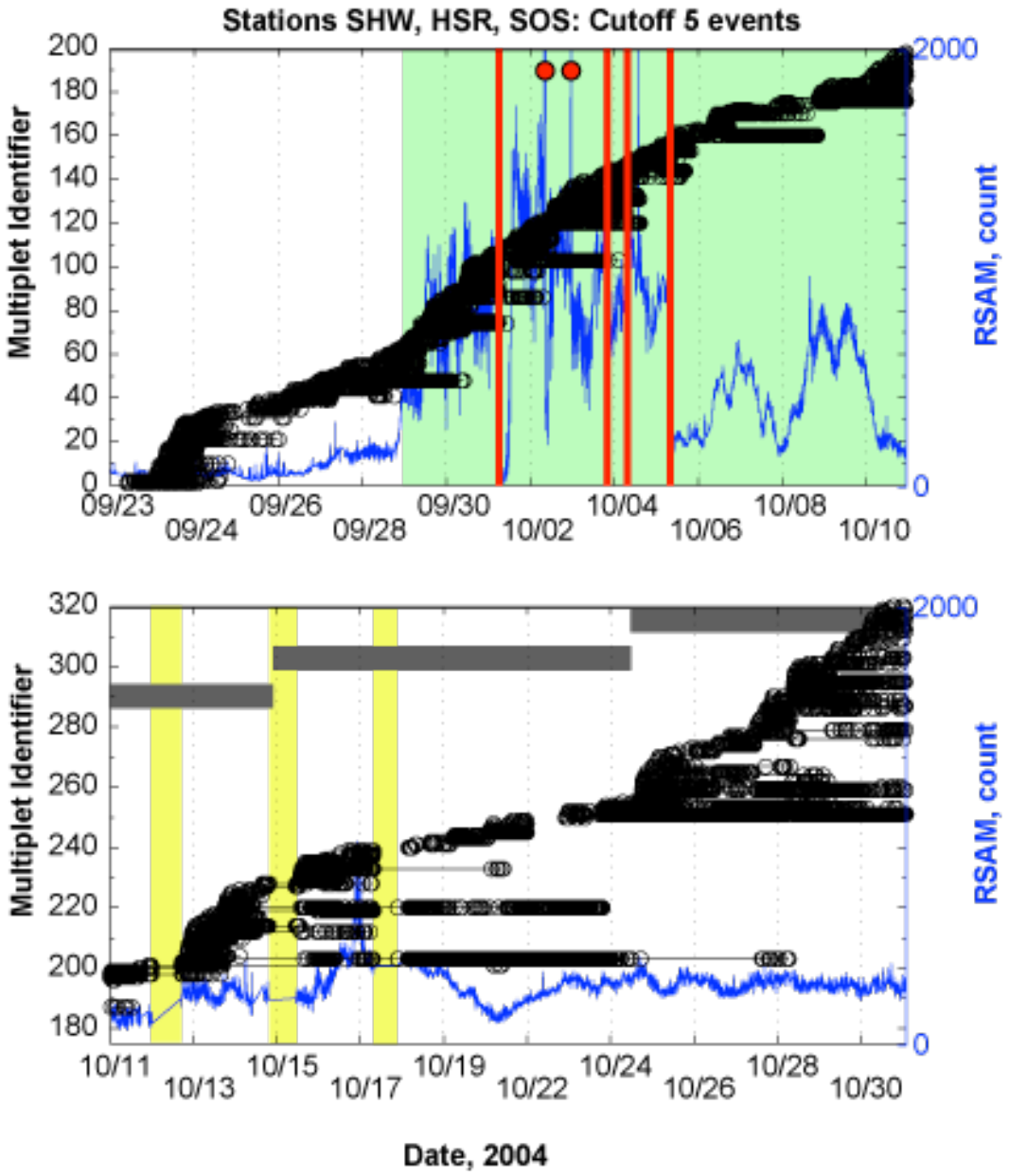

Figure 3.43: Near-field multiplet timeline from September 23, 2004 to November 1, 2004. Each black dot is an earthquake; black dots that lie on the same line are part of the same multiplet. The blue line is the rectified seismic amplitude on station SHW. Vertical red lines are confirmed explosions. Red circles are periods of tremor. The green box depicts when events were commonly clipped on the stations used here. Yellow boxes indicate outages of station SHW. Gray boxes refer to the 3 different dome phases that were present during the study period [Vallance et al., 2008]. Only multiplets with 5 or more events are included.

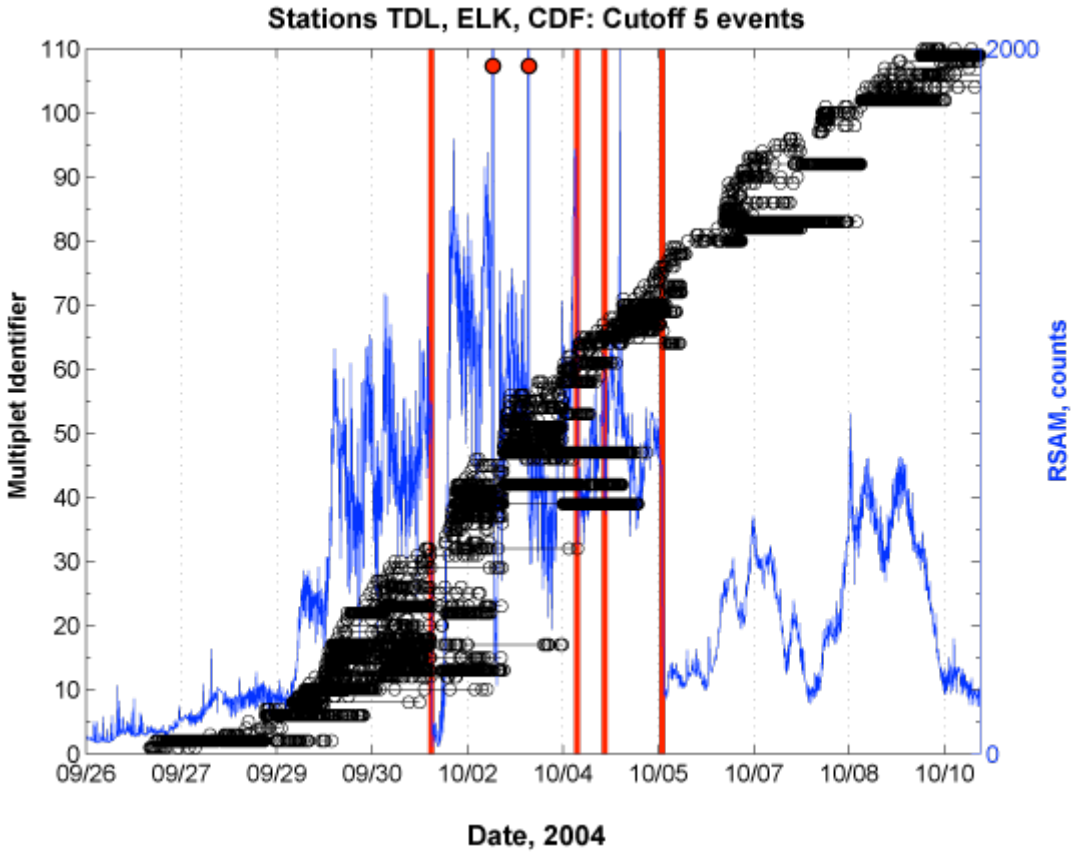

Figure 3.44: Far-field multiplet timeline from September 23, 2004 to October 11, 2004. Refer to Figure 3.43 for key to lines and symbols. Only multiplets with 5 or more events are included.

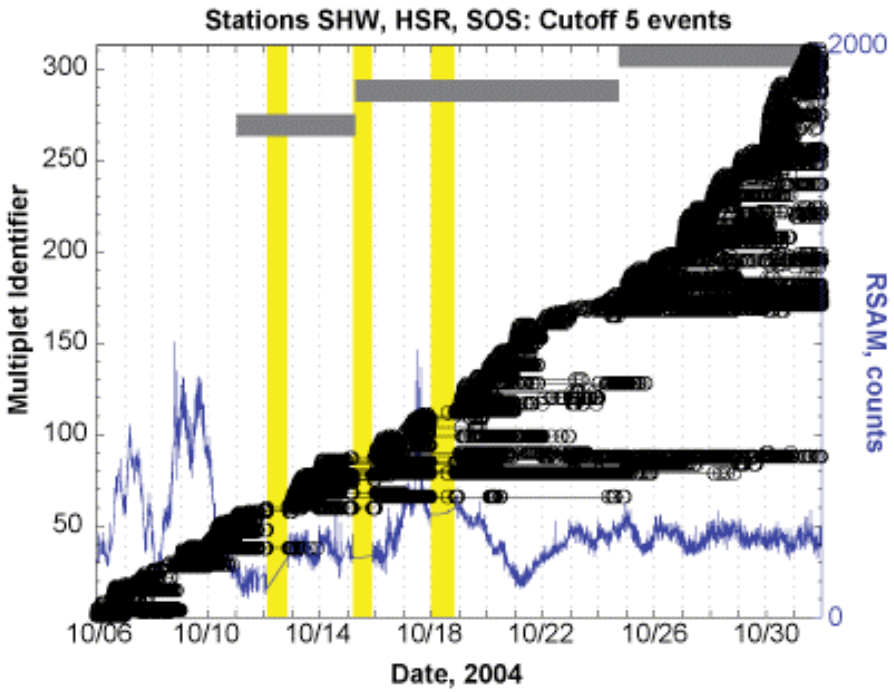

Figure 3.45: Filtered set multiplet timeline between October 6, 2004 and November 1, 2004. Refer to Figure 3.43 for key to lines and symbols. Only multiplets with 5 or more events were included.

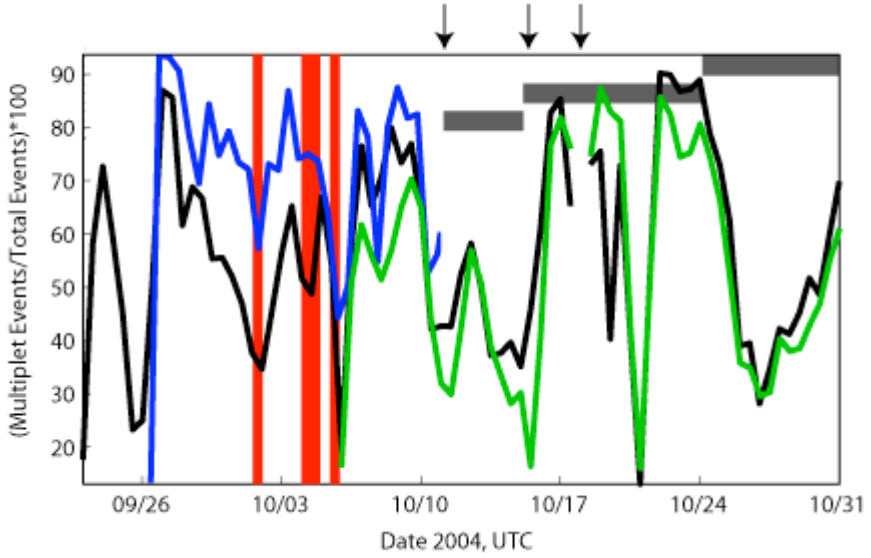

Figure 3.46: Multiplet proportion of total seismicity (MPTS) at Mount St. Helens. The black line is the MPTS measured on the near-field station set (HSR, SHW,SOS). The blue line is the MPTS as measured on the far-field station set (TDL, ELK, CDF). The green line is the MPTS using the filtered set. Low MPTS values on October 20 were from poor data quality that completely obscured the seismicity. Red lines are explosions. Gray boxes refer to the 3 different dome phases that were present during the study period. Black arrows refer to station outages.

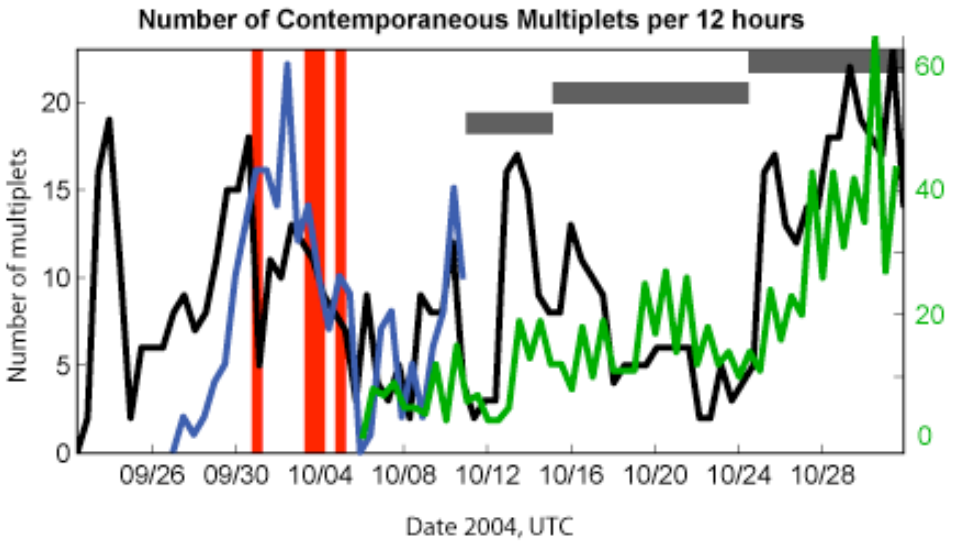

Figure 3.47: Number of contemporary multiplets at Mount St. Helens from September 23 to November 1. The number of contemporary multiplets is the number of multiplets active at a given time. The black line is the number of contemporary multiplets measured on the near-field stations (HSR, SHW, SOS). The blue line is the number of contemporary multiplets measured on the far-field stations (TDL, ELK, CDF). The green line is the number of contemporary multiplets from the filtered set. The green line uses the y-axis on the right side of the plot. Multiplets are tabulated every 12 hours. Red lines are explosions. Gray boxes refer to the 3 different dome phases that were present during the study period.

Figure 3.48: Amplitude and standard deviation of multiplets from the 2004 eruption at Mount St. Helens. A.) (left) Average maximum amplitude for each multiplet measured on station SOS. Horizontal bars represent the start and end times for the multiplet. (right) Standard deviation of the average amplitude of each multiplet measured on station SOS. Blue lines represent explosions. The plateau in amplitude near the explosions is due to clipping of the station. B.) Same as A with amplitudes measured on station ELK. Note that the time scales in A and B are different. C.) Same as A with amplitudes measured on station HSR using the filtered set. Note that the time scales in C are different than A and B. Gray boxes refer to the 3 different dome phases that occurred during the study period.

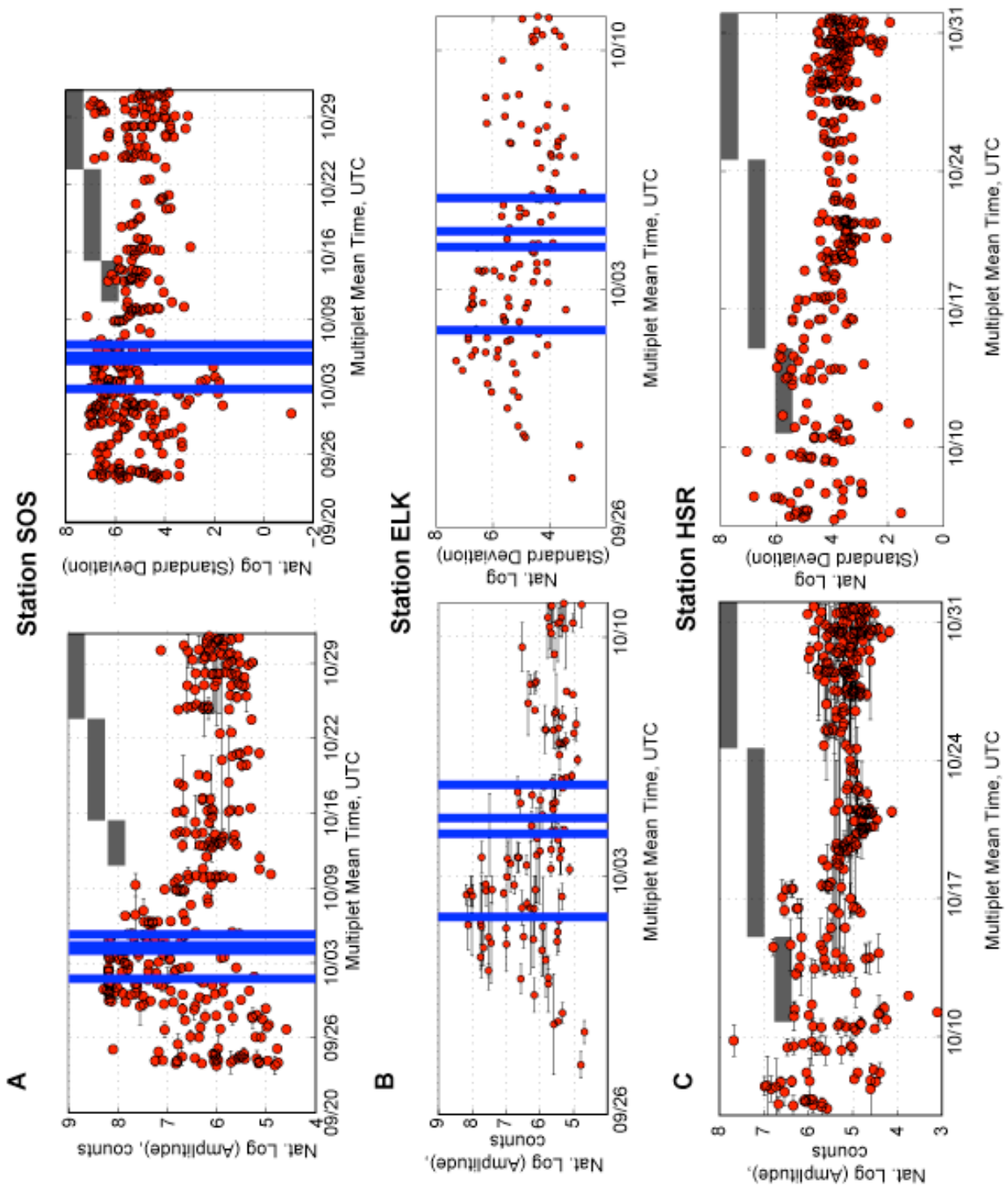
A
Station SOS
Nat. Log (Amplitude), counts
Nat. Log (Standard Deviation)
Multiplet Mean Time, UTC
09/20
09/26
10/03
10/09
10/16
10/22
10/29
B
Station ELK
C
Station HSR
10/10
10/24
10/31

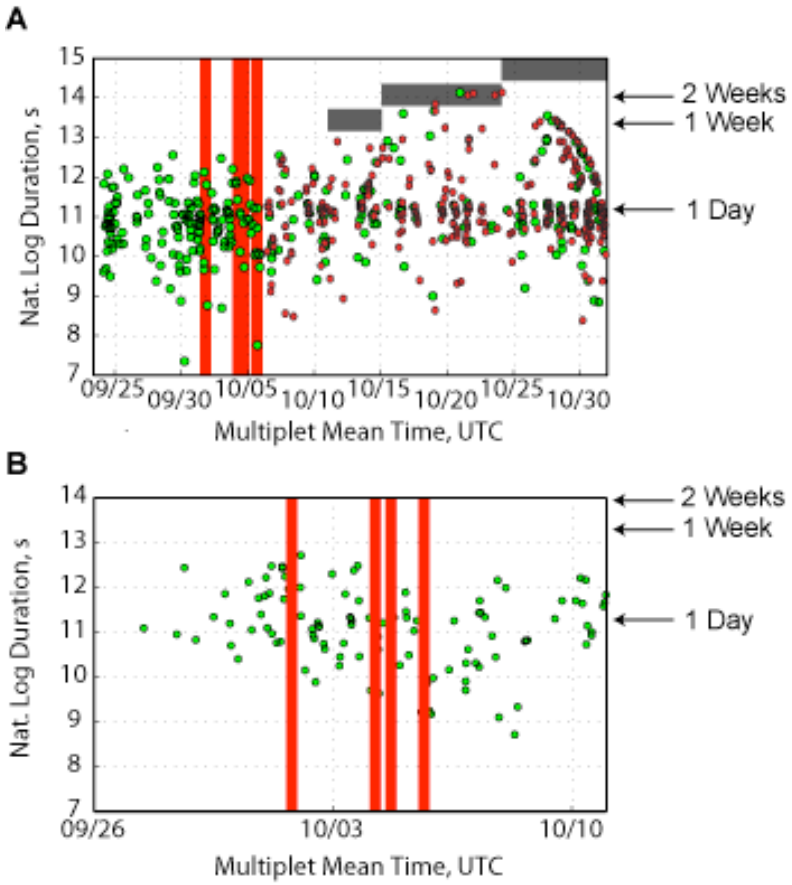

Figure 3.49: Multiplet durations during the beginning of the 2004 eruption at Mount St. Helens. A.) Multiplet duration, or time between the first and the last event in the multiplet, measured on the near-field stations (green circles). Red circles are from the filtered dataset. Red lines are explosions. The trend in multiplet duration at the right side of the plot reflects multiplets that are truncated by the end of the analysis. The duration of the multiplets near the end of the analysis is a minimum. B.) Multiplet duration measured on the far field stations. Red lines are explosions. Note that the time scales between A and B are different. Gray boxes refer to the 3 different dome phases that occurred during the study period.

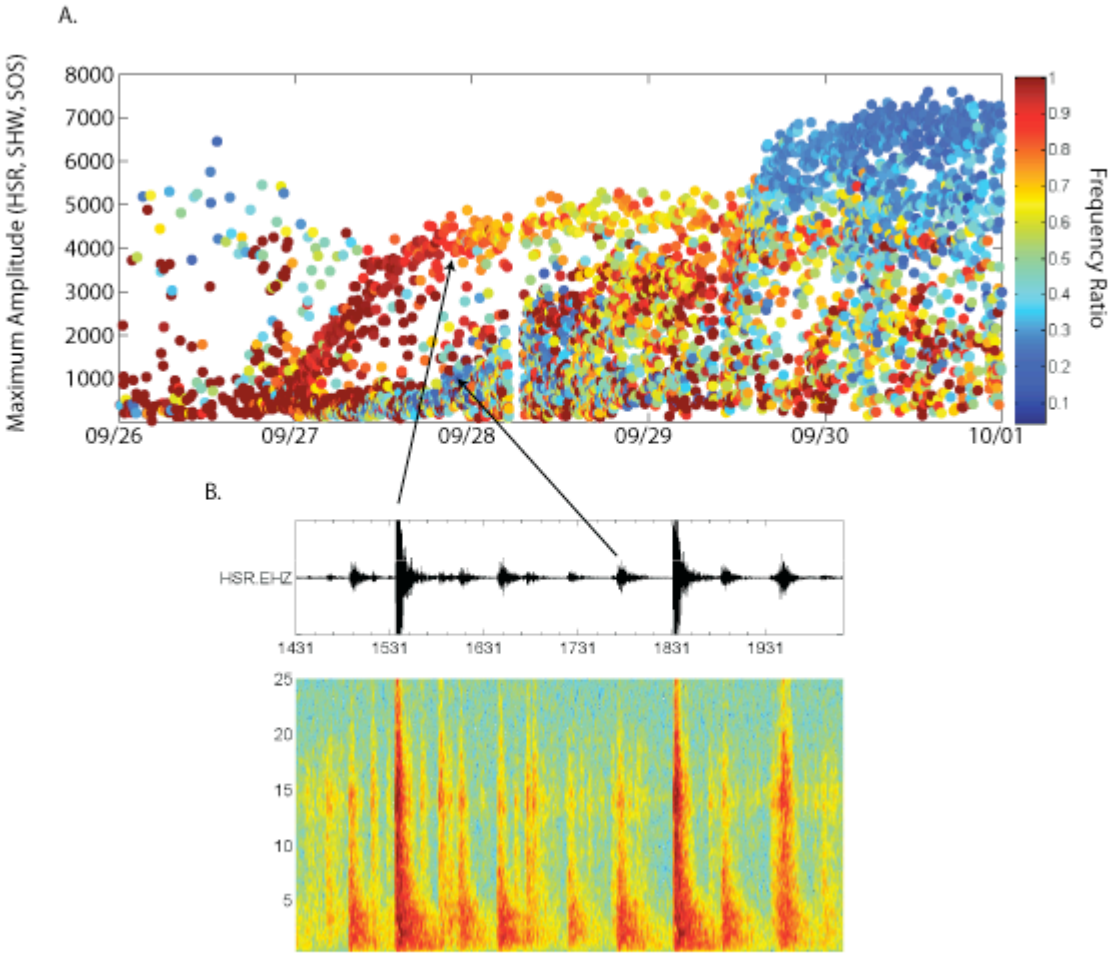

Figure 3.50: Example of source processes occurring contemporaneously. A.) Maximum amplitude of detected events on the near-field stations (HSR, SHW, SOS) from section 3.2. Circles are color-coded based on their frequency ratio. Red colors are high frequency events, orange and yellow events are hybrid events, and blue events are low-frequency events. B.) Example time series and spectrogram of several events on station HSR occurring on September 27, 2004.

Table 3.4: Table of stations used in the multiplet search during the 1980-1986 eruption at Mount St. Helens. All stations are vertical short-period stations. See Figure 3.39 for station locations.

Year	Stations
1980	LMW, MTM, BFW, RAN
1981	SHW, EDM, TIM, JUN, CDF
1982	SHW, EDM, JUN
1983	SHW, YEL, STD, JUN, TIM
1984	SHW, YEL, STD, EDM, JUN
1985	SHW, EDM, YEL, STD, JUN
1986	SHW, HSR, YEL, NSP

Table 3.5: Characteristics of different multiplet runs for the 2004 eruption of Mount St. Helens.

Analysis Name	**Dates**	**Stations**	**Advantages**	**Disadvantages**
Near-field	Sept. 23-Nov. 1	HSR, SHW, SOS	No distortion of clipped waveforms, good detection of small seismicity	Coda interference during strong seismicity
Far-field	Sept. 23-Oct. 12	TDL, ELK, CDF	Minor clipping, no interference between events	Poor recordings of smaller seismicity
Filtered	Oct. 5-Nov. 1	HSR, SHW, SOS	Improved event detection for low amplitude events	Distortion of clipped waveforms

IV. Comparison of Mount St. Helens, Washington and Bezymianny Volcano, Russia

While studying one volcanic center in detail is useful, it is never certain whether the observations and patterns at one volcano are applicable to another. General patterns may be better characterized by comparing volcanoes with similar characteristics. Further, differences between volcanoes may be exploited to learn something about the individual volcanic centers. As Bezymianny Volcano erupted 25 years prior to Mount St. Helens, we can use the similarities and differences between volcanoes to better understand if the activity currently seen at Bezymianny Volcano might be expected in the future at Mount St. Helens.

4.1 Conduit Structure

The conduit of a volcano is the path along which magma is transported from the base of the crust to the surface. The structure of the conduit and where magma chambers lie along that conduit are important to understand how magma arrives at the surface and where earthquakes may occur prior to eruption. The location and character of earthquakes under volcanoes are one of the best tools available to understand the conduit structure, and to identify magma chambers under a volcano.

4.1.1 Mount St. Helens

A dense network of seismometers installed at Mount St. Helens since the early 1980s has helped to accurately locate seismicity under the volcano and in the immediate vicinity. Seismicity at Mount St. Helens ranges from the surface to 22 km deep. A widening in the seismicity between 7 km and 9 km is interpreted as outlining

the top of the main magma chamber (Figure 1.6; Scandone and Malone, 1985). The magma chamber is hypothesized to extend to depths of 14 km or more below the surface, based on seismicity immediately following the 1980 eruption (Figure 1.4 and Figure 1.6; [Scandone and Malone, 1985]).

The shallowest structure of the conduit clearly changed with time after the catastrophic eruption in 1980. Domes between 1980 and 1986 formed in lobes, stacked vertically, suggesting a nearly vertical shallow conduit [Anderson and Fink, 1990; Chadwick and Swanson, 1989]. Additionally, earthquake locations extended in a pipe to 2 km depth or more prior to each dome forming eruption. During the 2004-2008 eruption, earthquake locations were located beneath the southern margin of the 1980-1986 dome (Appendix 1, Figure 3; Thelen et al., 2008). The cloud of earthquake locations suggested a northward dipping structure that intersected the surface near the site of the 2004-2008 vent. The dip of the structure is supported by the off-center location of the 2004-2008 vent on the south of the1980-1986 dome and the trajectory of the spines during the 2004-2008 eruption [Vallance et al., 2008]. A GPS instrument on the 1980-1986 dome also moved to the north (23.5 cm) and up (90 cm) prior to the first explosion on October 1 [Lisowski et al., 2008]. This motion is consistent with a pressure source under the 1980-1986 dome pushing it to the north [M. Lisowski, pers. comm., 2009]. The weight of the evidence above implies that the 2004-2008 conduit had been deflected by the cold, hard 1980-1986 dome creating a distinct bend in the shallowest levels of the conduit.

4.1.2 Bezymianny

The regional seismicity at Bezymianny, determined by two independent data sets, is much more elongated and displaced from the vent than the seismicity at Mount St. Helens (Figure 1.13, Figure 2.6, Figure 2.8). The epicentral displacement to the north is in an elongated cloud of seismicity coincident with regional trends of basement depths suggesting a northward striking fault structure. This is clearly different than the pull-apart basin within which Mount St. Helens is formed [Weaver et al., 1987].

Though laterally displaced the depths and relative sizes of magma or volatile chambers at Bezymianny are broadly similar to those at Mount St. Helens. At approximately 2 km depth, there is weak evidence of a small aseismic zone beneath the edifice of Bezymianny (Figure 2.8). At Mount St. Helens, the shallow chamber may act to regulate material flux to the surface. The seismogenic manifestation of this is the concentration of small earthquakes within a very narrow depth range. Given the network that has existed around Bezymianny since 1999, it is not clear that the seismicity associated with a cap, such as seen at Mount St. Helens, is detectable. The catalog at Bezymianny had a magnitude of completeness of 1.6 until 2004 when network upgrades improved the magnitude of completeness to 1.3 [West et al., 2007]. Figure 4.51 shows the same time-depth plot shown in Figure 1.4 including only earthquakes greater than M1.3. Clearly, the picture of seismicity at Mount St. Helens is much different when only larger earthquakes are included. Considering only earthquakes greater than M1.3, no seismicity cap at 2 km is evident at Mount St. Helens. Thus at Bezymianny with the network that existed prior to 2007, any concentration of seismicity similar to that seen at ~2 km depth at Mount St. Helens

would be undetectable. Future analysis using the PIRE network will inevitably determine whether this feature is present at Bezymianny or not.

Seismicity prior to and after eruptions since 1999 at Bezymianny usually extended from the surface to a depth of approximately 6 km (Figure 1.11). This is clear evidence of stress changes either due to pressurization or depressurization of the conduit feeding the eruption. If the seismicity is associated with pressurization, than the vertical distribution of earthquakes suggests inflation of a conduit. Even minor (~1 m) inflation of a conduit can lead to large changes in Coulomb stress many kilometers away from the conduit [Roman, 2005]. These large changes in Coulomb stress will lead to earthquakes on a variety of fault planes around the conduit. Given this model a magma chamber or other pressurization source may logically exist where the seismicity ceases at depth.

Depressurization of the conduit and magma chamber is also an efficient source of seismicity after an eruption [Scandone and Malone, 1985]. After the May 25 and June 12, 1980 explosions at Mount St. Helens seismicity outlined the top of the magma chamber, presumably indicating the source of magma during the eruption. The May 25 and June 12, 1980 eruptions had similar eruptive volumes to the bi-annual eruptions at Bezymianny (~10^6-10^7 m^3; [Scandone and Malone, 1985]; [Belousov et al., 2002]; [Belousova, pers. comm., 2009]). If I assume a similar relationship at Bezymianny as exists at Mount St. Helens between depressurization seismicity and magma withdrawal, then the deepest extent of post-eruptive seismicity should mark the top of the magma chamber. Alternatively, the seismicity could cease at depth if inflation below 6 km deep were too small to generate significant Coulomb

stress changes or if the depressurization at this depth was taken up by viscoelasticity in the crust. The presence of a deeper magma chamber is supported by a coarse gravity study [Balesta et al., 1976-77]. In this study, a magma chamber was postulated to have a center of mass at 10 km deep, which is consistent with the interpretation of a magma chamber top at approximately 6 km deep. The volume or lateral dimensions of the magma chamber is not constrained by the current seismic data.

The seismicity underneath and to the north of Bezymianny decreases rapidly below 6 km depth (Figure 1.11, Figure 1.14). Seismicity above the magnitude of completeness of the KBGS catalog is generally absent between 6 and 33 km depth, except for an interval between 18 and 23 km. The seismicity near 33 km depth consists of low-frequency repeating earthquakes with high b-values [West et al., 2007]. This area is interpreted to be a deep magma chamber at the base of the crust [S. Senyukov, pers. comm., 2007]. The geochemical signals at Bezymianny and Klyuchevskoy suggest that they come from the same high magnesium and low water basalts, and thus it is postulated that the magmatic zone at 33 km depth feeds both volcanoes [Ozerov et al., 1997]. As seismicity between the shallow and deep magmatic systems is sparse, it is not clear how the magma is transported between volcanoes.

4.1.3 Comparison of Plumbing Systems

The structure of the plumbing systems at Bezymianny Volcano and Mount St. Helens is compared in Figure 4.52. Both systems possess a mid-crustal magma chamber at around 7 km below the active dome. Additionally, both volcanoes have a

small shallow zone that may be filled with either magma or a separate gas phase, or both. The horizontal extent of both magma chambers under Bezymianny is poorly defined by the seismicity, and thus the volume of the magma chamber under Bezymianny is unknown. Even though the Bezymianny main crustal chamber is shifted to the north, the similarity of plumbing systems between volcanoes is similar, which may have implications for similarities in eruptive behavior [Costa et al., 2007] or the length of pre-eruptive sequences [Moran et al., 2008].

4.2 Behavior of Multiplets

Earthquake families, or groups of earthquakes with similar waveforms, are a common occurrence on a variety of volcanoes exhibiting unrest (e.g. [Fremont and Malone, 1987]; [Rowe et al., 2004]; [Petersen, 2007]; [Stephens and Chouet, 2001]). Though common, the sensitivity of earthquake families to changes in magma dynamics within the volcanic plumbing system is yet to be established. If a link between earthquake families and changes within the volcano can be established, it could aid volcanologists in improved interpretations and forecasts. Here, I compare multiplets characterized at Bezymianny and at Mount St. Helens together to analyze which factors are important in the creation and alteration of multiplets. Because only a few month's worth of data are available for Bezymianny I will generalize from this relatively short record keeping in mind that, even though it included three eruptions this record is not as extensive as that at Mount St. Helens. I then summarize observations of multiplets at other volcanoes and interpret the behavior with respect to the type of activity at each volcano.

4.2.1 Multiplet comparison at Bezymianny and Mount St. Helens

Multiplets were present at Bezymianny during the fall 2007 eruptions (Section 2.2) and at Mount St. Helens during the 1982, 1983-1986 and 2004-2008 eruptions (Section 3.1, 3.4, Appendix A; [Fremont and Malone, 1987]). The eruption at Bezymianny in December 2006 also had multiplets prior to eruption [West et al., 2007]. The most striking difference between the two volcanoes was the difference in the multiplet percentage of total seismicity (MPTS). With only one exception, the MPTS was less than 15% during the entire study period at Bezymianny (Figure 2.17). At Mount St. Helens during the 2004-2008 eruption the MPTS was between 25 and 90%, with most of the study period above 40% MPTS (Figure 3.8).

The difference in values of MPTS between volcanoes can be interpreted in terms of eruptive style. Mount St. Helens from 2004-2008 only had small explosions and dominantly consisted of viscous dome building extruded as spines. The October 2007 eruption at Bezymianny was explosive. There was no evidence for viscous dome building after the eruption [A. Ozerov, pers. comm., 2008]. The viscosity, temperature and gas content of the material within the conduit near the multiplet source area must have been different for each eruption [Eichelberger, 1995]. At Mount St. Helens during the 2004-2008 eruption, the extrusion of smooth and rigid whalebacks is good evidence for efficient degassing of a viscous plug within the shallow conduit. Though the MPTS was not quantitatively determined, the conspicuous presence of multiplets during the 1983 and 1984-1986 dome-forming eruptions suggests a high MPTS. The dome-building eruptions from 1983 to 1986 possessed a degassed, viscous plug that was emplaced at a lower extrusion rate than previous dome-building eruptions [Swanson and Holcomb, 1990; Anderson and

Fink, 1990]. A high MPTS, as seen at Mount St. Helens during the 1983-1986 eruptions (Figure 3.2) and the beginning of the 2004-2008 eruption, suggests a strong relationship between the presence of a viscous and degassing plug within the shallow conduit and the generation of multiplets. A degassing plug in the shallow conduit requires permeability, and efficient degassing of the plug will likely lead to effusive eruptions or viscous dome building [Eichelberger, 1995; Gonnermann and Manga, 2003].

Alternatively, the low MPTS observed at Bezymianny in October 2007, occurred without the extrusion of juvenile spines or viscous dome-building [Ozerov, pers. comm., 2008]. Similar eruptions in 1997 at Bezymianny were observed to push out a cold and dense plug prior to eruption [Belousov et al., 2002]. This suggests that the conditions in the shallow conduit around the plug at Bezymianny prior to an eruption are cooler with little or no degassing. At least for these two volcanoes, the presence of a cold and degassed plug is not as efficient at generating multiplets as a warm, viscous and actively degassing plug. The striking difference in MPTS between explosive and extrusive eruptions suggests that tracking MPTS in a pre-eruptive setting could be used to forecast the type of eruption to come.

Not all dome-forming eruptions will generate multiplets. As seen in Figure 3.2, dome building eruptions at Mount St. Helens in 1981 and the end of 1982 did not generate a significant number of multiplets. The rheology of the plug must have certain properties that are based on the viscosity, gas content, and extrusion rate. The early Mount St. Helens dome-forming eruptions extruded gas-rich lobes at high extrusion rates [Swanson and Holcomb, 1990] that did not produce multiplets. The

high extrusion rates seen in the early dome-building phase between 1980 and 1983 may not have allowed for complete degassing and crystallization of the magma in the shallow parts of the conduit. Thus the resultant magma was less viscous and multiplets were not a dominant part of the overall seismicity. The 1982 eruption at Mount St. Helens only possessed precursory multiplets, without vigorous multiplet generation during dome building. Clearly the state of the shallow edifice was not conducive to multiplet generation once the conduit was opened to gas flow and extrusion at the surface. The cessation of multiplets when dome building started suggests that the source of the multiplets can be associated exclusively with degassing of the ascending magma within a semi-closed system, and may be more akin to the generation of multiplets at Bezymianny.

The number of contemporary multiplets at each volcano displayed very different characteristics. During the 2004-2008 eruption at Mount St. Helens, the number of contemporary multiplets ranged from 5 to 20, compared to values of 0 to 13 at Bezymianny. The number of contemporary multiplets increased prior to the explosions at Mount St. Helens in 2004, which is opposite the trend seen at Bezymianny volcano prior to the October 2007 eruption. This may be evidence for separate multiplet source processes at each volcano that are differentially affected by increasing pressure within the conduit and plug.

When quantified, the characteristics of multiplets at both volcanoes can be divided into those associated with pre-explosive time periods and those associated with non-explosive or background time periods. The average amplitude, standard deviation of the average, and duration of multiplets had similar characteristics before

and during explosive phases and non-explosive phases at both volcanoes (Table 4.6). Prior to explosions, the average amplitudes and amplitude variability (standard deviation) of each multiplet was higher during explosive time periods than during non-explosive time periods at each volcano. The durations of multiplets prior to and during explosions were also shorter than during non-explosive time periods at each volcano. During the 2004 eruption at Mount St. Helens, multiplet durations prior to explosive activity ranged from several hours to days. In contrast, at Bezymianny Volcano, multiplet durations immediately prior to explosive activity were only several hours in length.

There are several characteristics of multiplets that may make them useful in determining the type of eruption from pre-eruptive seismicity, and in tracking the state of the shallow conduit. The prominence of multiplets in a pre-eruptive seismic sequence suggests the presence of a dense, degassing plug in the shallow conduit as opposed to a stiff, cold plug. The divergence in trends of MPTS and the number of contemporary multiplets in different types of eruptions at Bezymainny and Mount St. Helens suggests that by analyzing the pre-eruptive seismicity, the type of ensuing eruption may be characterized. The common trends in amplitude, standard deviation and duration at both volcanoes suggests that these characteristics may be an indicator of increasing stresses and gas turbulence in the conduit and thus could be useful for forecasts of explosions at both volcanoes. This is remarkable considering the different nature of volcanic products and the different types of eruptions.

4.2.2 Multiplet comparison to other volcanoes

Before I present a generalized model for the generation of multiplets, I will summarize observations of multiplets on several other volcanoes. It should be noted that multiplets are usually only recognized in cases when the largest events during a particular period are part of an earthquake family or when the dominant seismicity is made up of a limited number of different multiplets. When many families are active simultaneously, it is often difficult to track each individual family with time unless the families have a distinguishing characteristic. Particularly in cases when the proportion of total seismicity made up by multiplets is low, it is hard to track multiplets manually. Thus the lack of a published record of multiplets on a particular volcano does not mean that they did not occur, only that they were not likely a distinguishing feature of the overall seismicity.

Seismicity at Unzen Volcano, Japan during its dome-forming eruption from 1990-1995 was dominantly made up of multiplets [Umakoshi et al., 2008b]. Multiplets were found across a range of dominant frequencies within the uppermost kilometer of the dome. During the 1990-1995 eruption, dome-forming was both endogeneous and exogenous with solidification of the magma within the conduit at 600m to 1.2 km below the surface [Nakada et al., 1995]. Events within each family changed slowly with time and the duration of most families was less than two weeks [Umakoshi et al., 2008b]. Time periods with a high number of contemporaneous multiplets were strongly correlated with high rates of high-frequency earthquakes. When low frequency earthquakes dominated, fewer contemporaneous multiplets were present. The amplitudes of events within each multiplet varied smoothly with time. Brittle failure of the melt is plausible as a source of high frequency multiplets at Unzen

[Goto, 1999]. Some low frequency events were associated with weak gas emissions from the dome surface of Unzen, which suggests that a model associated with gas flux is also possible [Umakoshi et al., 2008b].

At Soufriere Hills Volcano, Montserrat, the presence of multiplets is well documented [Rowe et al., 2004; White et al., 1998; Green and Neuberg, 2006]. The published multiplets at Soufriere Hills dominantly consisted of hybrid events. During phreatic explosions and prior to dome extrusion (before November 1995), families lasted days and consisted of several hundred to a few thousand events. After dome building began multiplets lasted weeks and contained up to ten thousand events. Multiplet families during this time period were found to change slowly through time, eventually losing their high frequency onset. Amplitudes were remarkably stable. During a period of dome growth in June of 1997, a more detailed analysis was completed by Green and Neuberg [2006]. During this time period, many families were present contemporaneously, and the occurrence of certain families was associated with depressurization of the conduit. Event amplitudes and waveforms were remarkably similar over the lifetime of a multiplet. A dome collapse during the study period affected the occurrence of multiplets, changing the behavior of all of the multiplets that were occurring at that time. One multiplet family was precisely located at 1.5 km deep [Neuberg et al., 2006], although the overall eruptive seismicity ranges between 1 and 2 km deep [Rowe et al., 2004]. The source of the multiplets was attributed to fracture on the edges of the extruding plug [Neuberg et al., 2006].

Mount Pinatubo, Philippines, had one of the largest eruptions in the 20th century in 1991. Approximately one month after the massive explosive eruption,

dome building began and lasted for approximately four months [Newhall et al., 1996]. During this time period, over 23,000 low frequency events were recorded, many of which belonged to multiplets that lasted for many days [Ramos et al., 1999]. The amplitude of low-frequency events varied slowly through the course of their lifetimes, however there was a limited range of amplitudes that was shared by all multiplets during any given time period.

Multiplets are also documented prior to explosive eruptions. One such example is Redoubt Volcano, Alaska during the 1989 eruption. Beginning approximately 19 hours before the first explosion, three distinct multiplets dominated the seismic record [Stephens and Chouet, 2001]. Both multiplets lasted only a few hours. The amplitudes of the events within the multiplets varied over multiple orders of amplitude. The envelope of the maximum amplitudes in a given time period increased, then decreased smoothly with time. Both multiplets ceased prior to the first explosion. The source of the multiplets was attributed to choked flow in a hydrothermal crack 1-2 km deep. Dome growth was suspected prior to the 1989 eruption but never confirmed [J. Power, pers. comm., 2009]. The most recent eruption of Redoubt in 2009 had abundant multiplets during dome-building and prior to eruptions [W. Thelen, unpublished data, 2009].

One case of intense multiplet occurrence without any associated eruptive activity is at Shishaldin Volcano, Alaska [Petersen, 2007], where low-frequency multiplets are common, but one multiplet dominates at any given time. Multiplets make up anywhere from 19% to 45% of the total seismicity during periodic swarms. The dominant multiplet has a lifespan from 13 to 30 days. Multiplets changed slowly

with time, often staying stable, and then changing over the course of several days into another stable multiplet. Since multiplets became a prominent aspect of the seismic record, there have been no eruptions although there is evidence for 3 cm of inflation prior to the start of the multiplets [Petersen et al., 2006] . The location of the multiplets are 200 m below the crater of the volcano. The multiplets are attributed to the vigorous hydrothermal system under the volcano.

Using all of the cases above, several consistent characteristics stand out. These characteristics are summarized in Table 4.7. The difference between multiplet characteristics in explosive and dome-building eruptions is similar to the difference in behavior at Mount St. Helens and Bezymianny Volcano (Table 4.6). Multiplet durations prior to and during explosive eruptions were considerably shorter (hours) compared to multiplets during dome-building eruptions (days-weeks). The variability of events within multiplets was also less during dome-forming eruptions compared to explosive eruptions. Both the smooth variability and long durations of multiplets during dome forming eruptions suggests more stable stress and pressure regimes, resulting in slowly varying seismic sources. Alternatively, the high amplitude variability of events within multiplets and short durations suggest rapid changes near the seismic source for explosive eruptions. The number of contemporary multiplets is also lower during explosive eruptions than during dome-building eruptions. This is consistent with the observations of variability and duration. The MPTS of dome-building eruptions is generally higher than explosive eruptions. As mentioned before, multiplets are usually detected manually only when they are a conspicuous part of the overall seismicity. This is often the case when multiplets dominate the seismic

record. Assuming that published cases of manually detected multiplets represent periods of high MPTS, the MPTS during dome-building eruptions is much higher compared to explosive eruptions. One exception is the high MPTS prior to the explosion at Redoubt Volcano in 1989 although dome growth did occur at Redoubt approximately 7 days after the first eruption [Power et al., 1994]. The high MPTS at Redoubt suggests that the conditions within the shallow conduit consisted of a viscous and degassing plug, which fits with the inference of dome building prior to the first explosion [J. Power, pers. comm., 2009].

4.2.3 Generalized Model

I propose a general model where the emplacement of an actively degassing, viscous plug within a stable conduit will generate multiplets and that the percentage of multiplets relative to the total seismicity is a function of the stability of the conduit and the rheologic state of the plug. Stability in this context is defined as the systems ability to sustain several contemporary, long duration multiplets. In this model, a partially crystallized and degassing plug provides the environment most conducive to the generation of multiplets. The surface expression of such a plug is often the extrusion of a spine or whaleback. Alternatively, when the extrusion rate is too high to allow for crystallization and degassing (>1-3x10^{-4} m/s, [Cashman et al., 2008]), multiplets are not conspicuous. Likewise, when there is a plug of cold magma, such as a cap from a previous eruption, multiplet generation is not as efficient. This model has dramatic implications for forecasting, as the duration, number of contemporary multiplets and MPTS can be tracked in real-time to determine the type of eruption and the timing of explosions. When the plug is significantly disrupted or destroyed, as in

the case of an explosion, the multiplet sources present prior to the disruption do not occur after the disruption. This is true regardless of the state of plug within the conduit and supports the close relationship between the plug and the occurrence of multiplets. In special cases, such as that at Shihaldin, a system can generate pervasive multiplets with long durations without the presence of a degassing magma plug.

Mulitiplets have many forms, and understanding the source processes behind such phenomenon will help in understanding the significant observations of the model. Multiplets may be divided into three general sources: 1) repeated slip on a pre-existing weakness, 2) fluid-driven crack excitation and resonance, and 3) slip or fracture associated with a solidified plug in the presence of gases or fluids. Repeated slip on pre-existing weaknesses can be recognized by the presence of repeating high-frequency earthquakes. This source type may also generate hybrid events if there is gas or fluids nearby. They may occur at any depth. Two examples are the post-May 18, 1980 multiplet sequence and the September 23 – September 25, 2004 sequence at Mount St. Helens.

Fluid-driven excitation is a popular model that has been applied to many volcanoes to explain individual low-frequency earthquakes (e.g. Chouet, 2003). Its application as a multiplet source has also been demonstrated [Waite et al., 2008; Chouet et al., 1994]. This source may be present at any depth where a gas phase or magma is present. Fluid-driven excitation and resonance may or may not occur coeval with slip or fracture of the fractured plug, which makes them particularly hard to separate as multiplet sources. The deficiency of reported cases of multiplet

development prior to large explosive eruptions, where spines or whaleback structures were not extruded, suggests that fluid driven crack excitation alone is an inefficient way to generate a large number of conspicuous long duration multiplets. Few case studies of gas-driven crack excitation in a repeating earthquake sequence have been reported prior to an eruption when the conduit is closed (i.e. Redoubt, 1989 [Chouet et al., 1994]). This suggests that the permeability of the upper part of the edifice may play a role in the efficiency of fluid-driven crack excitation as a source of multiplets.

Many dome-forming eruptions are often reported as possessing many multiplets that are active for long time periods (Table 4.7). The movement of a solid plug may generate repeatable low-frequency and hybrid seismicity along the edges of the conduit [Neuberg et al., 2006; Goto, 1999]. Indeed, the frictional properties of the gouge on the outside of the 2004-2008 MSH plug support a stick-slip source on the plug margins[Iverson et al., 2006]. Many potential sources may exist around the perimeter of the plug as it moves upward, creating many contemporary multiplets. Magma fracture may also be a significant source of low-frequency multiplets when there is a constriction or geometrical change in the conduit [Massol and Jaupart, 2009]. These sources generally have depths in the upper 1.5 km under the dome. This is the depth coincident with the quenching of quartz microlites within the ascending magma again suggesting a relationship between the viscosity of the plug and the development of multiplets [Cashman et al., 2008]. Fluid-driven crack excitation may be aided by the presence of a solid degassing plug. If permeable conduit walls exist, then gas can escape into the surrounding country rock, potentially creating several contemporary multiplets in a dendritic network around the conduit.

As previously mentioned, this mechanism is likely most efficient in the presence of a closed system but before the stresses and pressures become large and chaotic prior to an explosion. The coincidence of extruded spines and whalebacks with pervasive multiplet development suggests that the fracture and slip of magma within the conduit is a more efficient generator of multiplets than fluid driven crack excitation.

4.3 Pre-eruption Signals

The ability to forecast the type and timing of eruptions is a major goal in volcano science. Both Bezymianny and Mount St. Helens have had eruptive periods over which successful forecasts have been issued (e.g. Swanson et al., 1985; Senyukov et al., 2004). Given the similar circumstances under which both volcanic sequences started, it is useful to look at the pre-eruptive buildup to eruptions from both volcanoes to understand if certain characteristics are unique to certain types of eruptions. Such an understanding of the variation, relative strengths and commonalities will aid in improved forecasts at both volcanoes in the future.

4.3.1 Pre-collapse seismicity

The pre-collapse sequence at both Bezymianny Volcano and Mount St. Helens are remarkably similar (Figure 4.53). The buildup of seismicity at Bezymianny before the relatively small first explosion lasted approximately a month and consisted of hybrid and low frequency earthquakes [Tokarev, 1981]. Similarly, at Mount St. Helens the initial buildup in moment release lasted 12 days, consisting mostly of volcano-tectonic (VT) earthquakes (Figure 4.53; [Endo et al., 1981]). The overwhelming majority of earthquakes at both volcanoes during the initial buildup were shallower than 5 km [Tokarev, 1981; Endo et al., 1981]. Depths were

particularly difficult to determine at Bezymianny because the closest station was 42 km away [Tokarev, 1981]. The first explosions occurred near the peak in energy and earthquake rate at both volcanoes.

After the initial peak in energy, seismic strain release and earthquake rate, the energy release in both sequences remained nearly constant (Figure 4.53). At Mount St. Helens, the decrease in the number of earthquakes per day followed an Omori-type decay, with a decay parameter that suggested a relatively slowly decreasing stress process [Neri and Malone, 1989]. At both volcanoes as the number of earthquakes decreased, the magnitudes of individual events increased, creating a relatively constant energy release (Figure 4.53;[Tokarev, 1981; Endo et al., 1981]). In both cases, the constant energy release was accompanied by phreatic explosions and deformation of the edifice of the volcanoes that was associated with the emplacement of a cryptodome [Gorshkov, 1959; Lipman et al., 1981]. Low frequency earthquakes were more conspicuous during this phase. At Bezymianny volcano, there was a sharp decrease in seismic and explosive activity about 1 month prior to the edifice failure on March 30, 1956. No such significant decrease in seismic parameters occurred prior to the collapse at Mount St. Helens. Overall, the pre-eruptive sequence at Bezymianny lasted approximately three times longer than the sequence at Mount St. Helens, even though the volumes of the emplaced cryptodomes were not significantly different (Table 4.8).

At both volcanoes, the earthquake associated with the dome failure was larger than any of the pre-eruptive earthquakes (Bezy: M4.9, MSH: M5.1; [Tokarev, 1981; Endo et al., 1981]). In addition, the lack of any significant increase in seismic

energy just prior to the collapse strongly supports a spontaneous failure of the edifice in both cases, which initiated the remainder of the eruptive sequence. This is supported by further analysis of the M5.1 event at Mount St. Helens, which shows the source process is most likely a single horizontal force, not a double couple as would be expected in a tectonic earthquake [Kanamori et al., 1984].

There was a bimodal distribution of density of erupted magmas at both volcanoes. The dense fraction was interpreted to reflect degassing of the stalled cryptodome in the shallow edifice [Thelen and Team, 2006; Hoblitt and Harmon, 1993]. The higher dominant frequencies and shallower depths in the beginning stages of the seismic swarm followed by an Omori-type decay to a relatively constant energy release with low frequency earthquakes suggests that the cryptodome was emplaced rapidly at first, then slower with time at both volcanoes [Neri and Malone, 1989]. At Mount St. Helens, the deformation rate was faster before April 20, 1980 as opposed to after, supporting an early, rapid emplacement of the cryptodome [Moore and Albee, 1981]. The longer pre-eruption sequence at Bezymianny may be due to the slightly larger cryptodome volume at Bezymianny compared to Mount St. Helens.

Assuming a similar failure strength for both edifices, the length of the pre-eruptive sequences at both volcanoes may be dependent on the intrusion rate. The average intrusion rate (total volume/length of precursory seismicity) at Mount St. Helens was almost double that at Bezymianny (20.9 m^3/s, 9.5 m^3/s, respectively). Based on the seismicity and deformation at both volcanoes, the cryptodomes were emplaced at similar depths under the edifice. A relatively slow intrusion rate would clearly allow for more cooling of the intruded magma prior to failure. A vigorous

hydrothermal system could have assisted in rapid cooling of the shallowest levels of the crytodome. Rapid cooling of the shallow conduit was shown at Unzen Volcano when the 1990-1995 conduit was drilled less than 10 years after the end of the eruption, only to find conduit temperatures of 160-180 degrees C [Ikeda et al., 2008]. The initial temperatures in the shallow conduit during the eruption were as high as 775 degrees C [Noguchi et al., 2008]. The cooled magma within the edifice of Bezymianny may have acted to strengthen the cone temporarily and allowed for the additional volume of magma intruded (Table 4.8). Both eruptions began with a landslide and lateral blast, and were soon followed by a plinian eruption [Mullineaux and Crandell, 1981; Gorshkov, 1959]. Failure of the edifice left a similar size crater at both volcanoes (Table 4.8).

4.3.2 Discrete Dome Forming Seismicity

After the collapse, the maximum magnitude of seismicity declined precipitously at both volcanoes, though the number of earthquakes remained high (Figure 4.54). Immediately after the edifice collapses, some explosive activity without dome formation occurred for 7 days and 6 days at Mount St. Helens and Bezymianny, respectively [Mullineaux and Crandell, 1981; Tokarev, 1981] . The first obvious dome formed on Mount St. Helens within 25 days of the collapse, while at Bezymianny volcano, it formed 7 days after the collapse [Mullineaux and Crandell, 1981; Tokarev, 1981]. Dome growth at Bezymianny then occured continuously at a very high rate for a year. Alternatively, explosive activity continued for 6 months at Mount St. Helens, destroying 2 small lava domes in the process. Interestingly,

although the intrusion rate was higher prior to collapse at Mount St. Helens, the dome at Bezymianny grew much faster after the failure of the edifice.

Discrete dome-building episodes began 21 months and 6 months after the edifice collapse at Bezymianny volcano and Mount St. Helens, respectively. Each dome-building eruption was preceded by an increase in seismicity, specifically shallow (<2 km deep) low-frequency earthquakes (Figure 4.54; [Tokarev, 1981; Malone et al., 1981]). At Mount St. Helens, discrete dome forming eruptions were also accompanied by surface events such as rock avalanches and small steam explosions[Malone and Pavlis, 1983]. Given the sparse network around Bezymianny, it is unlikely that such events were detectable. Discrete dome-forming events lasted 1-3 weeks at both volcanoes, with relative quiescence between eruptions. The similarity in the characteristics and timing of dome-building seismicity at Bezymianny and Mount St. Helens further suggests a similar conduit geometry [Costa et al., 2007]. Unlike Mount St. Helens, discrete dome-forming eruptions at Bezymianny were commonly associated with large explosions. This may be due to the increased gas content present at Bezymianny compared to Mount St. Helens (Table 4.8). At Bezymianny, the discrete dome-building phase lasted for about 4 years while at Mount St. Helens it lasted for approximately 6 years.

At Mount St. Helens, magma intruding into the dome during the discrete dome forming phase became more viscous with time, opposite the pattern shown at Bezymianny [Swanson and Holcomb, 1990; Tokarev, 1981]. Coincident with a more viscous magma was a larger number of earthquakes and larger moment releases seen in the eruptions at Mount St. Helens between 1984 and 1986 (Figure 4.54; [Neri

and Malone, 1989]). Mount St. Helens experienced a lull in activity between November 1986 and September 2004. Discrete intrusion at depth was ongoing, as evidenced by seismic swarms at magma chamber depths and focal mechanisms suggesting pressurization of a pipe (Figure 1.4; [Musumeci et al., 2002; Moran, 1994]). Bezymianny experienced nearly continuous extrusion at the end of the discrete dome building phase for 5 years before it became highly explosive[Tokarev, 1981].

The opposing trends in viscosity at Mount St. Helens and Bezymianny can likely be attributed to the changing compositions of magmas and changing magmatic temperatures. Assuming constant gas content within a given system, changes in SiO_2 content and temperature will dramatically change the viscosity [Witter, 2003]. Although initially similar in SiO_2 content, the erupted materials at Bezymianny dropped 2% (61% to 59%) between 1956 and 1970, while the erupted materials at Mount St. Helens increased by 4% (60% to 64%) between 1981 and 1986 [P. Izbekov, pers. comm., 2009][Pallister et al., 1992]. During the same time period, temperatures of crystallization rose at Bezymianny and fell at Mount St. Helens [P. Izbekov, pers. comm.., 2008; Cashman et al., 2008]. At Mount St. Helens, the increase in SiO_2 and the drop in temperature clearly increased the viscosity which may have been a factor in cessation of extrusion after 1986. The gas content decreased at Mount St. Helens during the 1980-1986 eruption, which would further increase the viscosity and make it more difficult to extrude magma (Table 4.8). At Bezymianny, however, the viscosity decreased with increasing temperature and

decreasing SiO_2, making it easier to utilize the existing plumbing system with time and enabling continued dome growth [Tokarev, 1981].

4.3.3 Continuous Dome Forming Seismicity

Beginning in 1965 and lasting for approximately 5 years, Bezymianny entered into a phase of continuous dome growth, which was marked by high rates of shallow (<2 km) hybrid and low-frequency seismicity with magnitudes similar to or higher than during the discrete dome-building phase (Figure 4.54; [Tokarev, 1981]). The extrusion of rigid blocks or viscous lava accompanied increased earthquakes and spasmodic tremor large enough to be recorded at the nearest seismic station 16 km away[Kirsanov and Studinikin, 1971]. By analogy to Mount St. Helens during the 2004-2008 eruption, closely spaced very shallow earthquakes may be highly attenuated at as little as 10 km away from the vent [Thelen et al., 2007], creating the apparent recording of spasmodic tremor in the far-field. Fluid lavas formed thin, short lava flows that accompanied deeper, high frequency seismicity. In 1966, spine extrusion occurred at the surface. In 1967, a smooth feature formed on the extrusive dome called the “Nautilus” [Kirsanov and Studinikin, 1971]. This feature was remarkably similar in form and dimension to the “Whalebacks” seen during the 2004-2008 dome forming eruption at Mount St. Helens (Figure 4.55). The entire eruption consisted of several periods of heightened seismic activity lasting 1-2 months, separated by 2-4 months of seismic quiescence. The shift from discrete to continuous dome growth at Bezymianny was attributed to a shift to less viscous magma [Tokarev, 1981]. The composition and mineralogy of magmas between the

discrete and dome forming phase at Bezymianny was unchanged [Bogoyavlenskaya and Kirsanov, 1981].

Between 2004 and 2008, Mount St. Helens exhibited a continuous phase of dome building that was broadly similar to the continuous phase of dome building at Bezymianny between 1965 and 1970. The eruption started in September, 2004 with very strong seismicity, over 4 times the moment release that had occurred during the entire dome forming process between 1980 and 1986 (Figure 4.56). Two cases of strong tremor occurred during a number of minor explosive eruptions starting approximately 7 days after unrest began. The first extrusion began 18 days after the first seismic unrest and soon extrusive spines were being emplaced at the surface (Figure 4.55). Like the continuous dome forming eruption at Bezymianny between 1965 and 1970, seismicity was dominated by shallow (< 2 km deep) low-frequency earthquakes over the entire extrusive phase of the eruption (Figure 1.4). Similar to Bezymianny, the composition of the magmas between the discrete dome building phase and the continuous dome building phase were largely unchanged [Pallister et al., 2008]. Unlike the eruption at Bezymianny, seismicity gradually declined throughout the course of extrusion roughly instep with the decline in extrusion rate, although the rate of moment release was still higher than at any point in the discrete dome building phase (Figure 4.56). At Bezymianny, the continuous dome-building phase was not notably larger in its 5-day seismic strain release rate, maximum magnitude, or earthquake rate compared to the discrete dome-building phase.

A significant difference between the two volcanoes was the repose time prior to the continuous phase. There was only a short hiatus in activity at Bezymianny

prior to the continuous phase of eruption, and as a result, the conduit was essentially open and extrusion continued with similar seismic characteristics to the discrete phase. A similar situation occurred during a year-long continuous dome-building phase at Mount St. Helens in 1983. There was less than 6 months repose time prior to the start of that continuous eruption, and thus, no significant cap had developed and seismicity during the continuous extrusion was not seismically notable with respect to the neighboring discrete eruptions (Figure 4.56). Prior to the 2004 eruption at Mount St. Helens, there was a nearly 18 year hiatus in surface extrusion. Clearly, this permitted a cap to develop within the 1980-1986 dome that had to be overcome before extrusion continued. Extruded magma was highly degassed and contained 65% SiO_2 which, intuitively would drive up viscosity and increase resistance compared to the 1980-1986 erupted products, creating higher seismicity as well [Pallister et al., 2008].

The relationship between repose time and moment release at Mount St. Helens followed a well-defined trend in log-log space (Figure 4.57). The magnitude-equivalent moment release was calculated using the earthquake catalog in Figure 1.4. The catalog is not complete below magnitude 3 prior to the May 18, 1980 eruption, or during the 2004 eruption, so the values shown are a minimum [Endo et al., 1981]. The 2004 eruption may be up to 0.5 magnitude units low [Moran et al., 2008]. Earthquakes were used in the magnitude-equivalent moment release calculation that occurred 14 days prior to the eruption. In the case of explosions with good timing, no earthquakes after the explosion were used. In the case of dome-forming eruptions where the onset of extrusion was not well defined, earthquakes

occurring on the day of the published start of the eruption were used [Swanson and Holcomb, 1990]. For the 2004 eruption, earthquakes within a time period up to the first extrusion of October 11 were used. For the 1980 eruption, the entire earthquake sequence after March 30, 1980 was used. The prior eruption to the 1980 eruption was the extrusion of the Goat Rocks dome in 1857 [Pallister et al., 1992]. The phreatic explosions between 1989 and 1991 were not included. Clearly, eruptions that occurred with a shorter repose time, defined as the time between the end of the last eruption and the start of the next, had a lower moment release than eruptions with a longer repose time. The relationship holds regardless of eruption type.

The strong relationship between repose time and moment release is very important in that it suggests that by knowing the time since the last eruption, you can estimate within a magnitude unit the moment release required for an explosive or extrusive eruption to begin. Physically, this relationship suggests that the strength of the rock in the uppermost conduit is the limiting factor in the emergence of juvenile material at the surface. Additionally, this relationship shows that explosive eruptions do not scale any differently than dome-forming eruptions with respect to the magnitude of the seismic moment release. The five eruptions that had the highest magnitude-equivalent moment release (excluding the 1980 eruption) also occurred when the largest dome volume was present at the surface. Three of the five eruptions lie above the best-fit line in Figure 4.57. This suggests that the lithostatic load of the dome on the crust may have been a second-order process dictating the strength of pre-eruptive seismicity.

The relationship between repose time and magnitude-equivalent moment release prior to eruptions at Bezymianny volcano is not as clear. The 1956 eruption and the eruptions between 1999 and 2009 at Bezymianny are plotted in Figure 4.57. There are several pitfalls in the analysis of repose times at Bezymianny. Since the volcano was not as well-monitored as Mount St. Helens, the start and stop times of eruptions are not well constrained. The timing of large explosions is precise; however the duration of dome-building and lava flows after the event is poorly documented. Thus the repose times, particularly between eruptions spaced closely in time, could be in error. To better estimate repose times, I considered an eruption finished at the first point when the KBGS classified the seismic activity to be at background levels. In this analysis, I considered seismicity 2 weeks prior to the eruption, unless precursory activity was documented to last longer. I included the seismicity on the day of the eruption as well, assuming the dome building and/or lava flows began in earnest after the explosions. Eruptions for which the seismicity was obscured by activity at Klyuchevskoy are not plotted.

The results of repose time compared to the moment release at Bezymianny are not conclusive. Eruptions have been frequent at Bezymianny since 1999, and thus there is not enough data at longer repose times to characterize a well-defined trend. Further, for short repose times, several eruptions may have been grouped into one eruptive sequence. The only constraint at long repose times was the 1956 eruption. I assumed a repose time of 1000 years [Braitseva et al., 1991], and found a similar relationship to that seen at Mount St. Helens between repose time and

moment release. This suggests, as at Mount St. Helens, that the competence of the cap rock is the controlling factor in the seismic energy release prior to eruption.

A long repose time explains the initially energetic seismicity at Mount St. Helens, but not the ongoing high rate of moment release once extrusion began and the conduit system was open. Seismic data during the extrusion of the Nautilus at Bezymianny shows that a solid plug could be extruded without an anomalously high rate of seismicity with respect to the discrete dome building seismicity (Figure 4.54). It is important to note that the Nautilus was extruded out of the top of the dome. Alternatively, the whaleback at Mount St. Helens was extruded through a new vent to the south of the 1980-1986 dome. Earthquake locations show a north-dipping conduit under the root of the 1980-1986 dome (Appendix A, Figure 3). All of the seismicity during the 2004-2008 eruption was within 2 kilometers of the surface, and thus in the zone where the conduit was required to bend to connect from the 1980-1986 conduit to where the extrusion was occurring. This bend is near the solidification depth of the plug and the source of tilt events ([Cashman et al., 2008]; [K. Andersen, pers. comm., 2008]). Perhaps a constriction developed where the solid plug bends between the 1980-1986 conduit and the new conduit. Constrictions in shallow conduits have been found to be sources of cracking of the plug [Massol and Jaupart, 2009]. Thus seismicity associated with cracking of the plug near a constriction may be a good candidate for the increased seismic energy release of the 2004-2008 eruption at Mount St. Helens.

4.3.4 Seismicity associated with explosive eruptions and lava flow formation

Since 1976, long, thick lava flows at Bezymianny have accompanied strong explosions that often destroyed large parts of the dome ([Bogoyavlenskaya and Kirsanov, 1981]). During the latest phase of activity, eruptions have occurred 1-2 times each year. Prior to eruptions associated with dome extrusion and lava flows, as defined by Venzke et al. (2008) , there was always an increase in catalog seismicity between 7 km deep and the surface (Figure 4.58). The cumulative moment release clearly accelerated prior to each eruption. The magnitude of completeness of the catalog is as low as M1, but was sometimes much higher depending on the activity at nearby Klyuchevskoy [S. Senyukov, pers. comm., 2008]. It is important to note, that much of the activity that characterizes the precursory phase of these eruptions is in the form of rockfalls from the surface of the dome, that are not located by the network, and thus do not show up in Figure 4.58. These signals are detectable with continuous data however, as shown by the increase in rockfall and LFLDEs prior to the October 14, 2007, eruption (Figure 2.11, Figure 2.22). Little locatable seismicity was present after each eruption, showing that the process of emplacing a lava flow produced generally small-magnitude seismicity that was not locatable by the network. In Figure 2.22, it can be seen that the lava flow was accompanied by high rates of low frequency earthquakes, high-frequency earthquakes and LFLDEs. Given the amplitude distribution in Figure 2.11, most of the high-frequency events detected in the continuous analysis are low amplitude signals that were not locatable by the local network. It should be noted that even though these eruptions produced powerful explosions and pyroclastic flows, the magnitude-equivalent moment releases were relatively low compared to Mount St. Helens (M2.3-M3.1).

There were variations in the general eruptive sequence at Bezymianny since 1976. Some eruptions did not include both dome building and lava flows, or occurred without an explosion. Some of the atypical eruptions since 1999 are shown in Figure 4.59. There were no clear differences in the number of events or cumulative moment release of locatable seismicity between eruptions with different eruptive characteristics. One exception may be in the case of exclusive dome building. In the single scenario since 1999, the number and moment release of locatable seismicity remained low until a week after the beginning of extrusion. Since this only represents a single case, more data is needed in order to establish if this was a feature unique to that eruption. Continuous data from the PIRE network should be closely monitored in the future to understand if there are microseismic patterns that discern one eruptive style from another, such as the peak in maximum frequency at 4 Hz associated with the October 14, 2007, lava flow.

4.3.5 The Future of Mount St. Helens

The activity at Mount St. Helens from 1980 to 2008 has had many parallels to the activity at Bezymianny Volcano since 1956. Both have gone through the emplacement of a crytodome and subsequent edifice failure, a discrete dome building phase, and a multi-year continuous phase of dome building. At Bezymianny, the continuous dome building phase was followed by an explosive phase that is continuing, which is marked by large explosions and lava flows. One potential model of the activity within the conduit at Bezymianny is shown in Figure 4.60. In this general model from Shinohara [2008], exsolved gases from convecting magma within the conduit collect under a hardened plug. Magma convection is probable in a

conduit containing silicic magma 5-20 meters across [Witter, 2003]. Accumulating gas pressure beneath the cool and rigid plug drives extrusion at the surface of the dome prior to the characteristic large explosion. An increase in low-frequency earthquakes prior to an eruption is likely associated with the movement of the cool plug and suggests that there are fluids and gasses present just below the hypocentral region. The extrusion of a cooled spine has been observed in a handful of cases at Bezymianny prior to large explosions [Belousov et al., 2002]. The rockfall signals and LFLDEs prior to an eruption are interpreted to be evidence of mass wasting from the cooled plug at the surface as it is rapidly deformed. A large explosion occurs when the gases that have collected under the plug reach the dome surface and decompress catastrophically. At Bezymianny, several explosions may occur during any single eruption, which likely represents second-order complexities in this very simple model. Explosions may also be aided by large weaknesses in the dome that have often been observed to fail during eruptions. Subsequent to the large explosion or explosions, lava effuses onto the surface. At Bezymianny, a lava flow pours out of the newly opened conduit until the flow in the conduit slows, or the lava gets too cool, in which case a plug develops and the process starts over again.

Is Mount St. Helens likely to follow the same pattern? Yes and no. Given their similar eruptive pasts, it is likely that Mount St. Helens, like Bezymianny, will enter into another discrete eruptive phase. However, even given the same conduit model for Mount St. Helens as for Bezymianny, the resultant activity may not be the same because of the divergence of SiO_2 content (57% Bezymianny, 64% Mount St. Helens), gas content and magmatic temperatures at both volcanoes. Future

eruptions with more than a few months of repose time will surely push up cold, hardened plug material initially. At Bezymianny, the seismic expression of the extrusion of a cold plug is minor shallow seismicity and increased rockfall off of the dome. At Mount St. Helens, the dome is not as large or unstable, and thus the seismic expression of the plug being pushed to the surface will likely be similar in the occurrence of event types to the seismic sequence in September 2004. In particular, a pre-eruptive seismic swarm will evolve from high-frequency earthquakes to hybrid earthquakes to low-frequency earthquakes. Prior to dome extrusion in 2004, a significant chunk of the old dome was uplifted, thus providing a quality seismic record of that particular phenomenon from which to be compared to in the future [Pallister et al., 2008]. Earthquakes will likely have an equivalent moment release in accord with the repose time since the last eruption (Figure 4.57).

Assuming that gas content at Mount St. Helens stays low, similar to that found in the magma in the 2004-2008 eruption, the decompression of the gas cap at the surface will result in relatively minor explosions. Only an increase in gas content, which ideally would be measurable at the surface prior to an explosion, would create large explosions as are currently seen at Bezymianny. At both volcanoes, the decompression of the gas cap trapped under the plug should be preceded by a dramatically increasing moment release. With earthquake location and moment release, it may be impossible to forecast which phenomenon will be present during a given eruption because of the variability in pre-eruptive sequences and the independence of total moment release and the size of explosions (Figure 4.57, Figure 4.58, Figure 4.59). It may be possible to forecast the type of ensuing eruption by

tracking characteristics such as MPTS and number of contemporary multiplet during the pre-eruptive seismic swarm.

Once the conduit is opened, many possibilities exist. At Bezymianny, lava flows are common after the explosive phase. Clearly, the dacitic composition of the current magmas at Mount St. Helens make this phenomenon a remote possibility. If conduit ascent rates are low (~1-3x10^{-4} m/s), than degassing and crystallization of the extruding magma can occur within the conduit, which will produce spines and whalebacks [Cashman et al., 2008]. If instead conduit ascent rates are higher, then dome lobes will form, such as those seen in 1980-1986. It is possible to see multiple compositions during a single eruptive sequence, as was seen in the combination of dacitic and andesitic eruptive products during the Goat Rocks eruption in the early 19^{th} century. If the composition changes to andesite, then lava flows are more likely due to the reduced viscosity of andesite compared to dacite. Seismicity during this open conduit phase at Mount St. Helens will consist of low-frequency and hybrid earthquakes, as largely seen at Mount St. Helens during the 1980-1986 sequence. Conspicuous multiplet sequences will also be present at low ascent rates.

This activity is also supported by previous eruptions, including the most recent Goat Rocks eruption. This eruptive sequence lasted nearly 60 years and was characterized initially by a large explosion and then effusive behavior [Pallister et al., 1992]. It is also clear from the pervasive dacite domes exposed within the wall of the crater, that effusive behavior is common in Mount St. Helen's eruptive history.

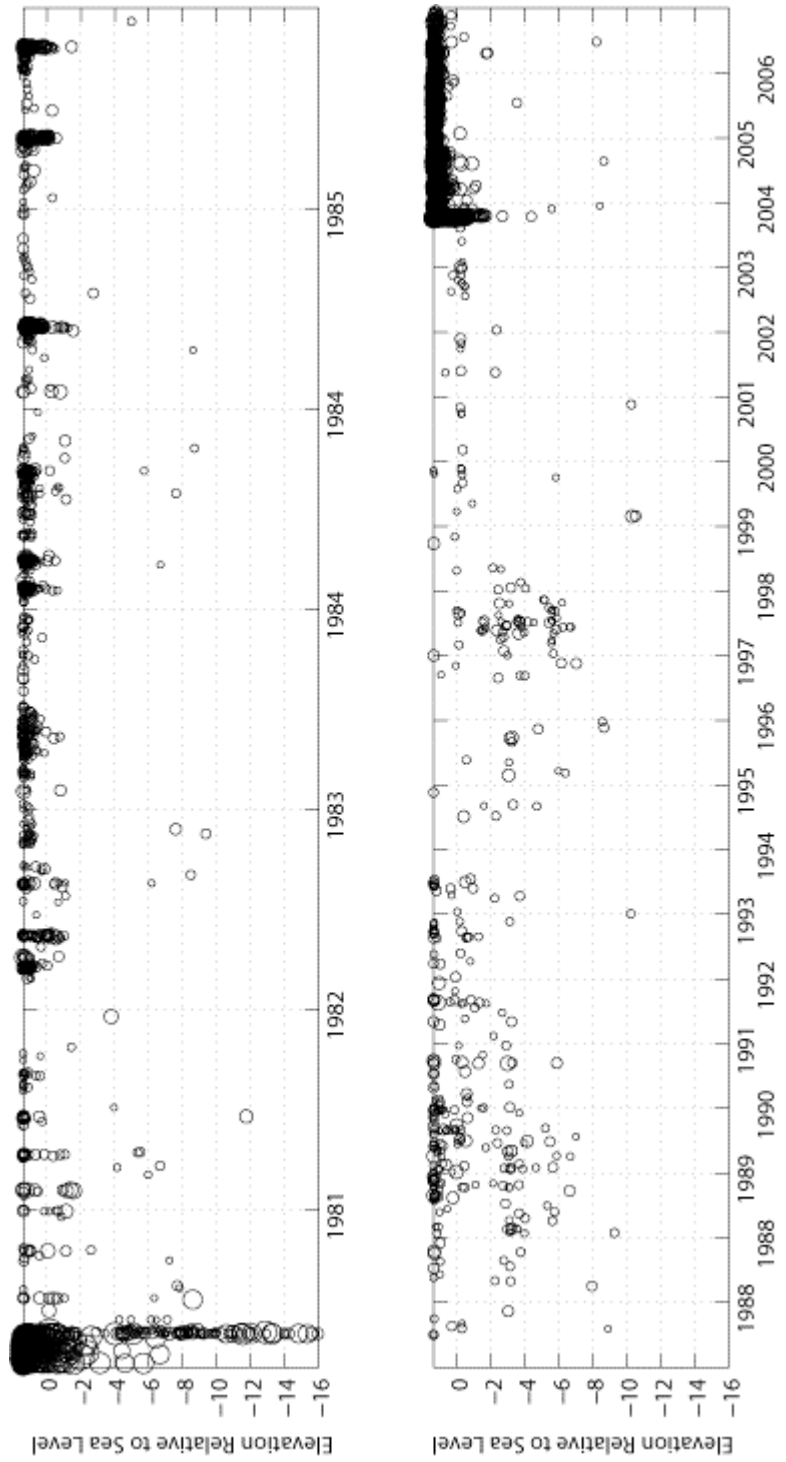

Figure 4.51: Mount St. Helens time-depth plot with earthquakes greater than M1.3. Compare to Figure 1.4.

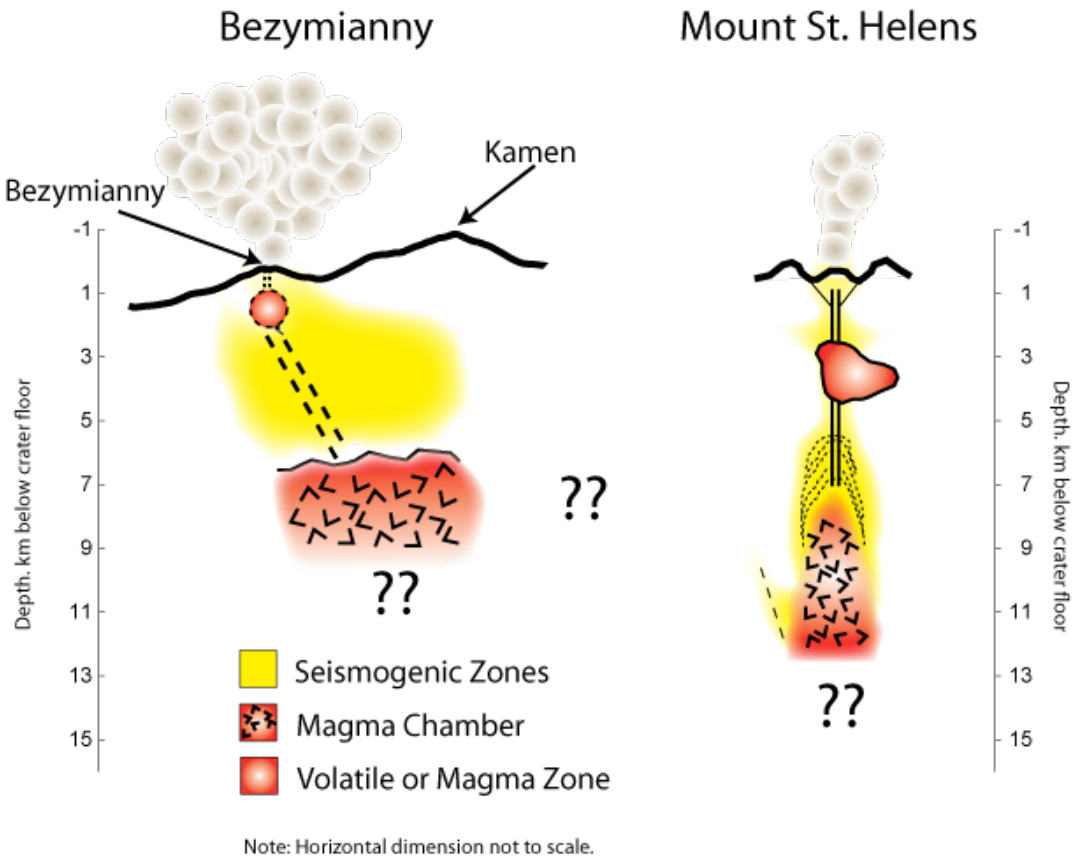

Figure 4.52: Schematic cross-section of plumbing systems at Bezymianny Volcano and Mount St. Helens. The horizontal scale within each system is accurate, however the horizontal scales between systems is different. For reference, the edifice of Mount St. Helens is about the same size as Bezymianny Volcano. Dotted lines on the Mount St. Helens model refers to magmatic stoping [Pallister et al., 1992]. The dashed line in the Mount St. Helens model refers to a fault. Mount St. Helens model modified from Pallister et al. (1992) and Waite et al. (2006).

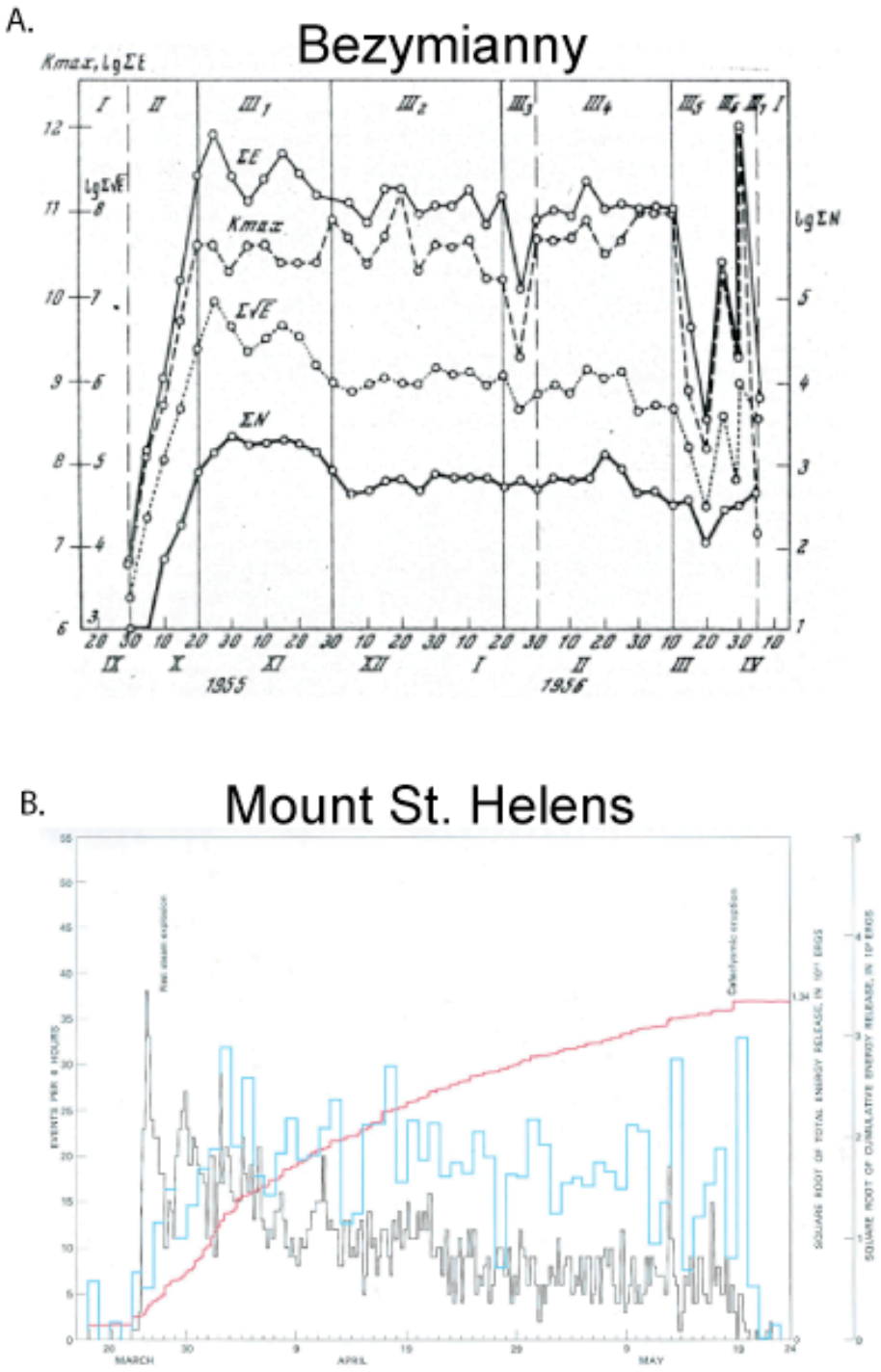

Figure 4.53: Comparison of pre-collapse seismicity at Bezymianny Volcano and Mount St. Helens. Refer to Figures1.8 and 1.2 for detailed explanations of A and B, respectively.

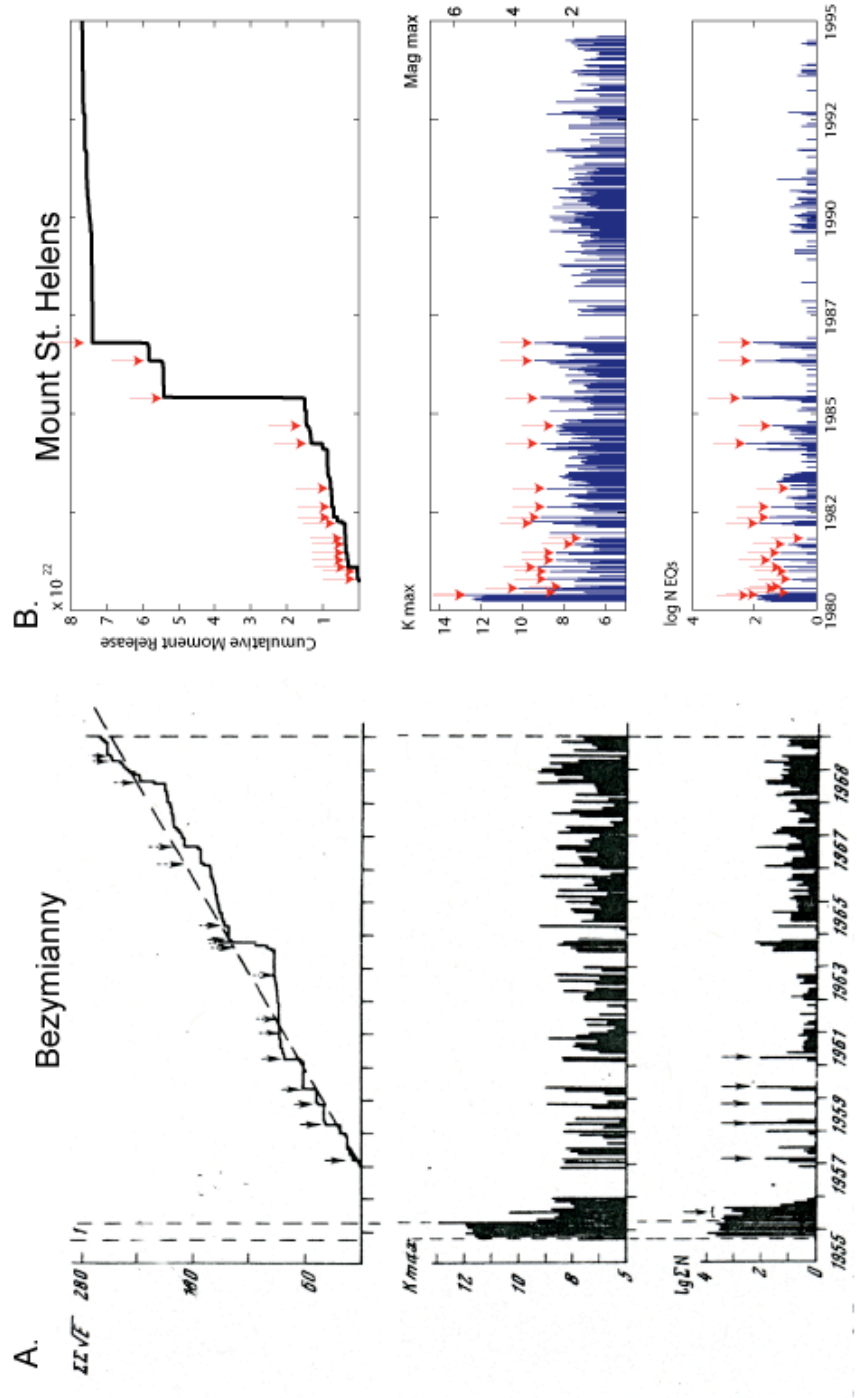

Figure 4.54: Comparison of post collapse seismicity at Bezymianny Volcano and Mount St. Helens. A. Same as Figure 1.9 with top middle plot missing. B. Similar seismic characteristic to A shown at Mount St. Helens over a similar duration. Earthquake catalog from Figure 1.4. B, Top: Cumulative moment release beginning in September 1980 to emphasize the dome-building period. Red arrows are documented eruptions. B, Middle: Maximum magnitude calculated every five days. B, Bottom: Number of earthquakes calculated each 5 days. The catalog was truncated at M1.1 to be consistent with the catalog at Bezymianny by Tokarev [1981].

Figure 4.55: Comparison of dome morphology during the 1965-1970 eruption at Bezymianny, and the 2004-2008 eruption at Mount St. Helens. Direction of extrusion is from left to right (top) and from right to left (bottom).

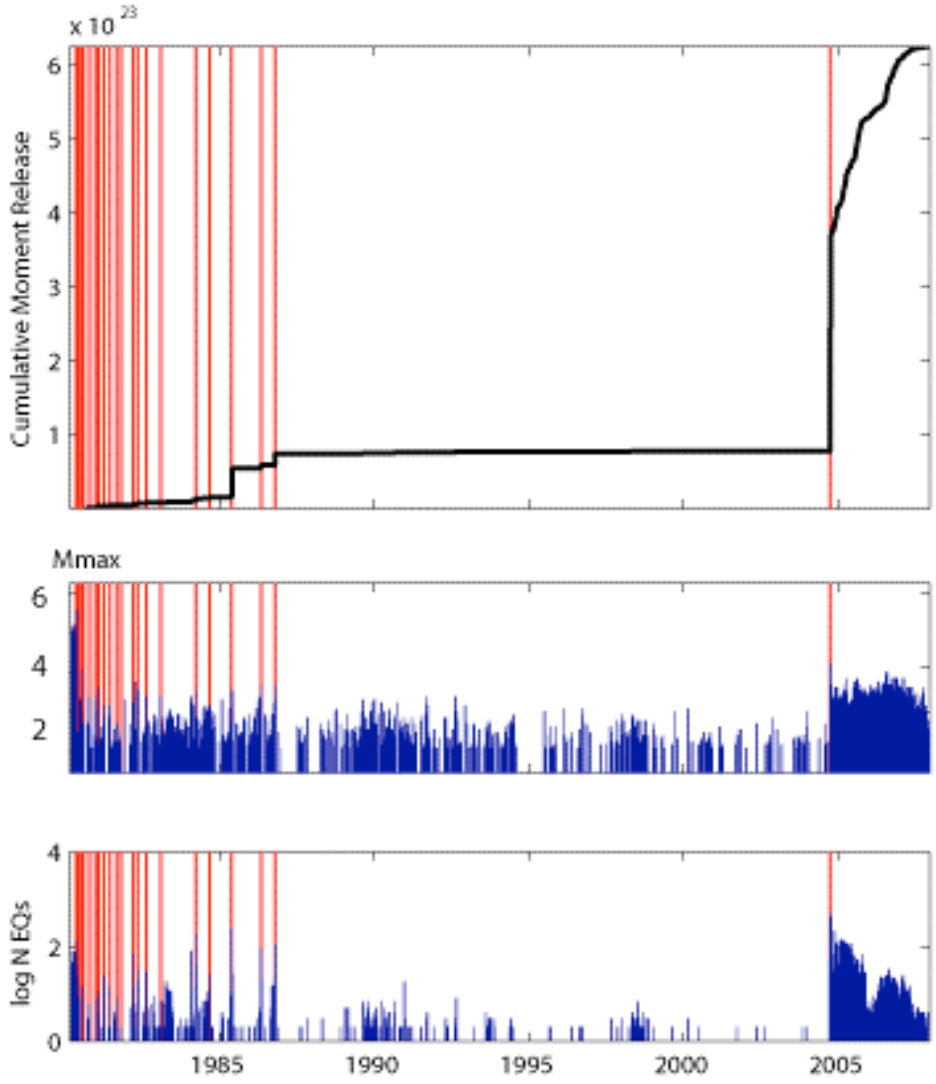

Figure 4.56: Seismic characteristics at Mount St. Helens between 1980 and 2008. Earthquakes are same that are used in Figure 1.4. Top: Cumulative moment release. Middle: Maximum magnitude every 5 days. Bottom: Number of earthquakes above M1.1. Magnitude cut is to mimic the sensitivity of the catalog at Bezymianny. The number of earthquakes, particularly after 2004, reflects as little as 3% of the total number [Thelen et al., 2008]. Red lines are eruptions.

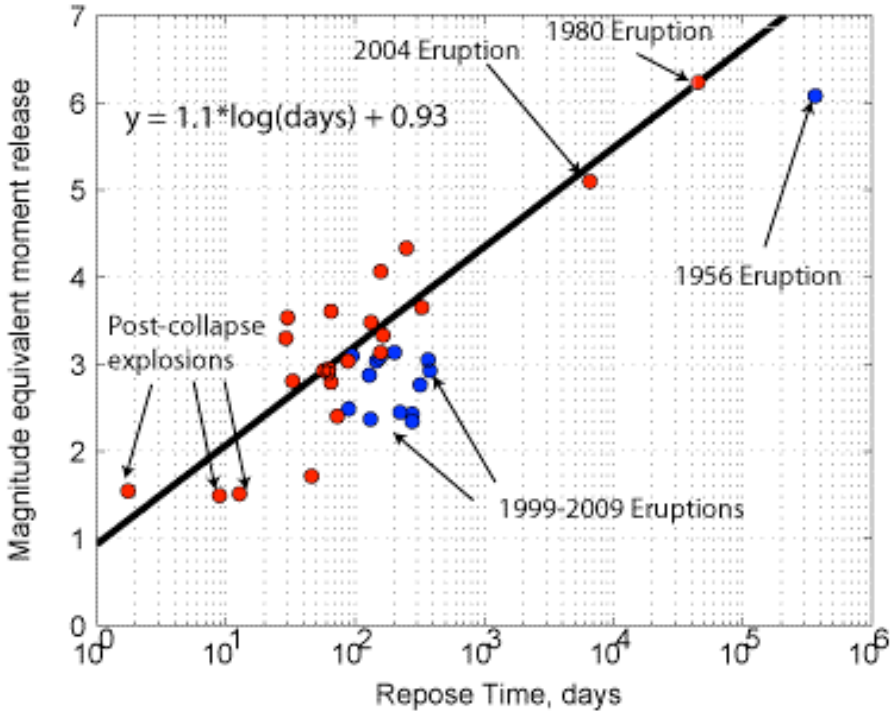

Figure 4.57: Relationship of repose time and equivalent moment release at Mount St. Helens and Bezymianny. Mount St. Helens eruptions between 1980 and 2009 are shown in red and Bezymianny eruptions in 1956 and between 1999 and 2009 are shown in blue. Repose time is defined as the time between the end of the last eruption and the start of the next eruption. The black line is the linear least squares fit to the Mount St. Helens data.

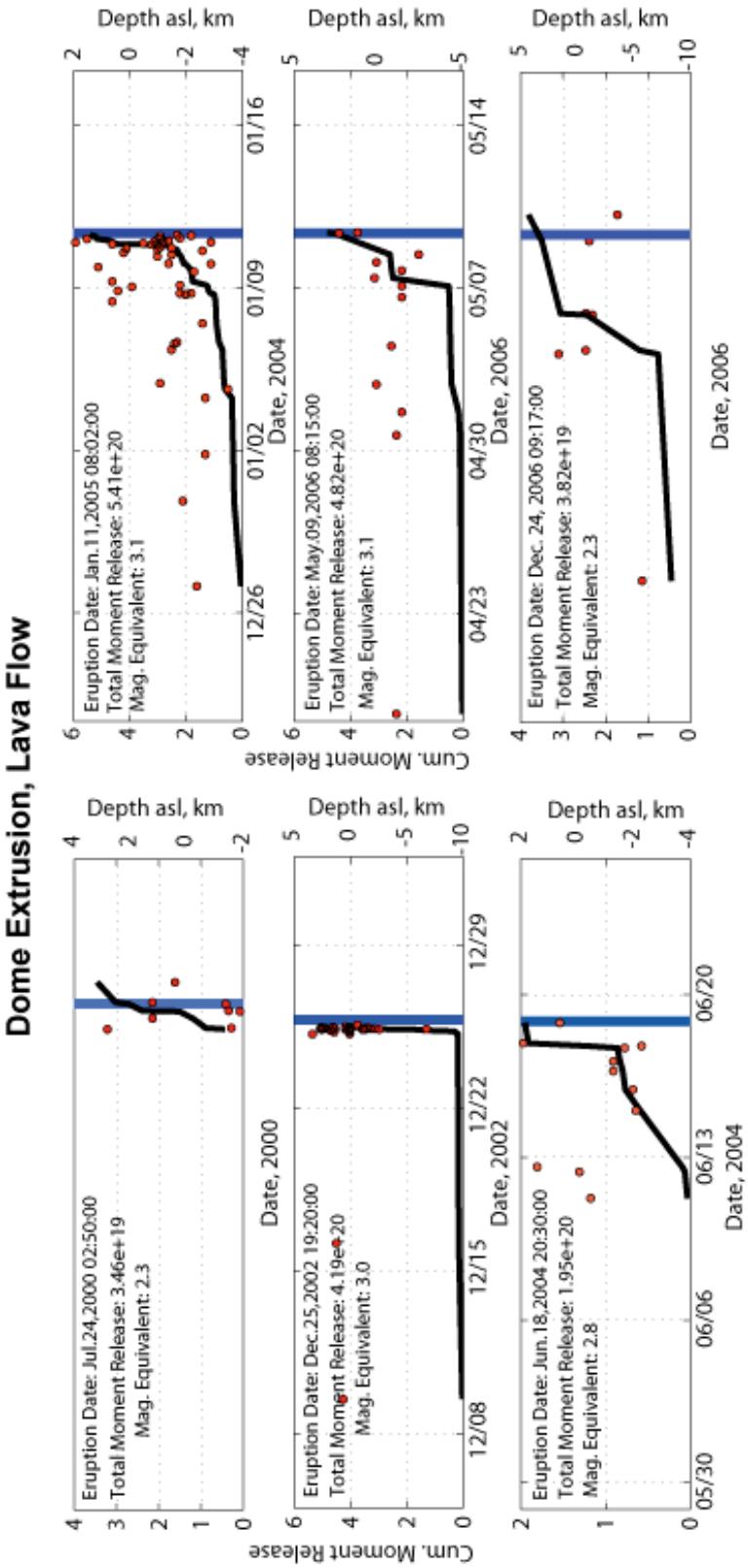

Figure 4.58: Cumulative moment release and time depth plot of explosive eruptions at Bezymianny Volcano beginning in 1999. Earthquakes are from the KBGS catalog. Black line is cumulative moment release, red circles are earthquakes plotted as a function of time and depth. Blue lines are explosions. Only eruptions that include both dome building and lava flows are included in this figure [Venzke et al., 2008].

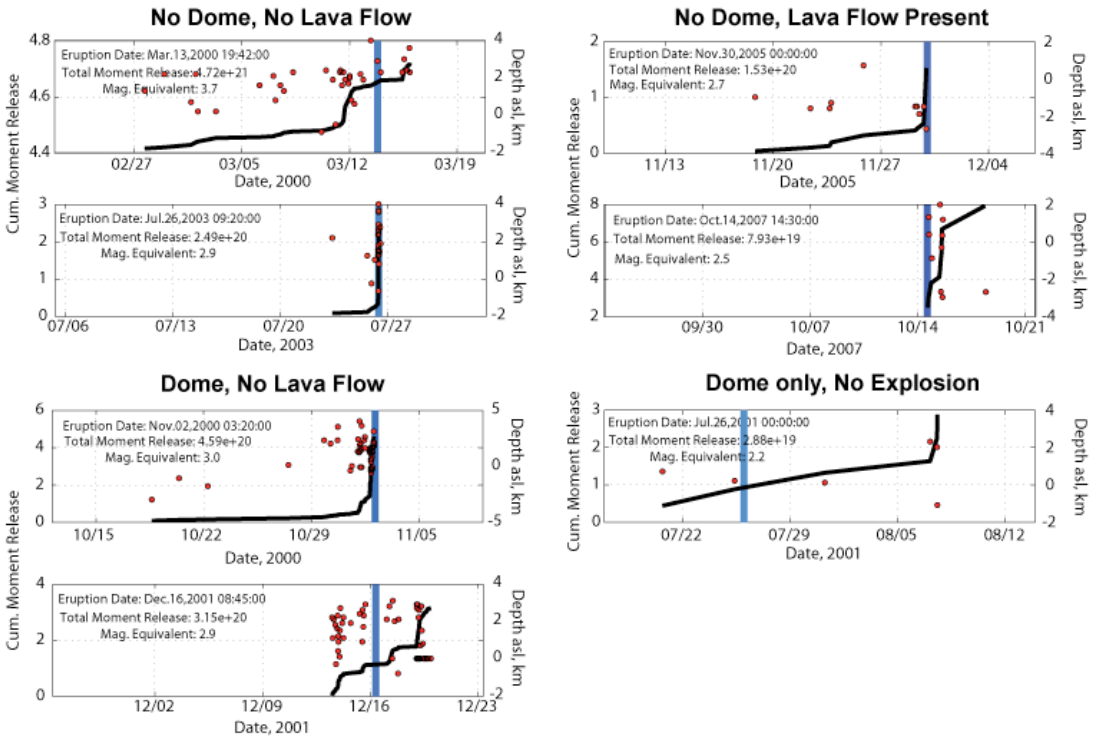

Figure 4.59: Cumulative moment release and time depth plot of atypical eruptions at Bezymianny since 1999. Lines and symbols are same as Figure 4.58

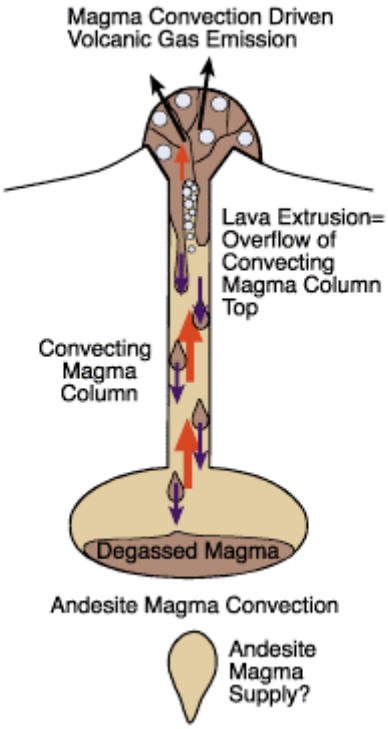

Figure 4.60: Schematic model of conduit processes prior to eruptions beneath Mount St. Helens and Bezymianny Volcanoes. Red arrows reflect the ascent of gas-charged magma up the conduit; black arrows show the descent of gas poor magma down the magma column. Gases exsolved from the ascending magma collect underneath the plug. Gases may escape to the surface through cracks. Figure from Shinohara [2008].

Table 4.6: Comparison of multiplet characteristics at Mount St. Helens and Bezymianny volcano. Terms such as “High” and “Low” are in reference to other multiplets during the study period at a particular volcanic center. Refer to Chapters 2 and 3 for details.

	Mount St. Helens (2004)		**Bezymianny (2007)**	
Multiplet Characteristic	**Non-explosive**	**Pre-explosion**	**Non-explosive**	**Pre-explosion**
Average Amplitude	Low	High	Low	High
Standard Deviation of Average	Low	High	Low	High
Duration	Hours-2 weeks	Hours-Days	Hours-2 weeks	Hours
Contemporary Multiplets	5-20	5-20	2 to 13	< 5
Multiplet Percentage of Total Seismicity	40-90%	25-90%, decreasing prior to eruption	10-30%	<15%, decreasing prior to eruption

Table 4.7: Common characteristics of multiplets during explosive and dome-building eruptions. Explosive eruptions are defined by plinian and sub-plinian eruption columns. Explosive eruptions may also include dome-building phases, which, if applicable, are included in the dome-building section of the table. A high MPTS is defined as > 20%. High contemporary multiplets are defined as > 5. Variability refers to the evolution of event amplitudes within multiplets. A low variability refers to stable amplitudes of events within a multiplet. The amplitudes may still change slowly with time. A high variability means that the amplitude of events within multiplets is variable.

Characteristic	Explosive	Dome Building
Multiplet Percentage of Total Seismicity (MPTS)	Low[1,2], High[3] Declined prior to explosion[1,2,3]	High[4, 5, 6, 7, 8]
Duration	Hours[1,2]	Days [6,7] to Weeks[4,5,8]
Contemporary Multiplets	Low[1,2,3]	High[5, 8]
Variability	High[2,3]	Low[5,6,8]

1. Bezymianny 2006, [West et al., 2007]; 2. Bezymianny 2007, this paper; 3. Redoubt 1989, [Stephens and Chouet, 2001]; 4. Unzen 1990-1995, [Umakoshi et al., 2008b]; 5. Soufriere Hills Volcano, 1995, [White et al., 1998; Green and Neuberg, 2006]; 6. Pinatubo, Oct. 1991 (Dome building), [Ramos et al., 1999]; 7. Mount St. Helens 1980-1986 (Dome building), [Fremont and Malone, 1987]; 8. Mount St. Helens 2004-2008, this paper

Table 4.8: Comparison of eruptive properties between Bezymianny and Mount St. Helens.

	Bezymianny	**Mount St. Helens**
Composition (% SiO_2)	Andesite (57%-61%, decreasing)[1,2,3]	Dacite (62-64%, increasing)[4]
Pre-eruption Duration	6 months[6]	2 months[7]
Cryptodome Volume km^3	0.15[8]	0.11[8]
Crater Dimensions	1.5 km x 2.8 km^2	1.5 km x 3 km^2
Measured SO_2 Gas Emission, Mt	7.2 (1956 eruption)[5]	1.0 (1980 eruption), 0.5 (1980-1986 eruption)[5]
Dome Building	>50 years[6]	28 years inc. quiescence
Current Dome Volume, km^3	0.367 (1976)[2]	0.125 (1987)[9], 0.225(2008 cumulative)[10]

References are as follows: 1. Belousov [1996]; 2. Bogoyavlenskaya et al. [1985]; 3. Pavel Izbekov, personal communication, 2009; 4. Pallister et al. [1992]; 5. Shinohara [2008]; 6. Tokarev [1981]; 7. Endo et al. [1981]; 8. Belousov et al. [2007]; 9. Swanson and Holcomb [1990]; 10. Vallance et al. [2008]

V. Summary

Many aspects of seismology have been explored at Bezymianny Volcano, Russia and Mount St. Helens, Washington as a part of this thesis. Through the comparison of the two volcanoes I have presented new interpretations that are only possible through a comparative approach. By utilizing the common and uncommon aspects between volcanoes, I have defined the parameters most important in producing the observed seismicity. At times I also used other volcanoes throughout the world to provide context for the observations and to develop more general interpretations.

5.1 Pre-collapse Seismicity

Bezymianny Volcano began erupting in 1956 and has continued to the present day with only minor breaks in activity. The 1956 eruption possessed many seismic characteristics that were similar to the 1980 eruption at Mount St. Helens. Similarities in the rapid seismic buildup and subsequent decrease in the number of earthquakes implied a steadily decreasing stress throughout the pre-eruptive sequence. This observation suggested that most of the emplacement of the cryptodome occurred at the beginning of the sequence. The pre-eruptive sequence at Bezymianny lasted three times longer than at Mount St. Helens. Given that the volumes of the cryptodomes were similar despite the longer activity at Bezymianny, the intrusion rate at Bezymianny was much lower than at Mount St. Helens. This slower intrusion rate allowed for the cooling of intruded magma, which temporarily strengthened the edifice.

5.2 Dome Building Seismicity

Activity at Bezymianny after the 1956 eruption was in the form of discrete dome forming events. This phase was similar in behavior and duration to the eruptive phase at Mount St. Helens between 1980 and 1986 suggesting similar conduit geometries between volcanoes. One key difference was the presence of large explosions at Bezymianny throughout this time period, presumably due to the increased gas content at Bezymianny with respect to Mount St. Helens. After the discrete dome building phase at Bezymianny, there was a 5-year period of continuous growth that included the extrusion of spines and whaleback-like structures. These structures were emplaced during times of increased seismic activity; however overall, the continuous eruption had a moment release rate and maximum magnitude of earthquakes that were similar to the discrete-dome building phase.

The continuous dome building phase at Bezymianny was not as well observed as the 2004-2008 Mount St. Helens eruption. Though the dome morphology was similar at both volcanoes, the basic seismic parameters that were observed at Bezymianny suggest some fundamental differences in the seismicity. In particular, the continuous dome building at Bezymianny had a similar rate of seismic energy release to the discrete dome-building phase. At Mount St. Helens the rate of moment release was much larger during the continuous phase of dome building than during the discrete phase of dome building. Presumably this is due to a bend in the shallow conduit around the 1980-1986 dome at Mount St. Helens.

The 2004-2008 eruption was exceptional in many ways. The eruption was well monitored seismically and visually. The 2004 eruption began on September 23, 2004 with a swarm of exclusively high-frequency earthquakes located approximately 1 km below the dome surface. After 2 days, the high-frequency swarm died off, only to be renewed by the occurrence of high-frequency, low-frequency and hybrid events, the latter a strong indication of the presence of pressurized fluids at seismogenic depths. A subset of these earthquakes had average depths that were approximately 200 meters shallower and to the south of the initial swarm. Amplitudes of all event types continued to build until the first explosion on October 1, 2004. Multiplets were common during the initial phases of unrest. Precise relocations of the multiplets prior to the first explosion show circular clouds of hypocenters 10-40 m across with little structure.

After the October 1 explosion, high-frequency events effectively stopped and the seismicity was dominated by high-amplitude hybrid and low-frequency earthquakes. After the October 5 explosion, hybrid and low-frequency events continued, however at reduced amplitudes compared to activity over the previous 6 days. Hybrid amplitudes were generally smaller and decreased faster than low-frequency events between October 5 and October 11. The difference in amplitudes and eventual cessation of hybrid events after October 11 suggests that the source giving rise to the hybrid events was related to plug breakup and fundamentally different than the source of the low-frequency events. Relocations of a multiplet during this time revealed tabular pattern in hypocenters over a source region 20 m in the long axis and 10 m in the short axis. This was the first indication of a possible

shift from a point source region into a tabular region of seismicity consistent with a depth-dependent genesis for seismicity.

Once extrusion started on October 11, 2004, the hybrid earthquakes essentially stopped and low-frequency earthquakes became the dominant source of seismicity. Absolute locations of earthquakes during this time were confined to the upper kilometer of the conduit. Multiplets tended to have much longer durations than multiplets prior to the explosive phase, suggesting a more stable and long-lived source mechanism. The cloud of relative locations of multiplets after extrusion began had horizontal cigar shape with strikes perpendicular to the direction of whaleback extrusion. The shape of the source region is consistent with a depth-limited generation of sources within a dike. The locations occur at a confined depth that suggests the source might be related to a pressure-dependent reaction in the conduit or to a constriction in the conduit at that depth. Possible sources include fracture at the conduit walls, fracture within the hardened plug at a bend in the conduit, or gas-driven crack excitation.

5.3 Seismicity of the Explosive Phase

After the continuous phase of extrusion, Bezymianny entered an explosive phase that was accompanied by lava flows. This activity is a clear departure from that seen at Mount St. Helens and likely represents the combined effects of a relatively high gas content, and a decreasing trend in composition from dacite to andesite to basaltic andesite.

Using continuous data, a 3-month period of unrest at Bezymianny was studied in detail, covering a variety of eruptive phenomenon included a large explosion and

lava flow. Rockfall signals were conspicuous during the pre-eruptive seismicity and are likely due to instability of the dome in response to deformation or the gravitational collapse of the extrusion of a hardened spine. Rockfalls that were preceded by a low-frequency signal (LFLDEs) were also only present in significant numbers in association with large explosions and lava flow extrusion, which suggested that their occurrence was related to degassing at the surface. Low-frequency events were common at Bezymianny with a dominant frequency of 1-2 Hz. Lava flow extrusion appeared to be associated with high-rates of events enhanced in frequencies above 5 Hz, LFFDEs and low frequency events with a dominant frequency between 3 and 5 Hz. Amplitudes of LFLDEs, high-frequency, and low-frequency events increased prior to large explosions and remained relatively high during lava flow extrusion.

5.4 Magma Plumbing System

The paths of magma from the middle crust to the surface at both volcanoes are broadly similar. Recalculated precise earthquake locations at Bezymianny using a dense network are oriented from the summit of the volcano to the north-northeast. The lineation is interpreted as a fault that is facilitating magma to the surface. The fault is sub-parallel to trends in bedrock topography. The skew in earthquake locations to the north of Bezymianny suggests that part of the neighboring Kamen plumbing system may currently be used at Bezymianny. On the other hand, seismicity at Mount St. Helens extending north and south of the volcano appears to be purely tectonic but with a right step in a right lateral system generating a pull-a-part structure for magma transport to the surface.

Both volcanoes have magma chambers at similar depths below the surface, however the magma chamber at Bezymianny is offset to the north. At Mount St. Helens, there is good evidence for a shallow magma or volatile chamber at 3 km below the surface. A similar shallow magma chamber may exist at Bezymianny within an earthquake-free zone under the edifice, however, more earthquakes are needed to define the extent of the shallow magma chamber. There is good evidence for similar geometries of the shallow parts of the conduit from the similar activity at both volcanoes during the discrete dome building phase.

5.5 Controls on the initiation of an eruption

At Mount St. Helens the energy of pre-eruptive seismicity was scaled to the time since the last eruption. In other words, more energetic precursory periods occurred after long repose times. The relationship holds regardless of the type of eruption. The connection between the precursor seismic energy release and repose time was loosely similar at Bezymianny. The scaling suggests that the strength of the cap rock is the controlling factor in the timing of an eruption. It may also suggest a common thickness of the plug between both volcanoes. The implication is that the repose time allows for cooling of the plug that propagates deeper with time. This process is likely uniform for similar width conduits. This relationship is profoundly important in volcano forecasting as it offers scientists an estimate of the amount of seismicity required prior to a large eruption or dome forming event. In cases where the seismic energy release is far less than expected from the scaling relationship, it may also offer an aid in determining the occurrence of a failed eruption.

5.6 Multiplets

Multiplets were present during many eruptive periods at Mount St. Helens and Bezymianny and their behavior was dictated by the viscous and degassed state of material in the shallow conduit. At Mount St. Helens prior to 1983, there was weak multiplet development related mostly to deep seismicity after the 1980 eruption and prior to the 1982 eruption. After 1983 at Mount St. Helens, multiplet development occurred during periods of spine extrusion and around eruptions when the volume extrusion rate was low, allowing for more complete degassing of the shallow conduit. During the 2004 eruption at Mount St. Helens, there was vigorous multiplet development prior to and accompanied by extrusion of a solidified plug at the surface. Bezymianny shows far fewer multiplets than Mount St. Helens, particularly prior to large explosions. This is presumably due to the cold, dense and completely degassed plug in the shallow conduit.

The observation of multiplets on volcanoes worldwide has revealed several general trends. Prior to eruptions, the relatively unstable environment produced high stress gradients, which I speculate acted to discourage the development of long duration multiplets. Further, in a system with a solidified cap rock, the low number of contemporaneous multiplets prior to an eruption suggested high stress concentrations over a small area. In explosions that did not include a solidified extrusive plug, a high number of contemporaneous multiplets may have been a sign of increased slip along several patches around the outside of the conduit or gas-driven crack resonance in a dendritic network around the conduit. The most striking difference in large explosive eruptions compared to dome-forming eruptions may be the dramatic difference in MPTS of multiplets. In explosive eruptions the MPTS of

multiplets is low, usually below 20%, compared to dome-forming eruptions where the MPTS of multiplets is usually above 20%, and often much higher.

5.7 Conclusions

The eruptive sequences after cryptodome emplacement and subsequent edifice failure are remarkably similar at both Bezymianny and Mount St. Helens. This similarity suggests that the eruptive behavior is at least somewhat dependent upon the initial conditions of sudden decompression of a magma chamber due to slope failure. Differences in the length and details of activity are likely due to the differential evolution of magmas through the volcanic sequence.

At both volcanoes the precursory moment release is a function of repose time with roughly the same relationship. The relationship holds regardless of the type of volcanic eruption. This suggests that a general process, such as the cooling of a magmatic plug, generates resistance that is reflected in the moment release required to have an eruption. This has dramatic implications for determining the timing of an eruption and in determining the possibility of a failed eruption.

Multiplet behavior was found at both volcanoes in a variety of different types of eruptions. Multiplet development is most productive in the presence of a viscous degassing plug. The presence of a cold and dense plug, or a hot and fluid shallow conduit results in the occurrence of few multiplets, if any. Temporal behavior of multiplet characteristics such as amplitude, standard deviation, duration, number of contemporaneous multiplets and multiplet proportion of total seismicity can be used in

concert to forecast explosions. Multiplets were also found to be annihilated during eruptions that extend to or below the multiplet source region.

5.8 Future Work

Several questions remain unanswered or stand to benefit from additional data and results. One question, “Do the plumbing systems of Klyuchevskoy and Bezymianny interact?” This may be answered with additional earthquake locations and improved integration of GPS and petrologic results. Another question, “Does the current phase at Bezymianny include continuous dome growth between large eruptions?” This may be answered with improved monitoring of seismic, geodetic and visual data streams.

Future work at Mount St. Helens should better determine the link between mutliplet behavior and dome growth. Such a relationship, if proven robust, could be used at Bezymianny to establish the presence of continuous dome growth. Of particular interest is the transition from one whaleback or spine to another. Corroboration between different datasets including GPS and tilt should help quantify the actual source of multiplets. The extrusion rate was also well documented and could be used to quantify under which conditions multiplet development is favored.

Reference List

Anderson, S. W., and J. H. Fink (1990), The Development and Distribution of Surface Textures at the Mount St. Helens Dome, in *Lava Flows and Domes: Emplacement Mechanisms and Hazard Implications:* edited by J. H. Fink, pp. 25, Springer-Verlag, Berlin Heidelberg, .

Balesta, S. T., A. I. Farberov, V. S. Smirnov, A. A. Tarakanovsky, and M. I. Zubin (1976-77), Deep Crustal Structure of the Kamchatkan Volcanic Regions, *Bull. Volcanol., 40*(4), 260.

Barker, S. E., and S. D. Malone (1991), Magmatic System Geometry at Mount St Helens Modeled from the Stress-Field Associated with Posteruptive Earthquakes, *Journal of Geophysical Research-Solid Earth and Planets, 96*(B7), 11883-11894.

Belousov, A. (1996), Deposits of the 30 March 1956 directed blast at Bezymianny volcano, Kamchatka, Russia, *Bulletin of Volcanology, 57*(8), 649-662.

Belousov, A., B. Voight, M. Belousova, and A. Petukhin (2002), Pyroclastic surges and flows from the 8-10 May 1997 explosive eruption of Bezymianny volcano, Kamchatka, Russia, *Bulletin of Volcanology, 64*(7), 455-471.

Belousov, A., B. Voight, and M. Belousova (2007), Directed blasts and blast-generated pyroclastic density currents: a comparison of the Bezymianny 1956, Mount St Helens 1980, and Soufriere Hills, Montserrat 1997 eruptions and deposits, *Bulletin of Volcanology, 69*(7), 701-740, doi: 10.1007/s00445-006-0109-y.

Bogoyavlenskaya, G. E., and I. T. Kirsanov (1981), Twenty-Five Year of Activity of Bezymiannyi Volcano, *Volcanology and Seismology, 2*, 3-13.

Bogoyavlenskaya, G. E., O. A. Braitseva, I. V. Melekestsev, V. Y. Kiriyanov, and C. D. Miller (1985), Catastrophic Eruptions of the Directed-Blast Type at Mount St-Helens, Bezymianny and Shiveluch Volcanos, *Journal of Geodynamics, 3*(3-4), 189-218.

Braitseva, O. A., I. V. Melekestsev, G. E. Bogoyavlenskaya, and A. P. Maksimov (1991), Bezymianny: Eruptive history and dynamics. *Volcanology and Seismology, 12*, 165-195.

Buurman, H., and M. West (in review), Seismic precursors to volcanic explosions during the 2006 eruption of Augustine Volcano, in *The 2006 eruption of Augustine Volcano:* edited by J. A. Power, M. L. Coombs and J. T. Freymueller, .

Calder, E. S., J. A. Cortes, J. L. Palma, and R. Luckett (2005), Probabilistic analysis of rockfall frequencies during an andesite lava dome eruption: The Soufriere Hills Volcano, Montserrat, *Geophys.Res.Lett., 32*(16), L16309, doi: 10.1029/2005GL023594.

Cascade Volcano Observatory, and University of Washington Geophysics Program (2007), Mount St. Helens, Washington Current Activity Archives, *2009*(April 7, 2009).

Cashman, K. V., C. R. Thornber, and J. S. and Pallister (2008), From dome to dust: shallow crystallization and fragmentation of conduit magma during the 2004–2006 dome extrusion of Mount St. Helens, Washington, in *A volcano rekindled; the*

renewed eruption of Mount St. Helens, 2004–2006, Professional Paper 1750 ed., edited by D. R. Sherrod, W. E. Scott and P. H. and Stauffer, United States Geological Survey, .

Cashman, K. V., and S. M. McConnell (2005), Multiple levels of magma storage during the 1980 summer eruptions of Mount St. Helens, WA, *Bulletin of Volcanology, 68*(1), 57-75.

Cervelli, P. F., T. Fournier, J. Freymueller, and J. A. Power (2006), Ground deformation associated with the precursory unrest and early phases of the January 2006 eruption of Augustine Volcano, Alaska, *Geophys.Res.Lett., 33*.

Chadwick, W. W., R. J. Archuleta, and D. A. Swanson (1988a), The Mechanics of Ground Deformation Precursory to Dome-Building Extrusions at Mount St-Helens 1981-1982, *Journal of Geophysical Research-Solid Earth and Planets, 93*(B5), 4351-4366.

Chadwick, W. W., R. J. Archuleta, and D. A. Swanson (1988b), The Mechanics of Ground Deformation Precursory to Dome-Building Extrusions at Mount St-Helens 1981-1982, *Journal of Geophysical Research-Solid Earth and Planets, 93*(B5), 4351-4366.

Chadwick, W. W., and D. A. Swanson (1989), Thrust Faults and Related Structures in the Crater Floor of Mount-St-Helens Volcano, Washington, *Geological Society of America Bulletin, 101*(12), 1507-1519.

Chen, K. H., R. M. Nadeau, and R. J. Rau (2007), Towards a universal rule on the recurrence interval scaling of repeating earthquakes? *Geophys.Res.Lett., 34*(16), L16308.

Chouet, B. (2003), Volcano seismology, *Pure Appl.Geophys., 160*(3-4), 739-788.

Chouet, B. A. (1996), Long-period volcano seismicity: Its source and use in eruption forecasting, *Nature, 380*(6572), 309-316.

Chouet, B. A., R. A. Page, C. D. Stephens, J. C. Lahr, and J. A. Power (1994), Precursory Swarms of Long-Period Events at Redoubt Volcano (1989-1990), Alaska - their Origin and use as a Forecasting Tool, *J.Volcanol.Geotherm.Res., 62*(1-4), 95-135.

Clynne, M. A., A. T. Calvert, E. W. Wolfe, R. C. Evarts, R. J. Fleck, and M. A. Lanphere (2008), The Pleistocene Eruptive History of Mount St. Helens, Washington, from 300,000 to 12,800 Years Before Present, in *A volcano rekindled; the renewed eruption of Mount St. Helens, 2004-2006*edited by D. R. Sherrod, W. E. Scott and P. H. Stauffer, pp. 856, .

Costa, A., O. Melnik, R. S. J. Sparks, and B. Voight (2007), Control of magma flow in dykes on cyclic lava dome extrusion, *Geophys.Res.Lett., 34*(2), L02303.

Dodge, D. A., G. C. Beroza, and W. L. Ellsworth (1995), Foreshock Sequence of the 1992 Landers, California, Earthquake and its Implications for Earthquake Nucleation, *Journal of Geophysical Research-Solid Earth, 100*(B6), 9865-9880.

Efron, B., and G. Gong (1983), A leisurely look at the bootstrap, the jackknife and cross-validation, *American Statistician, 37*(1), 36.

Eichelberger, J. C. (1995), Silicic volcanism: ascent of viscous magmas from crustal reservoirs, *Annu.Rev.Earth Planet.Sci., 23*, 41-63.

Endo, E. T., S. D. Malone, L. L. Noson, and C. S. Weaver (1981), Locations, magnitudes, and statistics of the March 20-May 18 earthquake sequence; The 1980 eruptions of Mount St. Helens, Washington, U. S. Geological Survey, Reston, VA, United States (USA), United States (USA).

Endo, E. T., and T. Murray (1991), Real-Time Seismic Amplitude Measurement (Rsam) - a Volcano Monitoring and Prediction Tool, *Bulletin of Volcanology, 53*(7), 533-545.

Fremont, M. J., and S. D. Malone (1987), High-Precision Relative Locations of Earthquakes at Mount St-Helens, Washington, *Journal of Geophysical Research-Solid Earth and Planets, 92*(B10), 10223-10236.

Geller, R. J., and C. S. Mueller (1980), Four similar earthquakes in central California, *Geophys. Res. Lett., 7*, 821.

Gerlach, T. M., K. A. Mcgee, and M. P. Doukas (2008), Emission Rates of CO2, SO2, and H2S, Scrubbing, and Preeruption Excess Volatiles at Mount St. Helens, 2004–2005, in *A Volcano Rekindled: The Renewed Eruption of Mount St. Helens, 2004–2006*edited by D. R. Sherrod, W. E. Scott and P. H. Stauffer, pp. 856, .

Giampiccolo, E., C. Musumeci, S. D. Malone, S. Gresta, and E. Privitera (1999), Seismicity and stress-tenser inversion in the central Washington Cascade Mountains, *Bulletin of the Seismological Society of America, 89*(3), 811-821.

Gonnermann, H. M., and M. Manga (2003), Explosive volcanism may not be an inevitable consequence of magma fragmentation, *Nature, 426*(6965), 432-435.

Gorshkov, G. S. (1959), Gigantic eruption of the volcano Bezymianny, *Bulletin of Volcanology, 20*, 77-109.

Goto, A. (1999), A new model for volcanic earthquake at Unzen volcano; melt rupture model, *Geophys. Res. Lett., 26*(16), 2541.

Green, D. N., and J. Neuberg (2006), Waveform classification of volcanic low-frequency earthquake swarms and its implication at Soufriere Hills Volcano, Montserrat, *J.Volcanol.Geotherm.Res., 153*(1-2), 51-63.

Gret, A., R. Snieder, R. C. Aster, and P. R. Kyle (2005), Monitoring rapid temporal change in a volcano with coda wave interferometry, *Geophys.Res.Lett., 32*(6), L06304.

Gudmundsson, A., and S. L. Brenner (2004), How mechanical layering affects local stresses, unrests, and eruptions of volcanoes, *Geophys.Res.Lett., 31*(16), 4, doi: 10.1029/2004GL020083.

Harrington, R. M., and E. E. Brodsky (2007), Volcanic hybrid earthquakes that are brittle-failure events, *Geophys.Res.Lett., 34*(6), L06308.

Herrmann, R. B. (1979), FASTHYPO–a hypocenter location program, *Earthquake Notes, 50*(2), 25.

Hildreth, W. (2007), Quaternary magmatism in the Cascades; geologic perspectives, *U.S. Geological Survey Professional Paper 1744,* , 125.

Hoblitt, R. P., and R. S. Harmon (1993), Bimodal density distribution of cryptodome dacite from the 1980 eruption of Mount St. Helens, Washington, *Bulletin of Volcanology, 55*(6), 421-437.

Ikeda, R., T. Kajiwara, K. Omura, and S. Hickman (2008), Physical rock properties in and around a conduit zone by well-logging in the Unzen Scientific Drilling Project, Japan, *Journal of Volcanology and Geothermal Research, 175*(1-2), 13-19, doi: DOI: 10.1016/j.jvolgeores.2008.03.036.

Ishikawa, T., F. Tera, and T. Nakazawa (2001), Boron isotope and trace element systematics of the three volcanic zones in the Kamchatka arc, *Geochimica et Cosmochimica Acta, 65*(24), 4523-4537, doi: DOI: 10.1016/S0016-7037(01)00765-7.

Iverson, R. M., et al (2006), Dynamics of seismogenic volcanic extrusion at Mount St Helens in 2004-05, *Nature, 444*(7118), 439-443.

Kanamori, H., J. W. Given, and T. Lay (1984), Analysis of seismic body waves excited by the Mount St. Helens eruption of May 18, 1980, *Journal of Geophysical Research, 89*(B3), 1856-1866, doi: 10.1029/JB089iB03p01856.

KBGS (2007a), OPERATIONAL REPORT ON THE KAMCHATKAN VOLCANOES AND ALAID VOLCANO (THE KURILE ISLAND) ACTIVITY ON TELEMETRIC DATA, , 1 pp.

KBGS (2007b), OPERATIONAL REPORT ON THE KAMCHATKAN VOLCANOES AND ALAID VOLCANO (THE KURILE ISLAND) ACTIVITY ON TELEMETRIC DATA, , 1 pp.

KBGS (2007c), OPERATIONAL REPORT ON THE KAMCHATKAN VOLCANOES AND ALAID VOLCANO (THE KURILE ISLAND) ACTIVITY ON TELEMETRIC DATA, , 1 pp.

Kirsanov, I. T., and B. I. Studinikin (1971), Dynamics of the Extrusive Eruption of Bezymiannyi Volcano in 1965-1968, *Biulleten Vulkanologicheskikh Stantsil, 47*, 15-22.

Klein, F. W. (1985), User's guide to HYPOINVERSE, a program for VAX and 350 computers to solve for earthquake locations, U. S. Geological Survey, Reston, VA, United States (USA), United States (USA).

Lahr, J. C., B. A. Chouet, C. D. Stephens, J. A. Power, and R. A. Page (1994), Earthquake Classification, Location, and Error Analysis in a Volcanic Environment - Implications for the Magmatic System of the 1989-1990 Eruptions at Redoubt Volcano, Alaska, *J.Volcanol.Geotherm.Res., 62*(1-4), 137-151.

Lees, J. M. (1992), The Magma System of Mount-St-Helens - Nonlinear High-Resolution P-Wave Tomography, *J.Volcanol.Geotherm.Res., 53*(1-4), 103-116.

Lees, J. M., N. Symons, O. Chubarova, V. Gorelchik, and Ozerov, Alexei Yu (Ozerov,Aleksei Yu) (2007), Tomographic images of Klyuchevskoy Volcano P-wave velocity; Volcanism and subduction; the Kamchatka region, *Geophysical Monograph, 172*, 293-302, doi: 10.1029/172GM21.

Lipman, P. W., J. G. Moore, and D. A. Swanson (1981), Bulging of the north flank before the May 18 eruption; geodetic data; The 1980 eruptions of Mount St. Helens, Washington, U. S. Geological Survey, Reston, VA, United States (USA), United States (USA).

Lisowski, M., D. Dzurisin, R. P. Denlinger, and E. Y. Iwatsubo (2008), GPS-measured deformation associated with the 2004–2006 dome-building eruption of Mount St. Helens, Washington, in *A volcano rekindled; the renewed eruption of Mount St. Helens, 2004–2006*, Professional Paper 1750 ed., edited by D. R. Sherrod, W. E. Scott and P. H. Stauffer, United States Geological Survey, .

Luckett, R., S. Loughlin, S. De Angelis, and G. Ryan (2008), Volcanic seismicity at Montserrat, a comparison between the 2005 dome growth episode and earlier dome growth, *J.Volcanol.Geotherm.Res., 177*(4), 894-902, doi: 10.1016/j.jvolgeores.2008.07.006.

Malone, S. D., and G. L. Pavlis (1983), Velocity structure and relocation of earthquakes at Mount St. Helens, *EOS Trans.Am.Geophys.Union, 64*, 895.

Malone, S. D., E. T. Endo, C. S. Weaver, and J. W. Ramey (1981), Seismic monitoring for eruption prediction; The 1980 eruptions of Mount St. Helens,

Washington, U. S. Geological Survey, Reston, VA, United States (USA), United States (USA).

Malone, S. D., C. Boyko, and C. S. Weaver (1983), Seismic precursors to the Mount St. Helens eruptions in 1981 and 1982, *Science, 221*(4618), 1376-1378.

Malone, S., and S. Moran (1997), Deep long-period earthquakes in the Washington Cascades; AGU 1997 fall meeting [modified], *EOS Trans.Am.Geophys.Union, 78*(46), 438.

Malyshev A., I. (1995), Evolution of Bezymyannyi eruptive activity in 1986-1987, *Volcanol.Seismol., 17*(3), 257-269.

Massol, H., and C. Jaupart (2009), Dynamics of magma flow near the vent: Implications for dome eruptions, *Earth and Planetary Science Letters, 279*(3-4), 185-196, doi: DOI: 10.1016/j.epsl.2008.12.041.

Mastin, L. G. (1994), Explosive Tephra Emissions at Mount St-Helens, 1989-1991 - the Violent Escape of Magmatic Gas Following Storms, *Geological Society of America Bulletin, 106*(2), 175-185.

Matthews, A. J., J. Barclay, S. Carn, G. Thompson, J. Alexander, R. Herd, and C. Williams (2002), Rainfall-induced volcanic activity on Montserrat, *Geophys.Res.Lett., 29*(13), 4, doi: 10.1029/200GL014863.

Miller, A. D., R. C. Stewart, R. A. White, R. Luckett, B. J. Baptie, W. P. Aspinall, J. L. Latchman, L. L. Lynch, and B. Voight (1998), Seismicity associated with dome growth

and collapse at the Soufriere Hills Volcano, Montserrat; The Soufriere Hills eruption, Montserrat, British West Indies; introduction to special section; Part 1, *Geophys.Res.Lett., 25*(18), 3401-3404.

Moore, J. G., and W. C. Albee (1981), Topographic and structural changes, March-July 1980; photogrammetric data; The 1980 eruptions of Mount St. Helens, Washington, U. S. Geological Survey, Reston, VA, United States (USA), United States (USA).

Moore, P. R., N. R. Iverson, and R. M. Iverson (2008), Frictional Properties of the Mount St. Helens Gouge, in *A volcano rekindled; the renewed eruption of Mount St. Helens, 2004-2006*edited by D. R. Sherrod, W. E. Scott and P. H. Stauffer, pp. 856, .

Moran, S. C., S. D. Malone, A. I. Qamar, W. A. Thelen, A. K. Wright, and J. Caplan-Auerbach (2008), Seismicity associated with renewed dome building at Mount St. Helens, 2004–2005, in *A volcano rekindled; the renewed eruption of Mount St. Helens*, Professional Paper 1750 ed., edited by D. R. Sherrod, W. E. Scott and P. H. Stauffer, United States Geological Survey, .

Moran, S. C. (1994), Seismicity at Mount St-Helens, 1987-1992 - Evidence for Repressurization of an Active Magmatic System, *Journal of Geophysical Research-Solid Earth, 99*(B3), 4341-4354.

Mullineaux, D. R., and D. R. Crandell (1981), The eruptive history of Mount St. Helens; The 1980 eruptions of Mount St. Helens, Washington, U. S. Geological Survey, Reston, VA, United States (USA), United States (USA).

Musumeci, C., S. Gresta, and S. D. Malone (2002), Magma system recharge of Mount St. Helens from precise relative hypocenter location of microearthquakes, *Journal of Geophysical Research-Solid Earth, 107*(B10), 2264.

Nakada, S., Y. Motomura, and H. Shimizu (1995), Manner of Magma Ascent at Unzen Volcano (Japan), *Geophys.Res.Lett., 22*.

Neri, G., and S. D. Malone (1989), An Analysis of the Earthquake Time-Series at Mount St-Helens, Washington, in the Framework of Recent Volcanic Activity, *J.Volcanol.Geotherm.Res., 38*(3-4), 257-267.

Neuberg, J. W., H. Tuffen, L. Collier, D. Green, T. Powell, and D. Dingwell (2006), The trigger mechanism of low-frequency earthquakes on Montserrat, *J.Volcanol.Geotherm.Res., 153*(1-2), 37-50.

Newhall, C. G., et al (1996), Eruptive history of Mount Pinatubo, in *Fire and mud; eruptions and lahars of Mount Pinatubo, Philippines*edited by C. G. Newhall and R. S. Punongbayan, Philippines (PHL), .

Noguchi, S., A. Toramaru, and S. Nakada (2008), Groundmass crystallization in dacite dykes taken in Unzen Scientific Drilling Project (USDP-4), *Journal of Volcanology and Geothermal Research, 175*(1-2), 71-81, doi: DOI: 10.1016/j.jvolgeores.2008.03.037.

Okumura, S., M. Nakamura, S. Takeuchi, A. Tsuchiyama, T. Nakano, and K. Uesugi (2009), Magma deformation may induce non-explosive volcanism via degassing

through bubble networks, *Earth Planet.Sci.Lett., 281*(3-4), 267-274, doi: DOI: 10.1016/j.epsl.2009.02.036.

Ozerov, A. Y., A. A. Ariskin, F. Kayl, G. Y. Bogoyavlenskaya, and S. F. Karpenko (1997), Petrologo-geokhimicheskaya model' geneticheskogo rodstva bazal'tovogo i andezitovogo magmatizma vulkanov Klyuchevskoy i Bezymyannyy, Kamchatka. Petrological-geochemical model for genetic relationships between basaltic and andesitic magmatism of Klyuchevskoy and Bezymyannyy volcanoes, Kamchatka, *Petrologiya, 5*(6), 614-635.

Pallister, J. S., C. R. Thornber, K. V. Cashman, M. A. Clynne, H. A. Lowers, C. W. Mandeville, I. K. Brownfield, and G. P. Meeker (2008), Petrology of the 2004–2006 Mount St. Helens lava dome—implications for magmatic plumbing and eruption triggering, in *A volcano rekindled; the renewed eruption of Mount St. Helens, 2004–2006*, Professional Paper 1750 ed., edited by D. R. Sherrod, W. E. Scott and P. H. Stauffer, United States Geological Survey, .

Pallister, J. S., R. P. Hoblitt, D. R. Crandell, and D. R. Mullineaux (1992), Mount St. Helens a decade after the 1980 eruptions; magmatic models, chemical cycles, and a revised hazards assessment, *Bulletin of Volcanology, 54*(2), 126-146.

Petersen, T. (2007), Swarms of repeating long-period earthquakes at Shishaldin Volcano, Alaska, 2001-2004, *J.Volcanol.Geotherm.Res., 166*(3-4), 177-192.

Petersen, T., J. Caplan-Auerbach, and S. R. McNutt (2006), Sustained long-period seismicity at Shishaldin Volcano, Alaska, *J.Volcanol.Geotherm.Res., 151*(4), 365-381.

Poupinet, G., W. L. Ellsworth, and J. Frechet (1984), Monitoring Velocity Variations in the Crust using Earthquake Doublets - an Application to the Calaveras Fault, California, *Journal of Geophysical Research, 89*(NB7), 5719-5731.

Power, J. A., J. C. Lahr, R. A. Page, B. A. Chouet, C. D. Stephens, D. H. Harlow, T. L. Murray, and J. N. Davies (1994), Seismic Evolution of the 1989-1990 Eruption Sequence of Redoubt Volcano, Alaska, *J.Volcanol.Geotherm.Res., 62*(1-4), 69-94.

Power, J. A., S. D. Stihler, R. A. White, and S. C. Moran (2004), Observations of deep long-period (DLP) seismic events beneath Aleutian arc volcanoes; 1989-2002, *J.Volcanol.Geotherm.Res., 138*(3-4), 243-266, doi: 10.1016/j.jvolgeores.2004.07.005.

Qamar, A. I., S. D. Malone, S. C. Moran, W. P. Steele, and W. A. Thelen (2008), Near-real-time information products for Mount St. Helens—tracking the ongoing eruption, in *A volcano rekindled; the renewed eruption of Mount St. Helens, 2004–2006*, Professional Paper 1750 ed., edited by D. R. Sherrod, W. E. Scott and P. H. Stauffer, United States Geological Survey, .

Qamar, A., W. S. Lawrence, J. N. Moore, and G. Kendrick (1983), Seismic Signals Preceding the Explosive Eruption of Mount St-Helens, Washington, on 18 may 1980, *Bulletin of the Seismological Society of America, 73*(6), 1797-1813.

Ramos, E. G., M. W. Hamburger, G. L. Pavlis, and E. P. Laguerta (1999), The low-frequency earthquake swarms at Mount Pinatubo, Philippines: implications for magma dynamics, *J.Volcanol.Geotherm.Res., 92*(3-4), 295-320.

Roman, D. C. (2005), Numerical models of volcanotectonic earthquake triggering on non-ideally oriented faults, *Geophys.Res.Lett., 32*(2), 4, doi: 10.1029/2004GL021549.

Rowe, C. A., C. H. Thurber, and R. A. White (2004), Dome growth behavior at Soufriere Hills Volcano, Montserrat, revealed by relocation of volcanic event swarms, 1995-1996, *J.Volcanol.Geotherm.Res., 134*(3), 199-221.

Scandone, R., and S. D. Malone (1985), Magma Supply, Magma Discharge and Readjustment of the Feeding System of Mount St-Helens during 1980, *J.Volcanol.Geotherm.Res., 23*(3-4), 239-262.

Schaff, D. P., G. H. R. Bokelmann, W. L. Ellsworth, E. Zanzerkia, F. Waldhauser, and G. C. Beroza (2004), Optimizing correlation techniques for improved earthquake location, *Bulletin of the Seismological Society of America, 94*(2), 705-721.

Scott, W. E., D. R. Sherrod, and C. A. Gardner (2008), Overview of 2004 to 2005, and Continuing, Eruption of Mount St. Helens, Washington, in *A Volcano Rekindled: The Renewed Eruption of Mount St. Helens, 2004-2006*, Professional paper 1776 ed., edited by D. R. Sherrod, W. E. Scott and P. H. Stauffer, United States Geological Survey, .

Senyukov, S. L. (2004), Activity Monitoring of the Kamchatkan Volcanoes using Remote Sensing, in *Integrated seismological and geophysical studies of Kamchatka.*edited by Anonymous , pp. 279, Kamchatkan Methodical Seismological Department, Geophysical Service, RAS, Petropavlosk-Kamchatsky, .

Senyukov, S. L., S. Y. Droznina, I. N. Nuzdina, V. T. Garbuzova, D. V. Droznin, and T. Y. Kozevnikova (2004), Sheveluch and Bezymianny Volcanoes Activity Investigations in 2000-2003 Using Remote Sensing, in *Integrated seismological and geophysical studies of Kamchatka.*edited by Anonymous , pp. 301, Kamchatkan Methodical Seismological Department, Geophysical Service, RAS, Petropavlosk-Kamchatsky, .

Sherrod, D. R., W. E. Scott, and P. H. Stauffer (Eds.) (2008), *A volcano rekindled; the renewed eruption of Mount St. Helens, 2004-2006*, 856 pp.

Shinohara, H. (2008), Excess Degassing from Volcanoes and its Role on Eruptive and Intrusive Activity, *Rev.Geophys., 46*(4), RG4005, doi: 10.1029/2007RG000244.

Siebert, L. (1984), Large Volcanic Debris Avalanches - Characteristics of Source Areas, Deposits, and Associated Eruptions, *J.Volcanol.Geotherm.Res., 22*(3-4), 163-197.

Stephens, C. D., and B. A. Chouet (2001), Evolution of the December 14, 1989 precursory long-period event swarm at Redoubt Volcano, Alaska, *J.Volcanol.Geotherm.Res., 109*(1-3), 133-148.

Swanson, D. A., and R. T. Holcomb (1990), Regularities in growth of the Mount St. Helens dacite dome 1980-1986; Lava flows and domes; emplacement mechanisms and hazard implications, International Union of Geodesy and Geophysics (IUGG) XIX general assembly, Vancouver, BC, Canada, 1987.

Swanson, D. A., T. J. Casadevall, D. Dzurisin, R. T. Holcomb, C. G. Newhall, S. D. Malone, and C. S. Weaver (1985), Forecasts and Predictions of Eruptive Activity at Mount St-Helens, Usa - 1975-1984, *Journal of Geodynamics, 3*(3-4), 397-423.

Swanson, D. A., T. J. Casadevall, D. Dzurisin, S. D. Malone, C. G. Newhall, and C. S. Weaver (1983), Predicting Eruptions at Mount St-Helens, June 1980 through December 1982, *Science, 221*(4618), 1369-1376.

Taisne, B., and C. Jaupart (2008), Magma degassing and intermittent lava dome growth, *Geophys.Res.Lett., 35*.

Thelen, W. A., R. S. Crosson, and K. C. Creager (2008), Absolute and Relative Locations of Earthquakes at Mount St. Helens, Washington Using Continuous Data: Implications for Magmatic Processes, in *A Volcano Rekindled: The Renewed Eruption of Mount St. Helens, 2004-2006*, Professional Paper 1750 ed., edited by D. R. Sherrod, W. E. Scott and P. H. Stauffer, United States Geological Survey, .

Thelen, W., and P. Team (2006), Twins across the Pacific; a comparison of Bezymianny Volcano, Russia and Mount St. Helens, USA; AGU 2006 fall meeting, *EOS Trans.Am.Geophys.Union, 87*(Fall Meeting Suppl.).

Thelen, W. A., S. D. Malone, S. C. Moran, and P. (. Cooper (2007), High or low? Frequency games at Mount St. Helens; SSA 2007 meeting announcement; Seismological Society of America, *Seismol.Res.Lett., 78*(2), 255.

Tokarev, P. I. (1981), *Volcanic Earthquakes of Kamchatka*, 47 pp., Publishing House of Science, Moscow.

Umakoshi, K., N. Takamura, N. Shinzato, K. Uchida, N. Matsuwo, and H. Shimizu (2008a), Seismicity associated with the 1991-1995 dome growth at Unzen Volcano, Japan, *J.Volcanol.Geotherm.Res., 175*(1-2), 91-99, doi: 10.1016/j.jvolgeores.2008.03.030.

Umakoshi, K., N. Takamura, N. Shinzato, K. Uchida, N. Matsuwo, and H. Shimizu (2008b), Seismicity associated with the 1991–1995 dome growth at Unzen Volcano, Japan, *Journal of Volcanology and Geothermal Research, 175*(1-2), 91-99, doi: DOI: 10.1016/j.jvolgeores.2008.03.030.

Vallance, J. W., D. J. Schneider, and S. P. Schilling (2008), Growth of the 2004–2006 dome complex at Mount St. Helens, in *A volcano rekindled; the renewed eruption of Mount St. Helens, 2004–2006*, Professional Paper 1750 ed., edited by D. R. Sherrod, W. E. Scott and P. H. Stauffer, United States Geological Survey, .

Venzke E, Wunderman R W, McClelland L, T. Simkin, J. Luhr, Siebert L, Mayberry G, Sennert S, and (2002-) (Eds.) (2008), *Global Volcanism, 1968 to the Present.*, Global Volcanism Program Digital Information Series ed., Smithsonian Institution, .

Vidale, J. E., W. L. Ellsworth, A. Cole, and C. Marone (1994), Variation in rupture process with recurrence interval in a repeated small earthquake, *Nature, 368*, 624-626.

Voight, B., et al (1999), Magma flow instability and cyclic activity at Soufriere Hills Volcano, Montserrat, British West Indies, *Science, 283*(5405), 1138-1142.

Waite, G. P., B. A. Chouet, and P. B. Dawson (2008), Eruption dynamics at Mount St. Helens imaged from broadband seismic waveforms: Interaction of the shallow magmatic and hydrothermal systems, *Journal of Geophysical Research-Solid Earth, 113*(B2), B02305.

Waite, G. P., and S. C. Moran (2006), Crustal P-wave speed structure under Mount St. Helens from local earthquake tomography; AGU 2006 fall meeting, *EOS Trans.Am.Geophys.Union, 87*(Fall Meeting Suppl.).

Waite, G. P., and S. C. Moran (2009), VP Structure of Mount St. Helens, Washington, USA, imaged with local earthquake tomography, *J.Volcanol.Geotherm.Res., 182*(1-2), 113-122, doi: DOI: 10.1016/j.jvolgeores.2009.02.009.

Waldhauser, F., and W. L. Ellsworth (2000), A double-difference earthquake location algorithm: Method and application to the northern Hayward fault, California, *Bulletin of the Seismological Society of America, 90*(6), 1353-1368.

Weaver, C. S., J. E. Zollweg, and S. D. Malone (1983), Deep Earthquakes Beneath Mount St-Helens - Evidence for Magmatic Gas-Transport, *Science, 221*(4618), 1391-1394.

Weaver, C. S., W. C. Grant, and J. E. Shemeta (1987), Local crustal extension at Mount St. Helens, Washington; Special section on Mount St. Helens [modified], *Journal of Geophysical Research, 92*(B10), 10,170-10,178, doi: 10.1029/JB092iB10p10170.

West, M., S. Senyukov, V. Chebrov, W. Thelen, A. Nikulin, and H. Buurman (2007), Eruption seismicity of Bezymianny Volcano, Kamchatka, Russia, *Eos Trans. AGU, 88*(52), Fall Meet. Suppl., Abstract V51D-0783.

White, R. A., A. D. Miller, L. L. Lynch, and J. A. Power (1998), Observations of hybrid seismic events at Soufriere Hills Volcano, Montserrat; July 1995 to September 1996; The Soufriere Hills eruption, Montserrat, British West Indies; introduction to special section; Part 2, *Geophys.Res.Lett., 25*(19), 3657-3660.

Wiemer, S., and S. R. McNutt (1997), Variations in the frequency-magnitude distribution with depth in two volcanic areas: Mount St Helens, Washington, and Mt Spurr, Alaska, *Geophys.Res.Lett., 24*(2), 189-192.

Williams, D. L., G. Abrams, C. Finn, D. Dzurisin, D. J. Johnson, and R. Denlinger (1987), Evidence from Gravity-Data for an Intrusive Complex Beneath Mount St-Helens, *Journal of Geophysical Research-Solid Earth and Planets, 92*(B10), 10207-10222.

Witter, J. B. (2003), Convection of Magma in Volcanic Conduits as a Degassing Mechanism at Active Volcanoes, PhD, University of Washington.

Appendix A: Excerpt from USGS Professional Paper 1750, “A Volcano Rekindled; the Renewed Eruption of Mount St. Helens 2004-2008

Vita

Weston Albert Thelen was born in Sacramento, California January 8, 1981. Beginning at age 7, Weston lived in Truckee, California. There he gained his appreciation of the outdoors and his wonder for the natural world. He also learned to ski, rock climb and mountaineer. He earned a double Bachelors of Science in Geology and Geophysics at the University of Nevada, Reno in 2004. In 2009, Weston earned a Doctor of Philosophy at the University of Washington in Geophysics.